HEL-2-18

RECENT SEDIMENTS OF MONTEREY BAY CALIFORNIA

by

T. E. YANCEY

HYDRAULIC ENGINEERING LABORATORY
COLLEGE OF ENGINEERING

UNIVERSITY OF CALIFORNIA
BERKELEY
JULY 1968

University of California
Hydraulic Engineering Laboratory

Technical Report
HEL-2-18

This work was supported by Contract DACW-72-67-C-0015
with the Coastal Engineering Research Center,
Corps of Engineers, U.S. Army

RECENT SEDIMENTS OF MONTEREY BAY, CALIFORNIA

by

T. E. Yancey

Berkeley, California
July 1968

CONTENTS

ILLUSTRATIONS

TABLES

ABSTRACT

Sediments of Monterey Bay are divisible into five heavy mineral provinces. Two of the provinces are from the Salinas and Pajaro rivers, the other three are not traceable to any known source. Sediments of the Salinas River have high garnet content, and the minerals glaucophane and lawsonite distinguish the Pajaro River sediments. A mineral province is restricted to beach sands along the north shore of the bay, and is carried into the bay by longshore drift from the northwest. The heavy mineral provinces do not coincide with the age differences of the sediment cover. The San Lorenzo River does not produce a detectable mineral province.

The grain size of the sediment cover decreases uniformly with water depth from the shoreline to a depth of 300 feet, then becomes coarser in a band along the edge of the continental shelf. Grain size modes correspond to conditions of wave agitation over most of the bay. Polymodal samples and samples not in agreement with this relationship can be shown to contain relict Pleistocene components. Sediment is being transported seaward from the shorelines by simple wave agitation, and deposited at various water depths according to grain size.

The sediment cover occurs in bands that are aligned subparallel to the depth contours. The outermost band on the continental shelf contains coarse sediment of Pleistocene age. The middle band is of very fine grained sediment of Holocene age. The nearshore band is of medium and coarse grained sediment probably of both Holocene and Pleistocene age. Pleistocene influences are found in this band at depths of 100 feet in the northeast corner of the bay.

INTRODUCTION

Monterey Bay, California's second largest bay, forms a large embayment into the linear trend of the Coast Ranges and is located on the central California coastline 70 miles south of San Francisco. It is located on a portion of the coast where the continental shelf is very narrow, and the outer limits of the bay floor correspond to the edge of the continental shelf. The bay contains the upper reaches of Monterey Canyon which has cut a deep trench across the floor of the bay all the way to the eastern shoreline. The character of the bay floor, smooth portions of continental shelf deeply cut by submarine canyons, is unusual and is restricted to the confines of Monterey Bay. North of the bay the continental shelf widens, and south of the bay the continental shelf disappears, giving place to a steeply sloping continental slope that begins at the shoreline (see Fig. 1).

Monterey Bay is the largest example of the open, semicircular type of bay that is the most common bay form in California. Most bays of this type contain sand beaches that are in delicate adjustment to prevailing conditions of wind and waves (Wiegel, 1964). The susceptibility of these beaches to alteration by human activities has created a need for understanding the processes of sediment transport to, along and off the beaches and into the bays they border. Prominent headlands at both ends of Monterey Bay make this a more protected bay than most and create sheltered conditions over large portions of the bay, especially in the northeast corner.

The bay is the focus of drainage for three rivers draining an area in excess of 6,000 square miles in the adjacent Coast Ranges (see Fig. 2). The possibility that Monterey Bay has served as the outlet for drainage

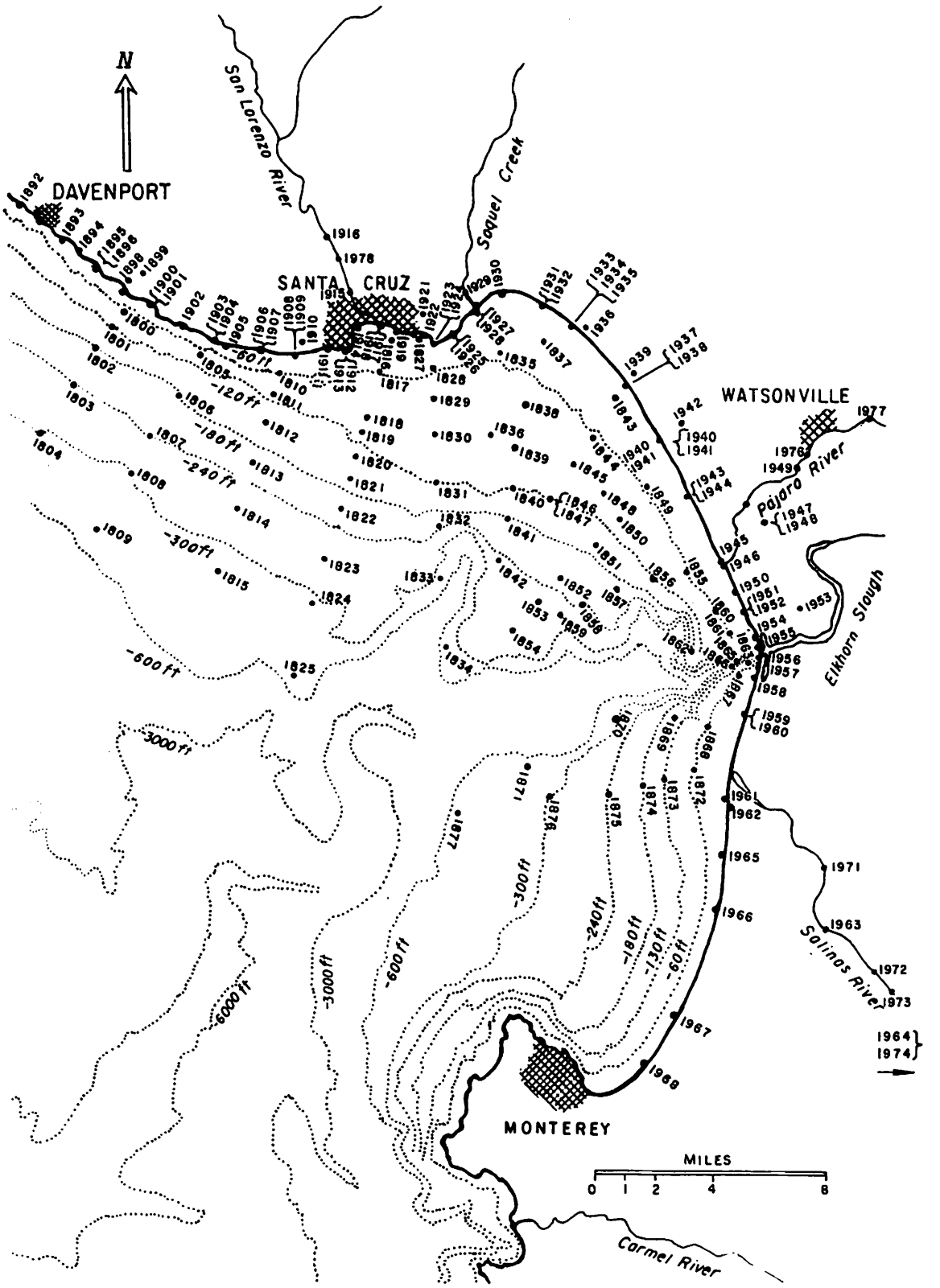

FIG. 1 LOCATION OF SAMPLES

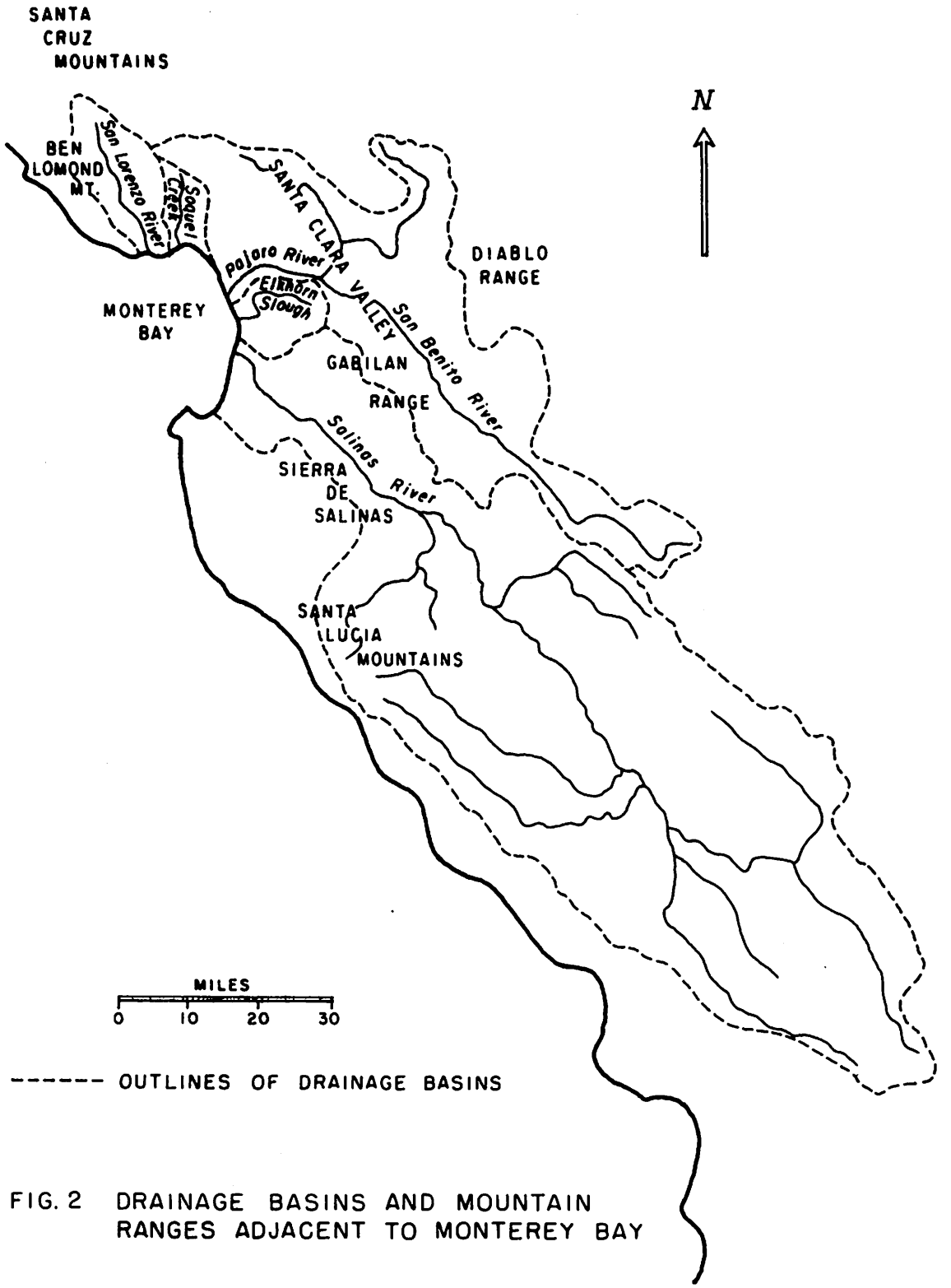

FIG. 2 DRAINAGE BASINS AND MOUNTAIN RANGES ADJACENT TO MONTEREY BAY

of the Central Valley during the late Tertiary has been suggested by many people (for example Allen, 1946; Baldwin, 1963) and the presence of the largest submarine canyon and the largest deep sea fan in California outside Monterey Bay is supporting evidence for this theory.

Early investigations of the submarine geology of Monterey Bay were made by Galliher (1932) during which a study was made of the general nature of the sedimentary cover on the continental shelf. Studies of various aspects of the bay's submarine geology have been conducted subsequent to Galliher's report (Galliher, 1935; Shepard & Emery, 1941; Wilde, 1965; Monteath, 1965; Martin & Emery, 1967), many of which have been completed within the past few years - a period of great expansion in oceanographic research. The most significant reports covering portions of the bay's submarine geology are Martin & Emery's (1967) report on Monterey Canyon and Wilde's (1965) report on the Monterey deep sea fan at the foot of Monterey Canyon. Geologic investigations of the subaerial sediments and bedrock outcroppings around Monterey Bay have been carried out for many years, and in considerable detail, the most relevant of them being noted on the Santa Cruz sheet (1959) of the Geologic Map of California.

The present work is primarily a description of the sediment cover in Monterey Bay and an analysis of the numerous variables controlling the distribution and accumulation of sediment within the bay. Investigation of the following problems has motivated the undertaking of this project and most of the work has been directed toward providing information on them:

1) describing the marine sediments,
2) determining the provenance of the sediments,
3) determining the geologic history of the sediment cover,
4) determining the processes of sediment transport into and within the bay, and,

5) describing the role of Monterey Canyon in the transport of sediment from the bay.

This project was undertaken with the support of the U.S. Army Corps of Engineers as part of their coastal sedimentation projects. Work was undertaken with the cooperation and encouragement of the Department of Geology and the College of Engineering at the Berkeley campus of the University of California, and facilities were provided by both divisions for the work. In addition, Scripps Institution of Oceanography, at La Jolla, California, provided facilities for part of the work and provided samples from several cores taken within Monterey Bay.

SUBMARINE PHYSIOGRAPHY

Monterey Bay is a semicurcular bay opening due west. It is 12 miles wide in an east-west direction and 25 miles wide in a north-south direction. Water depths reach 350 feet in many places, apart from the channel of Monterey Canyon which reaches a depth of 3,000 feet at 12 miles from the shoreline. Except for the channel of Monterey Canyon the bay floor is a wide gently sloping platform with an average gradient of 30-40 feet/mile, decreasing to about 20 feet/mile in the shallow portions of the northeast corner of the bay. The few submarine positive areas on the bay floor are low and small, and occur as a few low reefs and banks in the waters near Santa Cruz and Monterey.

The floor of the bay is divided into three major units, two smooth flat areas of continental shelf and the deep topographically rugged area of Monterey Canyon separating the two areas of continental shelf. The shelf portions of the bay floor are essentially smooth planar surfaces sloping evenly downward from the shoreline, and were formed as erosion surfaces cut across granitic and sedimentary bedrock underlying the bay (Martin & Emery, 1967). Prominent headlands on the north and south borders of the bay are composed of granitic rocks and siliceous mudstones highly resistant to erosion.

The continental shelf is relatively narrow within the bay, extending no further than 10 miles from the shore and breaks off into the continental slope at about a depth of 350 feet. The shelf-slope transition is rather abrupt in most places, corresponding to the rim of submarine canyons cut into the continental slope. Monterey Canyon is cut completely across the shelf and heads just outside the breaker zone at Moss landing. It is a deep, steep walled, V-shaped canyon with a high channel gradient which it maintains throughout its length. In depths of less than 5,000 feet the

channel is characterized by large meanders that are entrenched into late Tertiary sedimentary rocks of the bay floor. Soquel Canyon, another deep V-shaped canyon, is a small tributary on the north side of Monterey Canyon. It is cut a short distance across the continental shelf, but does not extend into the shallower part of the bay.

In addition to the major physiographic features discussed in this section, several minor submarine features around the head of Monterey Canyon provide direct evidence on the character of the canyon in premodern times and the features will be included in this discussion. These features appear to be directly related to the Salinas and Pajaro rivers, and include two erosional channels tributary to Monterey Canyon and a depositional fan south of the canyon.

Directly offshore from the mouth of the Salinas River the submarine contours show arcuate seaward deflections, revealing a broad thin wedge of sediment deposited by the Salinas River. The fan is built out over a sloping surface, covers an area of about 25 square miles, and is about 50-75 feet higher than neighboring areas equally distant from the shoreline. It is centered on the present mouth of the Salinas River and extends to a depth of about 300 feet, and is terminated on the north by Monterey Canyon. The shape of this sediment wedge resembles a subaerially deposited alluvial fan rather than a delta because its upper surface has a slope similar to adjacent parts of the bay floor which are not covered by the fan. Whether the fan originated above or below sea level is not clear from its morphology and its origin may be complex. The large volume of the fan indicates that it is mostly premodern in origin, and the shape is suggestive that it was formed during lowered stand of sea level. The position of the apex and shape of the fan show that the location of the present mouth of

the Salinas River has been maintained for the duration of the deposition of the fan. Thus the suggestion of Shepard & Emery (1941) that the Salinas River may have emptied through Elkhorn Slough for any significant period in the recent past can be discounted.

The two channels tributary to the head of Monterey Canyon are the Salinas Channel on the south side of the canyon, and the Pajaro Channel on the north side of the canyon. The Salinas Channel is a deep narrow channel carved across the continental shelf, ending at the edge of Monterey Canyon at a depth of 200 feet and extending shoreward to a depth of about 100 feet. It is cut into the submarine fan of Salinas River sediments throughout its entire length, and extends directly towards the mouth of the Salinas River. This channel does not extend to the shoreline and therefore is not being presently eroded. The Salinas Channel is within the depth range that appears to have been exposed at various times during the Pleistocene (Curry, 1960) and is certainly of subaerial origin. This feature then postdates the fan it is cut into and indicates that the fan is at least older than the last period of lowered sea level.

Located on the north side of the head of Monterey Canyon, the Pajaro Channel is a very short, wide, steep walled tributary that is much larger in size than the Salinas Channel. This channel extends directly toward the mouth of the Pajaro River, but does not reach the shoreline, losing its identity about two miles from the shoreline. It joins the main channel of Monterey Canyon in the same general area as the Salinas Channel, which enters on the south side of the canyon. Westward from this juncture area Monterey Canyon widens abruptly without noticeably changing its gradient. This widening appears to be directly related to the inflow of the two river drainages during the Pleistocene lower sea level stand.

SUBAERIAL PHYSIOGRAPHY

Leading into Monterey Bay are several valleys and rivers that have extensive drainage areas, draining most of the southern Coast Ranges. The Salinas Valley is the largest of these valleys, possessing a wide flat bottomed valley floor between adjacent mountain ranges, and fronting on a 10 mile portion of Monterey Bay. The Salinas Valley is a strongly linear drainage basin extending southeast from Monterey Bay nearly to Morro Bay and covers nearly 4,300 square miles. The center of the valley is covered with large areas of sedimentary fill, between adjacent highlands of mountain ranges that reach their highest elevations near the mouth of the Salinas Valley; that is, closest to Monterey Bay. The character of the valley changes little throughout its length and the river has a low gradient for its entire length. The mouth of the river is blocked off from the ocean by a wide sand bar and the last few miles of the river forms a lagoon or sluggish channel.

The Santa Clara Valley with its southern extension, the San Benito Valley, both drained by the Pajaro River, border the Salinas Valley on the northeast. This drainage basin is structurally similar to the Salinas basin although it is smaller in size, about 1,400 square miles. It is part of a NNW-SSE trending structural low occupied in the northernmost part by San Francisco Bay, but the southern half does not drain northward, instead draining westward into Monterey Bay through the narrow 600 foot deep Pajaro Gap cut across the northern extension of the Gabilan Range. The San Benito Valley is mostly bedrock floored, whereas the Santa Clara Valley is widely alluviated in a large basin around Hollister. West of the Pajaro Gap the Pajaro River flows in an alluvial valley like the Salinas Valley. The gradient for this portion is not as low as for the

comparable portion of the Salinas River and no lagoon is present at the mouth of the river. The river maintains a year round surface flow of water across the beach into the ocean but the flow is small and not large enough to modify the beach profile created by the ocean waves.

The other major river draining into Monterey Bay is the San Lorenzo River which drains most of the southern Santa Cruz Mountains. Its drainage basin is different from either the Salinas or Pajaro basins in, (1) being much smaller in area - 140 square miles, (2) having a high gradient, and (3) lying in a bedrock valley with alluviated portions small and confined to areas near the mouth. The drainage area is predominantly over 1,000 feet in elevation, and supports thick vegetation in all areas. The elevation and thick vegetation provide large amounts of runoff year round, and the river maintains a larger surface flow of water in the summer months than the Salinas or Pajaro rivers.

Monterey Bay lies within a major structural low that trends E - W across the Coast Ranges, similar to the structural low in the San Francisco region which contains the Golden Gate and Carquinez Strait, that serves as the outlet for drainage of the Central Valley. In addition to Monterey Bay itself, negative topographic features occurring within the Monterey structural low are Monterey Canyon, Pajaro Gap, and the Hollister Basin. Monterey Bay also serves as the center of drainage for most of the southern Coast Ranges. Topographically stronger structural trends of alternating highs and lows aligned NNW - SSE and corresponding to the dominant trends of the California Coast Ranges cut across the E - W trend. On the west are the Santa Lucia Mountains and their north extension, the Ben Lomond portion of the Santa Cruz mountains. Monterey Bay lies across this structural high in an area where it has been greatly downfaulted

(see Martin & Emery, 1967), and where it reappears on the north and south borders of the bay it is exposed as prominent headlands. Bordering this high trend on the east is a structural low which contains the Salinas and San Lorenzo rivers, and into which the bay has carved its smooth eastern boundary. These structural trends continue eastward, but the eastern-most one affecting the bay is the Gabilan Range, against which the eastern margin of the bay abuts. To the east another succession of structural low and high, the Santa Clara - San Benito valleys and the Diablo Range, complete the series that determine the physiographic character of the Monterey Bay region (Fig. 2).

GEOLOGY

Sediment supplied to Monterey Bay is derived from three general types of rocks; igneous and high grade metamorphic rocks, low grade metamorphic rocks of the Franciscan Formation, and lastly, sedimentary rocks overlying basements composed of the former two types. The granitic rocks are dominantly quartz diorites and adamellites with scattered remnants of metasediments consisting of schists, gneisses and carbonates (see Compton, 1966; Bowen and Gray, 1959; Leo, 1961), and are exposed primarily in the Ben Lomond portion of the Santa Cruz Mountains, in the northern Santa Lucia Mountains, and in the northern Gabilan Range.

Franciscan eugeosynclinal metamorphic rocks include some very distinctive lithologies, but exposures of them are much less extensive than exposures of granitic rocks. The assemblage is composed of serpentines, shales, bedded cherts and low grade metamorphosed graywackes and volcanics. Franciscan rocks are exposed on the west side of the Santa Clara Valley drainage basin, extensively in the center of the Diablo Range, and also in small areas on the west side of the Salinas Valley drainage basin.

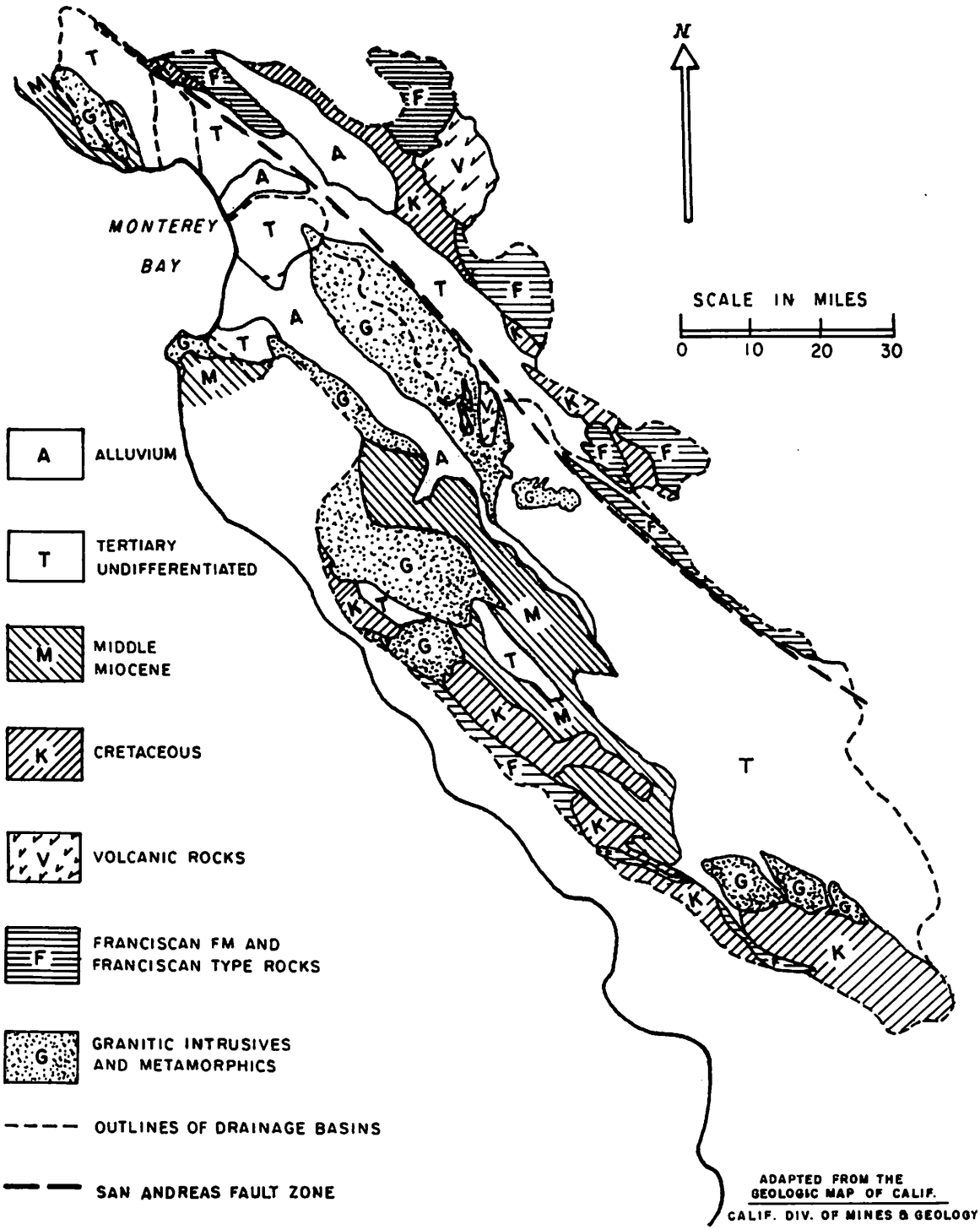

FIG. 3 GENERALIZED GEOLOGY OF THE MONTEREY BAY DRAINAGE BASINS

The granitic or Franciscan rock types everywhere form the basement rock of the drainage area of Monterey Bay, but in extensive areas they are deeply covered by Cretaceous and Tertiary sedimentary rocks. These sedimentary rocks crop out over much of the mountain ranges, especially as flanking units around the cores of mountains, and the younger rocks are present as deep valley fills. The major subunits of the sedimentary record in this area are (1) the Cretaceous age rocks along the Santa Clara Valley, which are predominantly sandstone, (2) the Miocene age rocks that crop out extensively along the Salinas and San Lorenzo valleys, and (3) the Pliocene to recent unconsolidated deposits that are generally confined to the central portions of the valleys. The Miocene age rocks include the Monterey Formation, a distinctive fine grained siliceous mudstone unit that crops out extensively north and south of Monterey Bay. Unaltered Tertiary vocanic rocks are sparingly present in the San Lorenzo Valley, Diablo Range and Gabilan Range.

The basements of granitic and Franciscan rock types occur in well defined structural blocks which are either wholly granitic or wholly Franciscan. Monterey Bay lies upon the Salinian block of quartz diorites, adamellites and high grade metasediments. Ben Lomond Mountain, the Gabilan Range and most of the Santa Lucia Mountains are formed of these rocks, and the Salinas and San Lorenzo valleys, totalling three-quarters of the total bay drainage area lie almost entirely upon this block. The Salinian block extends westward out to the continental slope in the Monterey Bay area (Martin & Emery, 1967). However, to the south the westward margin occurs within the Santa Lucia Mountains, and the complex Nacimiento-Sur fault system separates the granitic type rocks from a westward lying block of Franciscan-like metamorphic and sedimentary rocks. Only a very small

area of these Franciscan-like rocks is included in the Salinas Valley drainage basin.

The Salinian block is terminated on the east by the San Andreas Fault which extends for 150 miles across the area draining into Monterey Bay, separating the granitic type rocks of the Salinian block from the Franciscan metamorphic rocks of the Diablo block. The Diablo block with its Franciscan metamorphic rocks occurs no closer than 12 miles to Monterey Bay. It is the basement complex of the Santa Clara - San Benito valleys, which form one-quarter of the total bay drainage area. A topographic high occurs close to the San Andreas Fault line, and the drainage basin subdivisions correspond closely to geologic subdivisions. The drainage areas of the large valleys lie almost entirely upon either the granitic basement or the Franciscan metamorphic basement.

Dredgings carried out in Monterey Bay and reported by Martin & Emery (1967) reveal granitic rocks on the south wall of Monterey Canyon directly off the Monterey Peninsula, whereas Pliocene sedimentary rocks crop out on the north wall and along the shallower head regions of the canyon. West of the juncture of Monterey and Carmel canyons different lithologies appear to be present on the deeper parts of the continental slope, but insufficient sampling has been done to confirm this. Most of the continental shelf on the northern half of Monterey Bay is floored by Pliocene sediments which crop out in Monterey Canyon and on the shore east of Point Santa Cruz. Miocene bedrock crops out along the shore west of Point Santa Cruz, and probably floors large areas of the continental shelf off these shorelines. Thick deposits, probably Pleistocene, floor the eastern portion of the bay, in the region surrounding the head of Monterey Canyon and the mouths of the Salinas and Pajaro rivers. Wells drilled in this area on the shore reveal thick deposits of Pliocene and Pleistocene Age (Manning, 1963; Starke and Howard, 1968).

HYDROLOGY

Stream discharge records give a clear idea of the relative potential of each drainage system to transport sediment into Monterey Bay. The records of water flow for each basin show yearly variations that are very similar, an indication that the present climate of the Monterey Bay drainage basins is nearly uniform. The morphology of the basins, however, is not similar, and this difference modifies the flow characteristics of the rivers. The Salinas and Pajaro valleys are rather low, sparsely vegetated, and have extensive alluvial deposits. The San Lorenzo Valley is mostly over 1,000 feet in elevation, densely vegetated and with little alluvial cover. The differences show up in the discharge of the San Lorenzo River which is roughly equal to the flow of the Pajaro River, and yet has a drainage basin only one-tenth the size of the Pajaro. Because of its greater elevation and its location closer to the ocean, the San Lorenzo Valley receives more rainfall. In addition, the San Lorenzo Valley is a bedrock floored valley, which channels all water flow into the surface flow, whereas the alluviated Pajaro basin can channel appreciable subsurface water flow through its alluvial deposits.

The yearly discharge averages of surface water flow in the larger streams, compiled from gaging stations, are as follows:

Table 1

Drainage Basin	Drainage Area	10 Year Average Surface Water Flow
Salinas River	4300 square miles	320,000 acre-feet/year
Pajaro River above Chittenden, plus Corralitos Creek	1400 square miles	120,000 acre-feet/year
San Lorenzo River	140 square miles	106,000 acre-feet/year
Soquel Creek plus Aptos Creek	25 square miles	10,000 acre-feet/year

From Hendricks (1964)

Several small streams drain the west side of Ben Lomond Mountain, all having small drainage areas and steep gradients. Sediment transport may be high for local areas, but cannot be evaluated without more data. Elkhorn Slough has a small drainage basin also but the presence of an extensive salt water lagoon precludes sediment transport into the bay even by floods.

Over 90% of the runoff comes during the winter months from December to May. Within this interval and especially during floods most sediment transport takes place. Although Minard (1964) and Sayles (1965) argue, on morphological grounds, that significant amounts of sediment cannot be coming out of drowned streams or rivers that possess lagoons at their mouths, this argument does not appear to be valid when consideration is made of the fact that most sediment is transported during periods of high water flow and that afterwards water flow drops off rapidly to low levels. Wiegel (1964, p. 362) records a notable example of a stream with a deep lagoon nearly a mile long, blocked at its mouth by a beach bar, carrying a large volume of sediment through the lagoon into the ocean. In this case, Soquel Creek transported enough sediment to the ocean during the winter floods to form a delta into Monterey Bay, which was later dispersed by waves. Soquel lagoon did not fill up during this time, but acted as a channel instead, demonstrating that lagoons are not necessarily barriers to sediment transport into the ocean. Under conditions in which 50% of the water runnoff occurs in 10% of the time, the lagoons are stable to conditions of high water flow and intermediate flow does not last long enough to alter the bed pattern.

WAVE REFRACTION

Diagrams of refracting waves on shoaling bottoms along shorelines have been developed to analyze wave force for longshore components and

to predict direction of littoral currents, (see Johnson, 1953). Open ocean waves have straight wavefronts which will be retarded differentially by the differing topography of the sea floor as the waves approach the shoreline. Each wave has a motion at depth, an oscillatory motion extending in depth not more than one-half the wavelength, which decreases in force rapidly below the water surface. As the wave begins to strike bottom, those portions of it hitting bottom will be retarded and the wave height and wavelength change relative to the portions of the wave in open water.

When waves reach the shoreline they will strike it at an angle determined by the original direction of propagation and by the amount of refraction during the shoaling of the wave. This angle will be 90 degrees only if the original wavefront was parallel to the shoreline and underwent no refraction during shoaling. Most waves do not meet this condition and as a result they provide a component of force parallel to the beach which creates longshore drift or littoral transport of sand. Other actions of the waves, such as wash and backwash on the beach, are oscillatory processes which give no net gain in transport direction. Refraction of waves is then the predominant factor in determining the direction of longshore drift (Ingle, 1966).

Charts prepared by the National Marine Consultants (1960) show wave data in terms of swell conditions at points in deep water at several locations off the California coast. Swell conditions rather than total sea conditions are used because these are more directly related to shoreline development (Johnson, 1956). Figure 4 shows a three year averaging of swell conditions for a station at 37.5° North latitude and 123.6° West longitude, 55 miles off San Francisco. Swell conditions for a location at 35.5° North latitude and 122.0° West longitude, off Cape San Martin, are nearly identical in magnitude and direction. Seasonal variations are

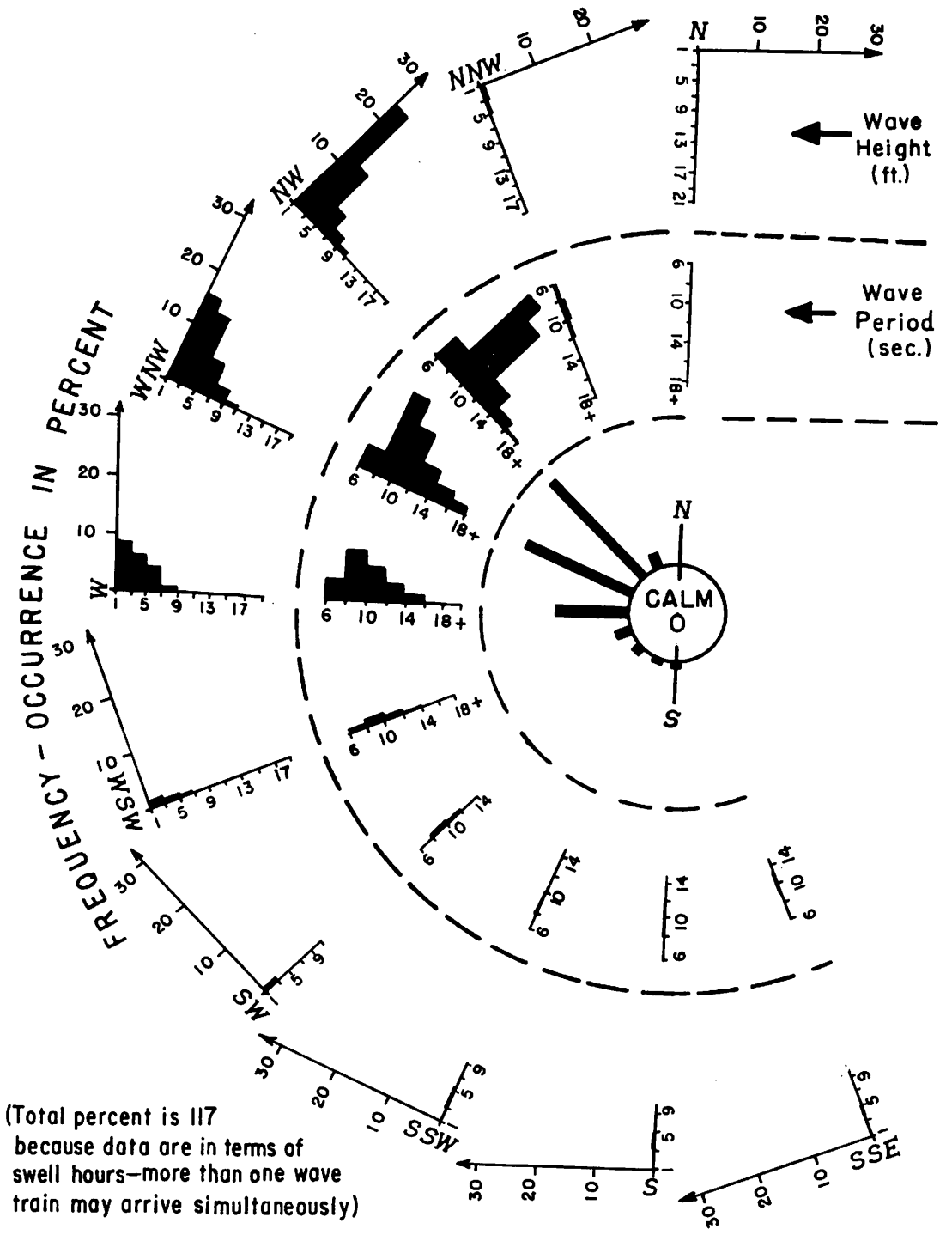

FIG. 4 AVERAGE SWELL CONDITIONS OFF CENTRAL CALIFORNIA COAST (FROM CHERRY, 1964)

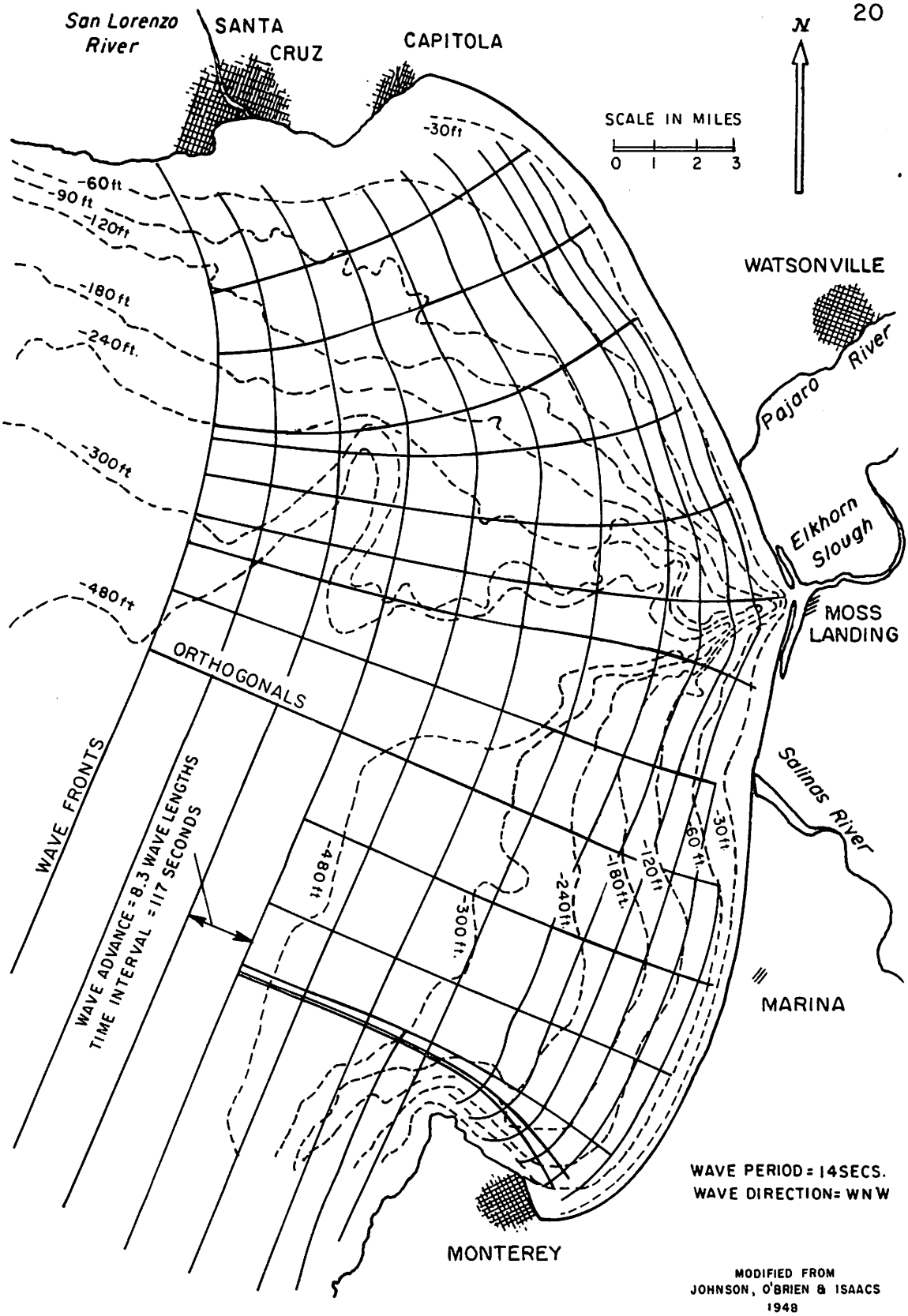

FIG. 5 WAVE REFRACTION DIAGRAM FOR MONTEREY BAY

averaged in this total and do not show the marked predominance of northwesterly swell during the summer months which give way to westerly conditions during the winter months. The average, however, does show the narrow limits of this variation. A swell direction of WNW is then a valid yearly average not requiring separate analysis of seasonal variations.

The effects of short period waves are considered the predominant influence on beach sand movement. Long period waves (storm waves) are infrequent and Wilson and others (1963) show that such waves are refracted far from shore and approach the shoreline almost normally everywhere. A refraction diagram for Monterey Bay is shown in Figure 5 for wave conditions of 14 seconds wave period from the WNW. The fit of the wave pattern to the shoreline is close enough to make it clear that the shoreline is highly responsive to wave control. The fit is not perfect to the entire bay so a prevailing direction of longshore drift should occur in several areas.

The north margin of the bay and the south margin along the Monterey Peninsula are areas in which the shoreline is at variance with the prevailing wave fronts, and both areas have a resultant strong component of eastward littoral drift. This eastward drift moves beach sands into the inner portion of the bay from beaches along the headlands of the outer bay, a unidirectional movement in continuous operation. Along the north bay margin the trend is interrupted briefly by Santa Cruz beach. The wave refraction diagram is not sufficiently detailed in Figure 5 to show it, but due to westward protection, the beach is essentially in equilibrium with local wave conditions. This beach is the only large body of sand along the north bay and it appears to act as a reservoir for sand drifting

eastward. Any net longshore drift along the beach will be dependent upon a building up of the beach by material supplied from the west which would be drifted eastward until original beach conditions prevail. The volume of sand moved along the north bay margin must be low, but locally where sediment is transported into the bay this material must be rapidly dispersed.

The reverse conditions occur along the east margin of the bay. Here, wave fronts nearly always parallel the shoreline and the component of longshore drift is small, but the beaches are wide and extensive. Such beaches are highly sensitive to small components of longshore drift. Fig. 5 shows that under average conditions only the southeast corner of the bay is in exact equilibrium with the waves, other portions are at slight variance. The southeast corner of the bay is also the most openly exposed to waves coming into Monterey Bay.

In the northeast corner of the bay the shoreline is not aligned to the WNW average wave conditions and an average southward component of longshore drift is predictable for the area. This has proven to be the case in a morphologically similar area, the northeast corner of Halfmoon Bay (see Sayles, 1965) where the construction of a breakwater has ponded sand on the north side and removed it from the beaches south of the breakwater. In the northeast corner of Monterey Bay sand drifted from the north margin of the bay, and sediment washed from the adjacent high cliffs of poorly consolidated sands is expected to supply a strong southward directed longshore drift.

In the central part of the bay two features cause deviations from the otherwise smoothly rounded outline of the bay. These are a slight embayment at the head of Monterey Canyon and a slight outbuilding at the mouth

of the Salinas River. The shoreline in these areas closely approximates the wavefront, which is refracted by the deep submarine canyon and the fan-shaped sediment wedge off the Salinas River. These sinuosities are well enough adjusted to wave conditions so that under average conditions they do not create prevailing longshore drift, except for a short distance south of the mouth of the Salinas River where a southward drift is expected. These sinuosities undoubtedly create strong, diverse and short-lived conditions of longshore drift under varying wave conditions but their long-term effect will be small.

The result of these conditions is an eastward flow of sand into the inner portions of Monterey Bay along the north and south margin of the bay. The northeast corner of the bay has a small but definite component of southward directed longshore drift, and the volume of sand movement may be high. An area of equilibrium exists from Monterey to Marina, and longshore drift in other portions of the bay is directed toward this area. There are two specific areas where sand is lost from this system. The first is at the head of Monterey Canyon where some sand is swept out of the littoral zone and down the canyon, but as Ingle (1966) has demonstrated, most sand transport takes place between the breaker zone and swash zone on the beach and sand can be transported past Monterey Canyon without being lost. The other area of loss occurs at the beach between Monterey and Marina where sand is blown off the beach and onto the dune field in back of it.

PROCEDURES

The sampling for this study was done in September 1966 from R/V Tage of Hopkins Marine Station, Pacific Grove, California. 75 submarine samples were taken and 37 beach samples were taken during the sampling program. See Fig. 1 for location. The marine samples were collected by

means of a five inch diameter pipe dredge which was towed a short distance over the sea floor. Samples obtained by this method are composite samples from several microenvironments on the sea floor, which is a beneficial result for this study because it reduces the effects of local variation in sediment composition. Sampling localities were spaced semi-regularly across the sea floor to include samples from all depth zones, and sampling was carried out on the continental shelf along the north half of Monterey Bay from off Davenport, California to off the mouth of the Salinas River. Restricted areas in the south part of the bay adjacent to Fort Ord Army Base prevented sampling throughout the entire bay.

The beach samples were obtained by driving a three inch pipe about one foot into the beach at mid tide level to obtain a composite sample of sand layers accumulated during the summer aggradation of the beach. Inherent in taking beach samples is the danger of obtaining samples whose mineral composition has been altered from the average mineral composition of the beach by selective sorting of waves. The pipe method of sampling minimizes this danger by obtaining portions of several layers in the beach profile, each deposited under different hydraulic conditions. River samples were taken from the bedload of the major streams and rivers, at several places near their mouths, and bedrock samples of all the major lithologic units surrounding the bay were collected at regular intervals from seacliffs at several points around the bay.

In the laboratory the samples were divided by sediment splitter into portions for size analysis and mineral analysis, after the removal of a small portion for clay analysis. For mineral analysis the sample was washed on a 52 micron screen and heavy mineral separations were made of the sand, using bromoform with a density of 2.88 grams per cubic

centimeter. Heavy mineral grain mounts were prepared after eliminating mineral grains larger than 500 microns. This removal facilitates making slides and procedures of identification are simplified because large grains create thick slides in which the finer grains cannot be brought into focus. Grains above 500 microns ordinarily are opaque or semi-opaque, and in this series of samples represent much less than 1% of the sample. For a few samples of coarse sand, slides were prepared from grains of 750 microns and less.

100 nonopaque and nonmicaceous mineral grains were identified along line counts in each slide. Biotite, opaque and aggregate grains were tabulated separately. To check the accuracy of the counts, a recount was made on 15 samples from two traverses across the bay, and the results of the second count were within a few percent of the original count.

The sand fraction was analyzed by use of the settling tube at Scripps Institution of Oceanography (see van Andel, 1964). The settling tube provides analyses based on settling velocity, which in addition to grain size, allows for hydraulic variables of shape and specific gravity of the mineral grains. Samples were washed and sieved to remove all silt and clay, then split to approximately three grams for each run. A weight cumulative curve is produced from a continuous recording of the weight of the sediment as it settles through a column of water. Quartile measurements, or any other percentage measures, are read directly off the curve by means of an overlay. Silt was analyzed by pipette using the procedure described in chapter 6 of Krumbein & Pettijohn (1938).

The use of settling tubes provides an easy and rapid method for determining size analyses of sediments. This method appears not to be as accurate as sieving for measuring grain size distribution (Folk, 1966),

but it more accurately represents the dynamic behavior of the sediment and records a cumulative curve determined at all points. Quartile measurements were read directly off the recording, improving the accuracy of these measures considerably over curves determined at $\frac{1}{2}\Phi$ or $\frac{1}{4}\Phi$ intervals.

STATISTICAL PARAMETERS

Much current work in sedimentology is being directed toward relating the statistical parameters of sediment grain size distribution to environmental conditions and to show differences resulting from different environments of deposition (for example, Folk, 1966). Differences in statistical parameters are usually determined by the interaction of several factors and therefore are not easily analyzed. The most frequently used statistical parameters are the median diameter, modes, sorting coefficient, skewness, and kurtosis, of which median diameter, modes, sorting coefficient, and skewness are used here.

Great exactitude is possible in computing statistical parameters, but this has exceeded the accuracy of measuring the grain size distribution of the sediment. In addition, the different methods are not strictly comparable in the properties they measure, and in consequence, only the values of the elementary statistical parameters such as median diameter and sorting coefficient are closely comparable between different methods or even different workers using similar methods.

Objective measures of the sediment grain size distribution are necessary to describe sediments, and regardless of the difficulties in standardizing these measures, examination of Figs. 6, 8, 9 and 10 show that significant trends in the statistical parameters are associated with environmental changes. By comparing these trends with the modern environment of Monterey Bay a measure is obtained of the control of modern con-

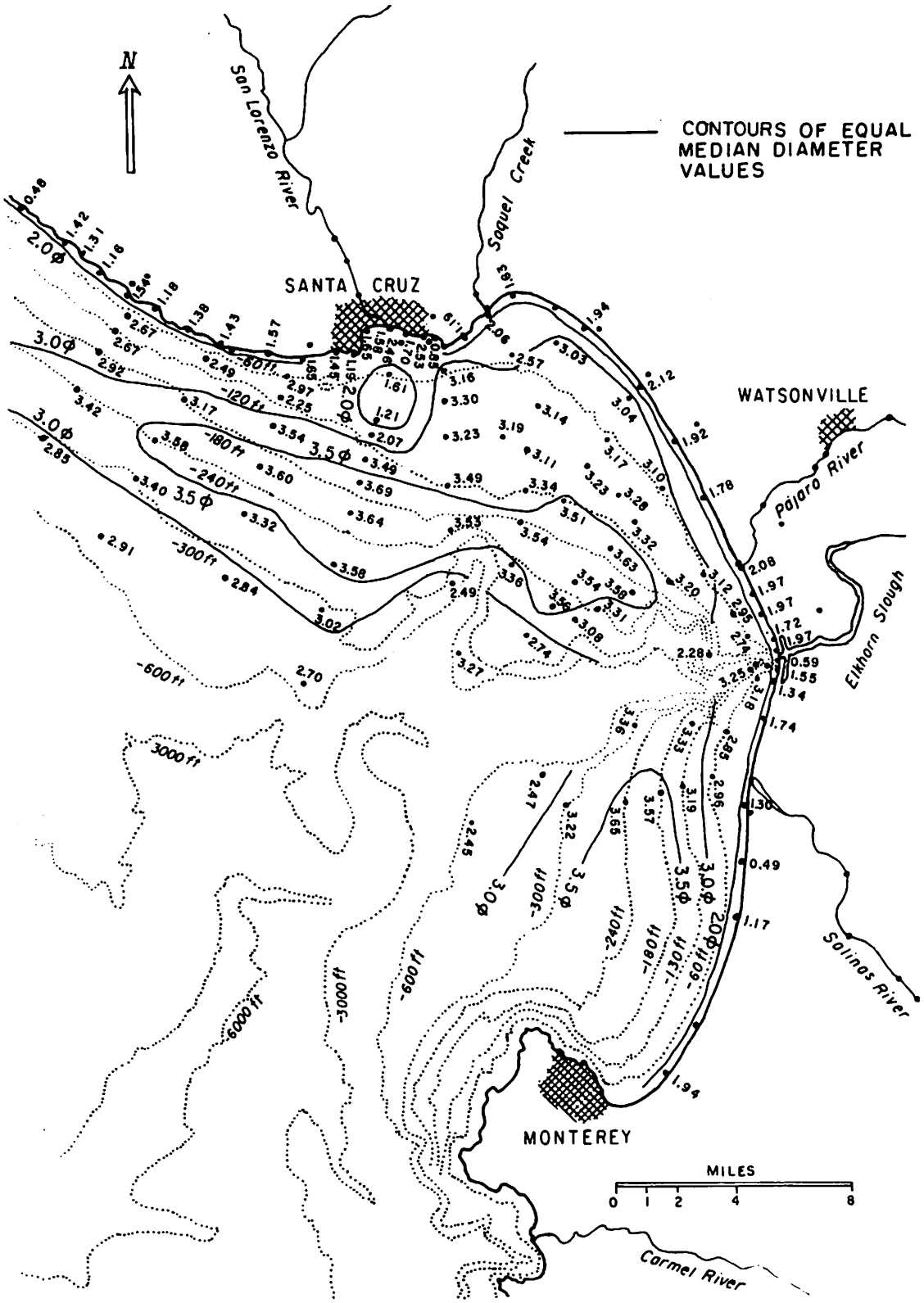

FIG. 6 MEDIAN DIAMETER IN PHI (φ) UNITS OF THE SAND (>62 μ) FRACTION OF BEACH AND MARINE SAMPLES

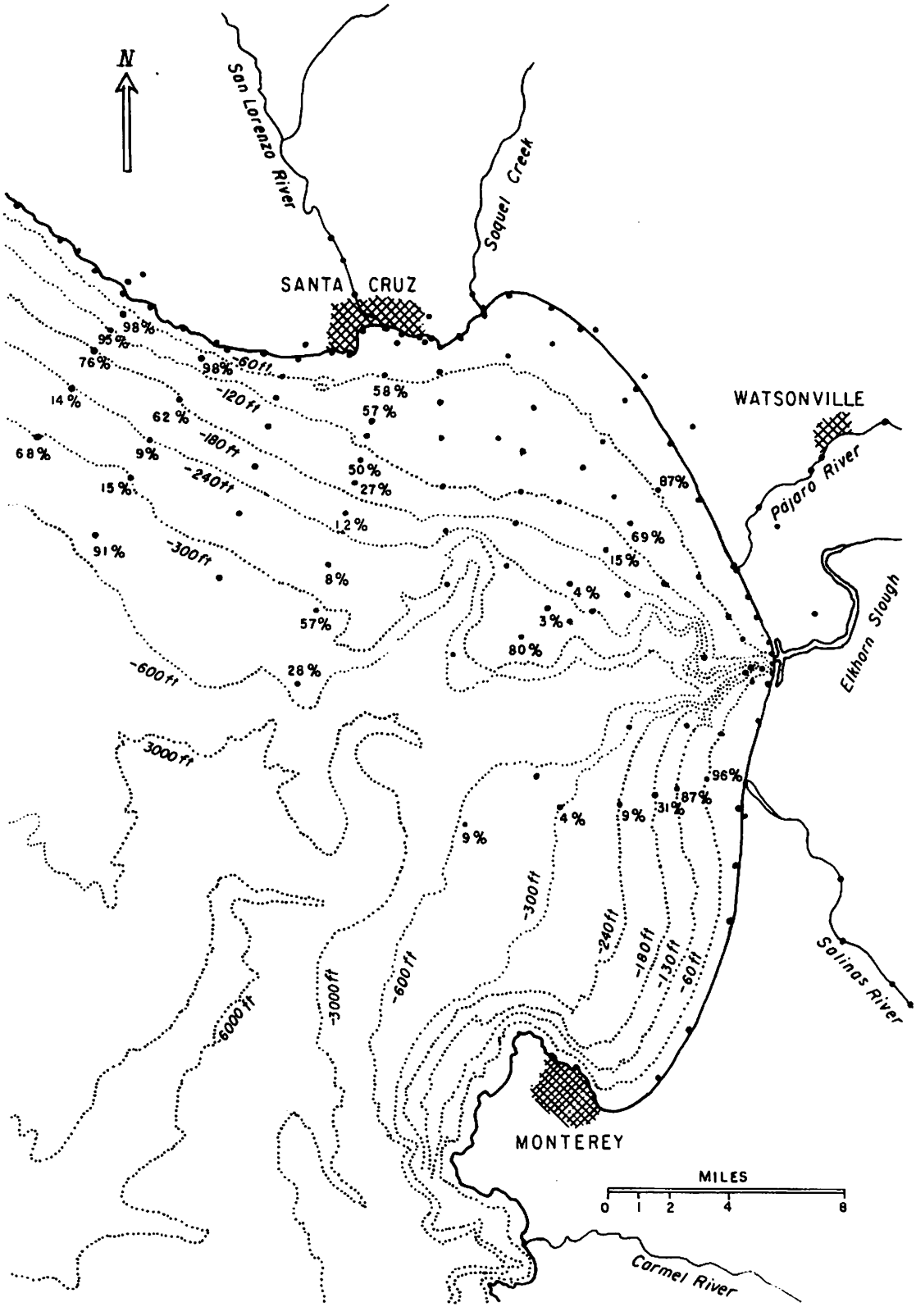

FIG. 7 PERCENTAGE OF SAND FRACTION IN MARINE SAMPLES

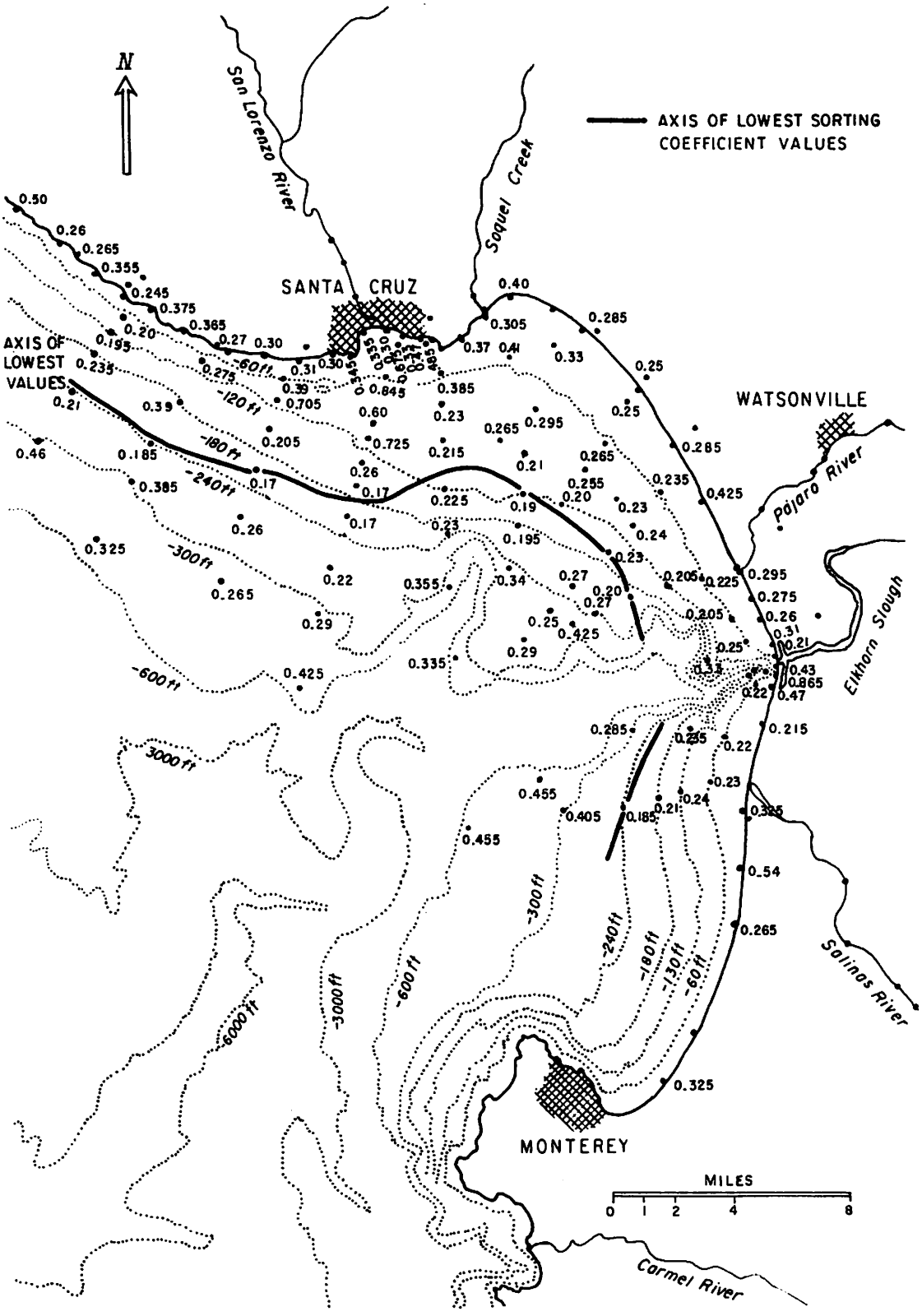

FIG. 8 PHI SORTING COEFFICIENT $\left[S_o = \frac{Q_3\phi - Q_1\phi}{2} \right]$ OF SAND FRACTION OF BEACH AND MARINE SAMPLES

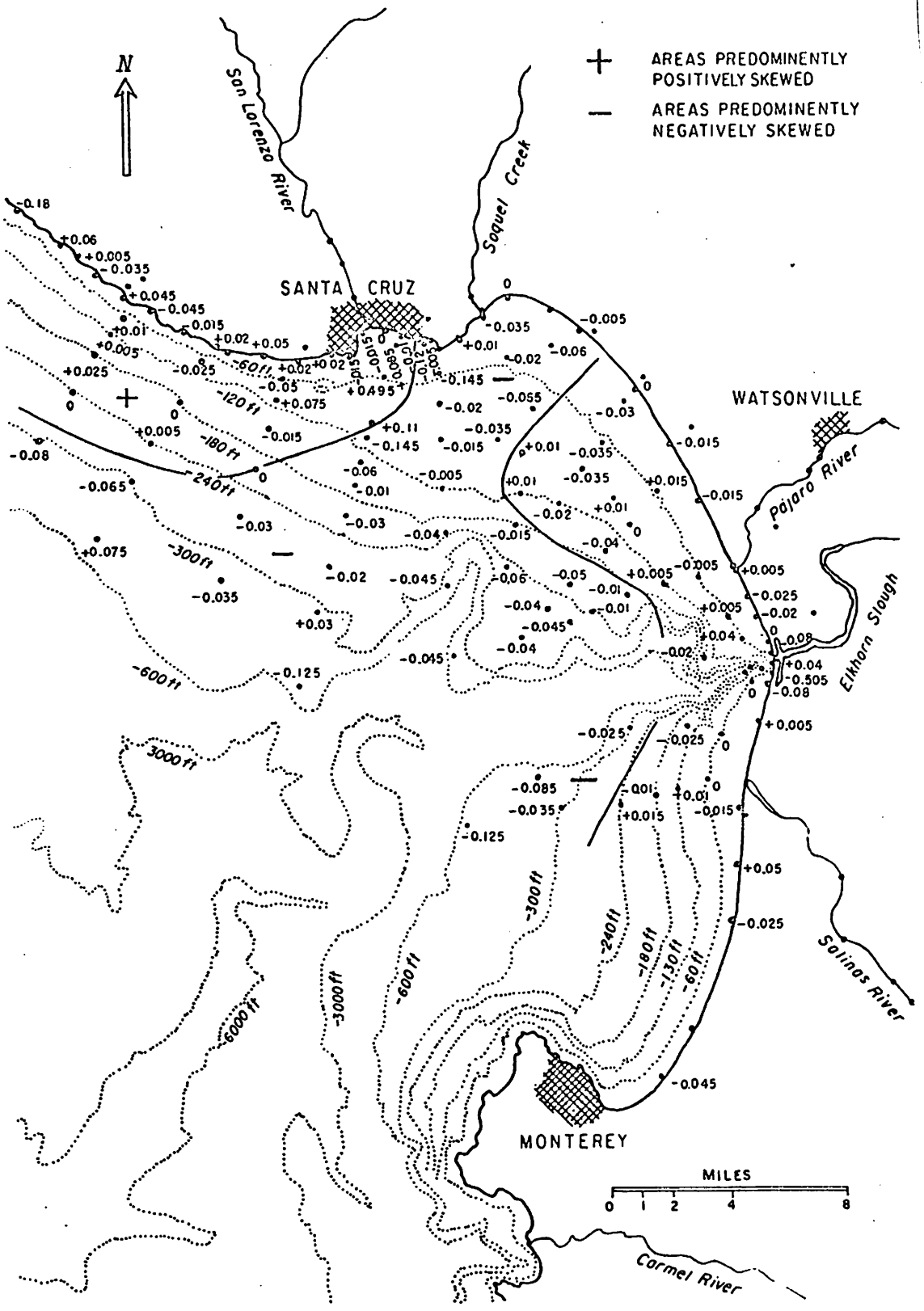

FIG. 9 QUARTILE SKEWNESS $S_k = \left[\frac{Q_{3\phi} + Q_{1\phi} - 2Md\phi}{2}\right]$ OF SAND FRACTION OF BEACH AND MARINE SAMPLES

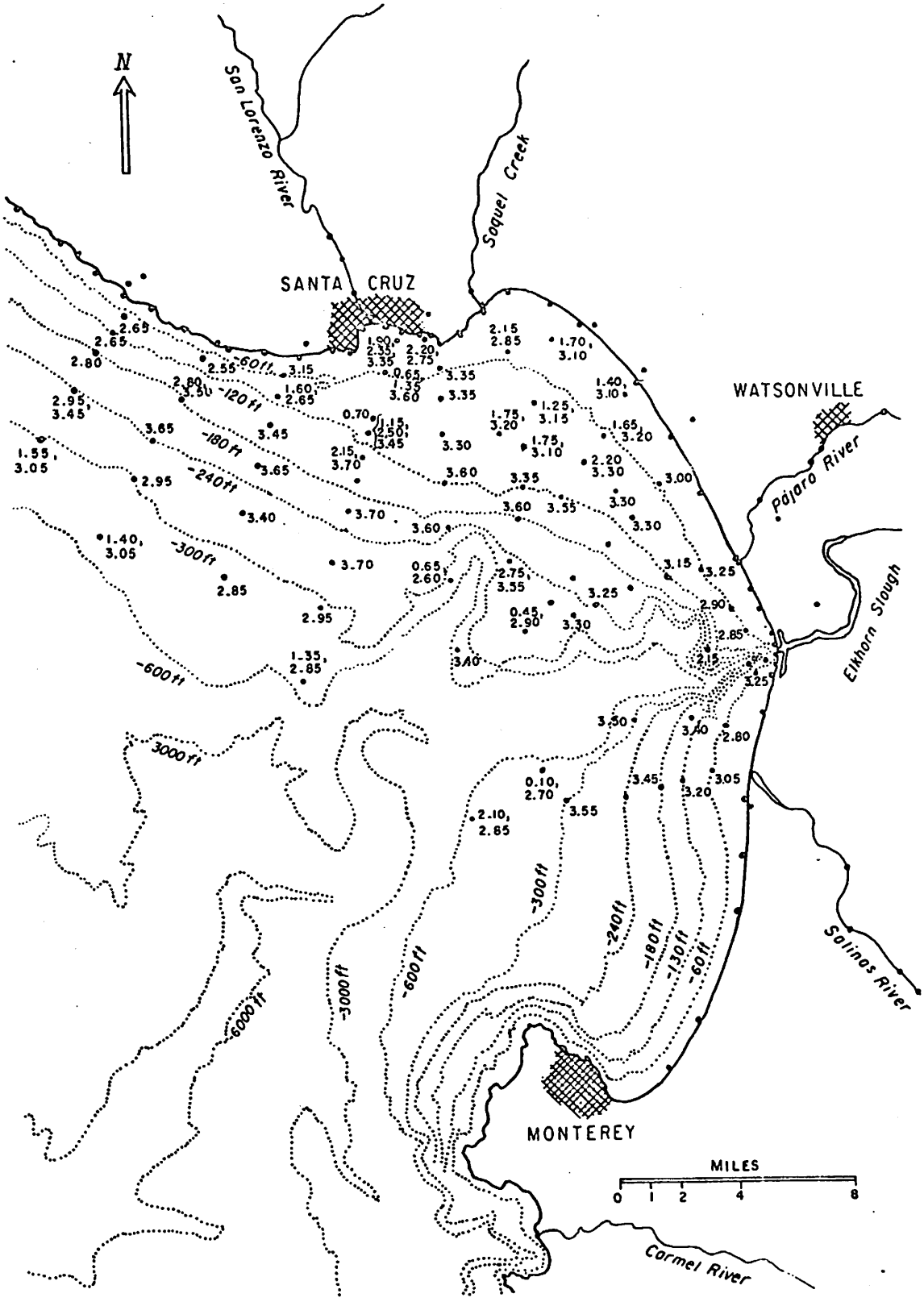

FIG. 10 MODES IN PHI (ϕ) UNITS OF SAND FRACTION OF MARINE SAMPLES

ditions on the sediment cover of the bay. The most obvious example of sediment discrepancy with modern conditions is the band of coarse sediment on the outer edge of the continental shelf, which is similar to bands of sediment in other regions that have been dated as late Pleistocene (Curry, 1960). Statistical analysis can be used to semi-quantitatively measure the influences of modern and premodern conditions in the sediment cover, and to detect them in areas where the sediment cover is predominantly of one regime or another.

Values of median diameters of the sand fraction of the submarine samples are plotted on Fig. 6. Contours of equal grain size are aligned subparallel to the depth contours, but vary in position in response to exposure of the coastline and areas of rough topography on the bottom. In all areas there is a progressive decrease in grain size with increasing depth, a trend which is reversed about halfway out on the continental shelf and the sediments become coarser in the 300-400 foot depth range on the outer edge of the shelf.

In depths of less than 300 feet the trend of decreasing grain size is directly related to the strength of bottom agitation - a factor which is controlled by the water depth and the degree of exposure to open ocean waves. The reef areas south of Santa Cruz break this trend abruptly, but their influence is limited to the immediate environs of the reefs. They are fairly regular rock bottoms with thin covers of sediment in most places rather than prominent projecting reefs, and do not break or deflect the force of waves shoaling toward the shoreline. Their marked effect on the statistical parameters is caused by residual concentrations of coarse sediment and by the great abundance of shell material produced in the area.

The decrease in median diameter is fairly uniform on the shoreward portions of the continental shelf, areas in which the sediments contain high percentages of sand. On the seaward portions of the shelf this ends in a zone one-half to two-thirds the distance out on the shelf having closely similar median diameter values, which corresponds to a belt of very fine grained muds in which the sand fraction constitutes only a few percent of the total sample. Values in this belt all fall below 3.5Φ, yet the decreasing grain size trend is still readily apparent.

The increasing median diameters on the outer part of the shelf result from a belt of relict and authigenic sediments in the 300-400 foot depth range. The sediments in this belt become coarser and more poorly sorted in the direction approaching the edge of the shelf. They often contain small percentages of gravel, but the sorting is very poor and their median diameters are less than for many areas of nearshore sediment.

The lowest median diameters are found in a zone not farthest from the shore or in the deepest water, but about midway out on the continental shelf. It would be expected that the sediments with the lowest median diameters would be those with the least percentage of sand in the sediment, but the relation does not prove true, and the lowest median diameters consistently lie shoreward of the least percent of sand fraction (see Figs. 6 and 7). The values of the sorting coefficient also show their lowest values consistently shoreward of the line of least percent of sand fraction. The logical boundary between the modern sediment cover of fine grained muds and the coarser relict sediments lies along the line of least sand percent, yet these statistical parameters do not follow this boundary, and are clearly very sensitive to the origin of the sand fraction. A small amount of relict origin sand is being mixed

into the cover of muds deposited on the middle of the continental shelf and displacing the boundaries of statistical parameters. The relict sand is clearly much less well sorted than the sand carried out and deposited with the silts and clays under modern conditions.

The chart of sorting coefficient values, Fig. 8, shows trends similar to that revealed by the chart of median diameters. The lowest values occur midway out on the continental shelf, and the axis of lowest values closely parallels the zone of least median diameters of sand fraction. Shoreward and seaward of this axis the sorting values increase irregularly but consistently and become less well sorted. Close to the shore, near the surf zone, many samples are better sorted than samples in slightly deeper water but this sorting only interrupts the trend slightly.

The sector of continental shelf between the shoreline and the branches of Soquel and Monterey canyons in the northeast corner of Monterey Bay has higher values of sorting coefficient than comparable areas to the west or south. A zero value denotes perfect sorting and high values mean poor sorting, with average values for sorting of sediment on the open continental shelf in this report ranging between .18 to .25. Within the northeast corner of the bay values consistently range .01 to .02 higher than on portions of the continental shelf to the west and south, and in the northernmost portion of the bay, off the mouth of Soquel Creek, the values are very much greater. This corresponds to the smaller median diameter of sediments found in this portion of the bay and appears to be the result of reduced wave action, as this area is partially protected from the prevailing northwesterly waves. Samples off the mouth of Soquel Creek also contain larger amounts of organic matter (shells) than is usual and this raises the sorting values, in addition to a visible

component of very coarse sand grains, usually comprising a few percent of the sample.

In comparing values of sorting from different areas in Monterey Bay, the majority of samples fall within the range of .18 to .25. There are almost no lower values and higher values are associated with areas of reefs, beaches, or shelf edge sediments. The following table compares the class limits of sorting from various formulae for obtaining measures of sorting, and the common occurrence of each class of sorting.

Table 2

Standard Deviation σ	Sorting Coefficient of Trask $S_o = \sqrt{Q_1/Q_3}$	Phi Sorting Coefficient of Krumbein $S_o = \frac{Q_{3\Phi} - Q_{1\Phi}}{2}$	Common Environmental Occurrence
0.0 ----	1.00 ----	0.0 ----	
Very Well Sorted			Most dune sands, many beach sands, many marine sands above wave base
0.35 ----	1.17 ----	0.23 ----	
Well Sorted			Most beach sands, most marine sands above wave base, many dune sands
0.50 ----	1.20 ----	0.26 ----	
Moderately Well Sorted			Most river sands, most continental shelf sands below wave base, most inland dune sands
0.71 ----	1.35 ----	0.425 ----	
Moderately Sorted			Many river sands, some continental shelf sands below wave base, many glaciofluvial sands
1.00 ----	1.87 ----	0.91 ----	
Poorly Sorted			Glaciofluvial sands
2.00 ----	2.75 ----	1.47 ----	
Extremely Poorly Sorted			
2.60 -----			

Modified from Friedman (1962)

Friedman (1962) determined the size classes for values of standard deviation and Trask sorting coefficient, and to determine the comparable size class values for Krumbein phi sorting coefficient, conversions were made from a table prepared in Krumbein and Pettijohn (1938). The Krumbein equation for sorting coefficient is the same as the Trask equation, except that it is written in logarithmic form, however, values obtained by each formula from the same set of data are systematically different and Trask and Krumbein values cannot be converted back and forth by a simple logarithmic conversion, necessitating the use of a table compiled by empirical computations.

The environmental interpretations of Friedman (1962) do not bear out well in this study, probably because of slightly different techniques used in sampling and determination of size frequencies. Beach samples are not well sorted because composite samples were taken of several beach strata, and marine samples appear to be better sorted because of the use of only the sand fraction in size frequency determination. However in the studies of Sayles (1965) and Moore (1965), their values of sorting of marine sediments to depths of 200 feet also clustered predominantly in the very well sorted and well sorted classes, closely comparable to values obtained in the present study. Only a few samples were obtained in depths less than 60 feet and these do not indicate any appreciable change in sorting values as the surf zone is approached, in accordance with the observations of Ingle (1966, p. 42) on samples taken through the surf zone.

The chart of skewness values is shown on Fig. 9. Skewness measures show a few rather widespread trends, the strongest being a negative skewness associated with the outer shelf sediments. A negative skewness value means that there is a greater spread of sizes coarser than the median

diameter than of sizes finer than the median diameter. The occurrence of extreme sizes of coarse material in the shelf edge sediments agrees well with trends found in the sorting and median diameter measures. The inner shelf sediments show greater variation, and on the north shore of the bay are widely variable, while on the east side of the bay they are much closer to neutral values. Along the east side of the bay many samples have values of .01 or less, both negative and positive, which suggest that the sorting over this area is essentially not skewed, being very closely adjusted to hydraulic conditions.

A chart of the modes from the submarine samples, Fig. 10, shows in nearly all traverses across the shelf a decrease in grain size of the modes away from shore almost to the edge of the shelf. The trend is interrupted only by a sudden increase in grain size at the outermost edge of the shelf, where in many cases the samples are bimodal, the coarsest mode being weak in all cases, but persistently present. The shelf edge sediment samples with bimodal sand content are also the samples which show greater percentage of sand fraction than neighboring samples. High sand percentage in the samples and coarse sediment particles show that these samples contain much sediment of relict origin, but the finer than sand size portion probably contains much deposited under modern conditions.

Polymodal samples are present in the reef area south of Santa Cruz, a condition due mainly to the presence of reef rocks. In the northeastern part of the bay, in the most sheltered portion, are several samples at depths of 100 feet or less, which are bimodal with a small mode at 2Φ and the major mode at 3Φ to $3\frac{1}{4}$Φ. The 3Φ to $3\frac{1}{4}$Φ mode is one developed by modern conditions, as determined by neighboring samples, while the 2Φ mode is not relatable to any modern process. The 2Φ mode is probably

caused from coarser sediment formed by a paleoshoreline, because, first, the bimodality is similar to the bimodal condition of the extensive relict deposits at the edge of the continental shelf, and second, the samples are from similar depths, and third, sample 1818 at about 100 feet depth and west of the other samples, has large well rounded pebbles of a cherty type that could not be derived from breakdown of the adjoining reefs and represents a littoral concentrate. The preservation of relict grains can be correlated with the relative protection from waves which inhibits good sorting of bottom sediments. Other shallow areas receive greater bottom agitation, and in deeper areas enough fine material appears to settle out in the quiet waters to cover the coarser sediments of earlier origin.

SEDIMENTARY ENVIRONMENTS

The surface sediments in Monterey Bay are roughly divisible into three types, (1) a coarse grained relict sediment type (with authigenic components) which is located in a band on the outer edge of the continental shelf, (2) a fine grained modern sediment type completely of modern origin covering a band on the middle of the continental shelf, and (3) a medium to coarse grained sediment type of modern origin in most areas but showing some relict components, located in the nearshore parts of the bay. The width of relict band of sediments at the edge of the shelf is 2-3 miles wide on the north side of the bay west of Soquel Canyon, and is much narrower on the east side of the bay, no more than a mile wide and probably less in most places. This is being overlapped by a cover of modern sediments that extends out to about eight miles from the shoreline. West of Santa Cruz and outside the bay this blanket extends no more than five miles from shore. The boundary of the relict and modern sediment covers is marked by changes in the values of median diameter

and sorting for sand fraction between depths of 250-300 feet, and indicates a thinning of the modern sediment cover, pinching out on the outermost edge of the shelf.

Data from the median diameter, sorting, modes and percentage of sand fraction all show that the sediments are predominantly in adjustment with the modern conditions of wave agitation, and presumably are of modern origin, except for a zone on the outer edge of the continental shelf. The fine grained sediments on the middle shelf are certainly of modern origin because the rise in sea level at the close of the Pleistocene would have dispersed any premodern sediments of this grain size. These sediments have been deposited in a cover thick enough to completely mask the coarser sediments formed during or before the last rise in sea level.

Premodern sediments are present on the outer shelf, modern sediments are present on the middle shelf and the surface sediments of the middle and inner shelf are well adjusted to modern conditions, so it would be expected that the cover of modern sediments thickens shoreward. This may not be the case, because influences of relict sediments are obvious along the north shore of the bay in depths of 100 feet. Thicker accumulation of sediment in deep water is a possible result of the dominance of very fine grained sediments (clays and silts) transported into the bay.

Once it is established that sediment is moving across the continental shelf and reaching the outer portions of it, it becomes possible to use the size frequency data to measure the size of sediment that is moving to any specified depth. Pipette analysis of the silt fraction of the samples demonstrate that the trends seen in the charts of sorting, modes and median diameter of the sand fraction continue into the silt sizes. With several composite size frequency curves calculated from both settling

tube and pipette analysis, the effect of this sorting is seen and measurable as modes, and are seen in all samples within the modern sediment cover. The presence of modes in a sample indicates that sorting, whether by wave agitation or by settling characteristics, preferentially favors the accumulation of a certain size range, and it follows that particles finer than this size range will be carried farther out to quieter areas, and that particles coarser than the size range are not carried abundantly to the site of deposition.

The dominant grain size mode was determined and plotted against depth of water (Fig. 11) for samples 1818, 1820-1823, 1829, 1868, 1872-1876, representing two traverses across the continental shelf in areas of similar exposure and in areas receiving sediment from rivers. The relationship between mode grain size and depth is simple and linear for sediments in the fine sand and silt size range. Sediment grains smaller than 3Φ are transported into deeper water and deposited, the size of the particle largely determining the depth of deposition. For example, sediment of $3\frac{1}{2}$Φ size (very fine sand) is preferentially deposited at 125-150 foot depth, of 4Φ size is preferentially deposited at 175-200 foot depth, and of 5Φ size at 250-275 foot depth. Below this depth the sorting of the silt fraction becomes much less, and the relationship of grain size to depth becomes obscure.

The size range of 3Φ to 6Φ appears to be the total range in which the relationship between depth and grain size holds up. Ingle (1966) plotted median diameters (= modes in his samples) against location in the surf zone, and most of the samples were in the 2Φ - 3Φ range. Comparing with the depth-mode graph obtained in this paper, 3Φ emerges as a size stable over a depth range of at least between 40 feet to 100 feet.

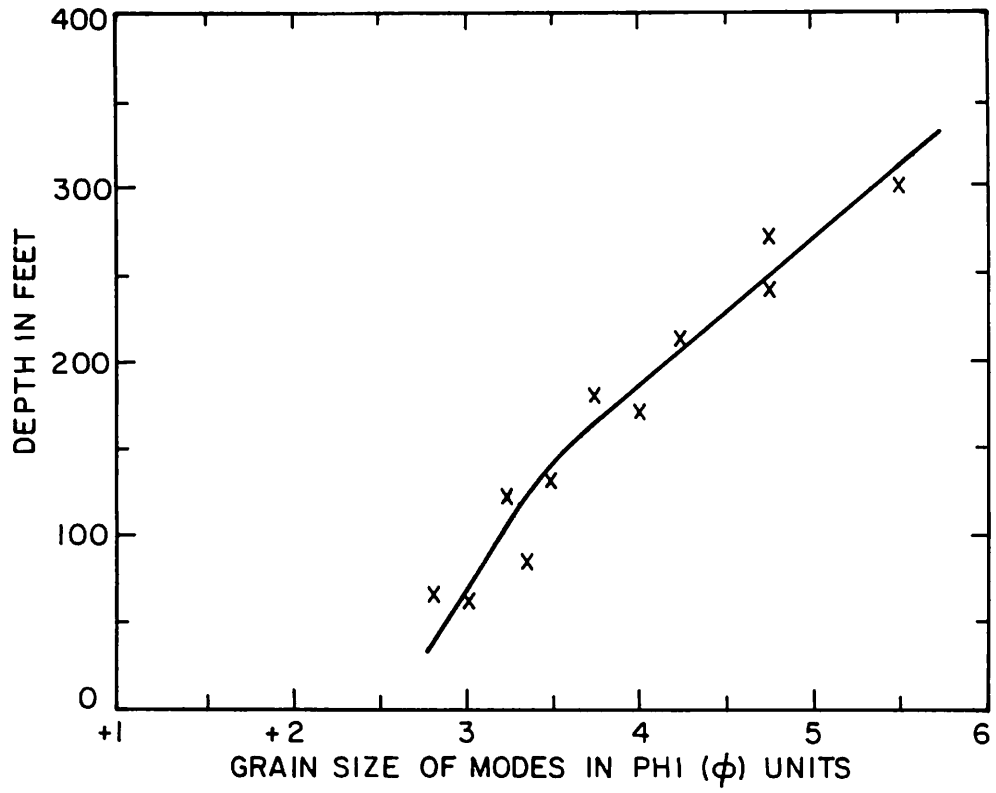

FIG.11 RELATION OF WATER DEPTH TO SEDIMENT MODES

The ability to transport silt is easily acquired by water masses, either by direct wave surge or by suspensions that flow downslope from areas of high turbulence, but the transporting of sand other than by currents is not so clearly established, and the wide exposures of the bay floored by fine sand raises the question of whether or not sand size material is consistently transported across the shallow portions of the continental shelf. If material as fine as 3Φ is concentrated within the surf zone, the mechanism of transporting sand out to the 100 foot depths, where the sediment finer than 3Φ accumulates, is unexplained. Studies by Ingle (1966) and Vernon (1966) on the dynamics of shallow marine sediment transport, demonstrate that within the zone of shoaling waves sediment transport is multidirectional and complex, and is not primarily in an offshore direction. Close to shore the direction of sediment transport, both seaward and shoreward of the breaker zone, is into the line of breakers, so that seaward of the line of breakers the sediment is moving in a shoreward direction.

Vernon (1966) investigated in deeper water and confirmed the existence of the null point, a dividing line between shoreward moving sediment moving toward the breaker zone, and seaward moving sediment away from the shore and breakers. The null point in the tests he conducted was in depths of between 10-20 feet, but this would vary depending on the strength of the surf. In tests using fluorescent tracer sands in depths near 30 feet, sediment moved distinctly in a seaward direction. On analyzing the movement of different size classes of fluorescent sand in 30 foot depths, the finest portion had moved seaward markedly, while the medium sizes remained fairly stationary, and the coarsest portion became less abundant without any observable reason for its dilution.

Vernon's experiment demonstrated several points relevant to the question of transport of sand size material in the shallow parts of Monterey

Bay. The sand sample was completely sorted into size classes which behaved differently in the same environment; the finer sand was transported seaward, and the coarser sand which was in adjustment with the average wave conditions remained in the original location. These characteristics are what is predicted to occur in the nearshore environments of Monterey Bay if sand is transported across the shallower depths, and sediment that is carried beyond the null point by rip currents, etc., will be gradually dispersed into deeper water. The grain size this is effective for is fine sand size, so the shallower parts of Monterey Bay (100 feet and less) are in adjustment with hydraulic conditions, and fine sand undoubtedly is transported below wave base and across these depths.

CLAY MINERALOGY

The detrital clay minerals were investigated for 28 submarine samples selected to include all depths and all portions of the area studied, and three river samples, from the San Lorenzo, Pajaro and Salinas rivers, and seven source rock samples. For each of these localities a portion of the sample was set aside for clay analysis before the sample was subjected to any procedural steps for other purposes. A suspension of the clay bearing sediment was made, and particles of size less than two microns were sedimented onto slides and X-ray diffraction records were prepared.

The clay mineralogy of the samples is uniform over all parts of the area under study. Montmorillonite is the dominant clay mineral of this suite, accompanied by lesser amounts of kaolinite and smaller amounts of mica. The proportions of the three clays is quite similar in all the submarine samples examined and in a comparison of peak heights, using the montmorillonite peak as a standard of 100, kaolinite has a peak height of 40-50 and mica has a peak height of 10-20 (see Fig. 12).

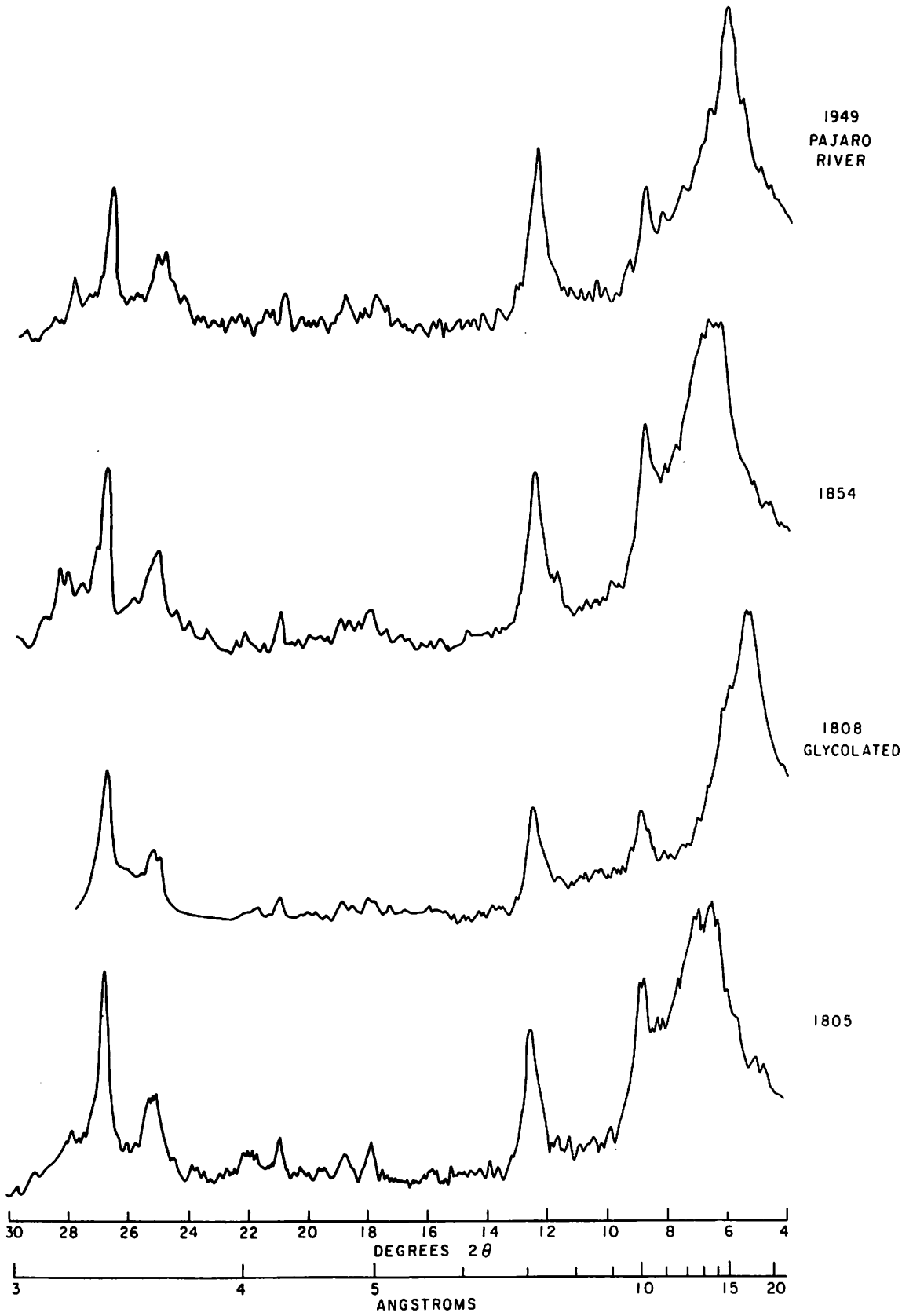

FIG 12 X-RAY DIFFRACTION DIAGRAMS (Cu Kα) OF MONTEREY BAY CLAYS

Clays of the Salinas and Pajaro rivers are similar to the submarine clays in composition and proportion. Clays from the San Lorenzo River contain the same minerals, however they are present in different proportions with kaolinite and mica producing peak heights proportionally as high as montmorillonite. Clay minerals from cliff forming Pliocene sediments on the northeast side of the bay in two samples, 1928 and 1932, are composed of montmorillonite exclusively, and in another sample, 1938, show montmorillonite and kaolinite in equal amounts. From the fine grained Pliocene cliff rocks at Soquel Point, 1924, and Point Santa Cruz, 1913, montmorillonite is the major component with secondary kaolinite, having $^{Ik}/_{Im}$ peak intensities of 20 and 40. From the very fine grained cliff rocks of the Miocene on the north side of the bay, two samples 1901 and 1904, show high silica content of quartz and cristobalite and equal peak heights for montmorillonite and mica, with no detectable kaolinite.

The mineral montmorillonite is identified from a dominant 13 - 14 Å peak which shifts to 17-18 Å upon treatment with ethylene glycol and shifts to 10 Å upon heat treatment at 550 ° C. for one half hour (Brindley, 1951). Kaolinite was identified from a peak at 7 Å and a companion peak at 3.5 Å which are greatly reduced with the above heat treatment, and not affected by soaking in warm dilute acid for one half hour, distinguishing it from the chlorite group. The mica type minerals produce peaks at 10 Å and 3.35 Å, of which the sharp 10 Å peak is not variable under differing humidity conditions, precluding the hydrous micas and indicating the true micas (Warshaw and Roy, 1961). Muscovite is probably the mica mineral present because it is a conspicuous component of the fine grained submarine sediment samples and because of its relative abundance in the bedrock surrounding the bay and this source of detrital mica is adequate

to create the 10 Å peak in all records.

The widespread uniformity and similar proportions of clay minerals in the submarine samples is very striking, as is their identical character to the clay mineralogy of the Salinas and Pajaro river samples. A few of the samples near the coast west of Santa Cruz suggest a slight enrichment in kaolinite, but the difference is slight and may not be significant. That the marine clays should be so close in composition to the clay content of the Salinas and Pajaro rivers, which provide 80% of the water entering the bay, is no surprise but that there is so little indication of departure from this rather uniform character in areas farthest from the rivers and closer to other local sources is somewhat unexpected. Kaolinite is more abundant in the San Lorenzo drainage area (Santa Cruz Mountains) than any other, yet the influence of this contributor is minimal, being masked by detritus from more distant sources. The possibility of the clays changing in composition once they enter the ocean, coming to a compositional equilibrium with the marine environment cannot be discounted, especially when it is known that the clay mineral glauconite is forming currently (Galliher, 1935), and that clay conversion can be very rapid (Grim, 1953, p. 344), but the similarity of marine and river samples makes it doubtful that this process affects the composition of the marine clays, apart from the formation of glauconite.

The importance of cliff erosion providing clay for deposition in the bay can be discounted because of the slowness of erosion and the large quantities of silt and clay laden waters that are discharged each year into the bay by the rivers. The source area for most of the clay can be determined as the Salinas and Pajaro rivers. These rivers have clay fractions identical with the clay fractions of the marine samples and both discharge large volumes of water into the bay at times of

flood. Contributions from the San Lorenzo River are not detectable and it is possible that this river carries relatively small amounts of clay due to the heavily forested nature of the watershed. Circulation of currents within the bay is sufficient to spread clay of the Salinas and Pajaro rivers in a blanket covering the entire bay and out at least as far as the open shelf off the west side of Ben Lomond Mountain (Skogsberg and Phelps, 1946).

The separate clay minerals cannot be identified with any distinctive source area. Montmorillonite forms by weathering in areas of low rainfall and alkaline soils (Keller, 1957). These conditions are prevalent in all the drainage basins of the rivers flowing into Monterey Bay and cannot be preferentially associated with either the granitic or sedimentary rock types. Kaolinite forms under conditions of complete leaching of metal ions, and because of its occurrence in the same proportions with montmorillonite in the Salinas River draining large areas of granitic rocks and the Pajaro River draining almost no granitic rock areas, it does not associate preferentially with any rock type. Much of the clay is probably derived secondarily from breakdown of existent sedimentary rocks, of which the clay mineralogy is seen to be heterogeneous but similar in composition to the river and marine clays, and is not helpful in provenance studies.

HEAVY MINERALOGY

The mineralogy of the heavy mineral fraction of Monterey Bay sediments is similar to the mineralogy of continental shelf sediments in the San Francisco region to the north, with the addition of very small amounts of the minerals tourmaline, staurolite and sillimanite. Most of the heavy mineral assemblage of the sediments consists of hornblende, augite and hypersthene, accounting for 75 percent to 90 percent of the assemblage in all but a few samples. In the remainder of the assemblage a much greater variation in composition occurs, and it is chiefly on the minor constituents that the mineral provinces are distinguished.

Hutton (1959) and Sayles (1966) have determined the heavy mineralogy for samples of Monterey Bay beach sands; Hutton's study being limited to a few samples but being very detailed in mineral identification. Beveridge (1960) and Spotts (1962), students of Hutton, have made heavy mineral studies on bedrock in the Monterey Bay drainage basins. Spotts (1962) confined his work to heavy mineral studies of the Coast Ranges batholith north of Monterey Bay, and Beveridge (1960) studied marine sediments of Eocene age in the Santa Cruz Mountains.

Hornblende colors range from pale green to dark green to brown. The category brown hornblende is used for grains that are completely brown, and gradations between brown and green were all counted with green hornblende. Very small grains of green hornblende are easily confused with tremolite-actinolite, because they are very pale green or colorless, often with a flaky or prismatic habit, so the few distinguishable grains of tremolite-actinolite were counted with green hornblende.

Brown augite, a category used by Hutton (1959) for heavy minerals in Monterey Bay sands, was not counted because of the rarity of truly brown

colored augite, the bulk of the augite being pale green. Epidote occurs as granular light to dark colored grains, and only rarely showed the bright green pleochroism it is noted for. The category for clinozoisite is used for colorless grains with the morphology of epidote grains with very low angle of extinction and positive optic axial sign. Pumpellyite was searched for but could not be distinguished in grain form.

Lawsonite, a mineral of great value in tracing sediments of Franciscan Formation origin, was distinguished by its cleavage, and optic axial properties when they could be determined, but pleochroism was usually lacking and was very pale colored or colorless. The few grains of jadeite were distinguished by grain morphology and by high dispersion of the optic axis.

SELECTIVE SORTING

The composition of mineral suites are initially controlled by the composition of the source rock from which they are derived, but during sediment transport the proportions of minerals present in the suite can be changed by selective sorting (see Pettijohn, 1949; van Andel, 1959; etc.). Selective sorting concentrates mineral grains with similar hydraulic characters and usually enriches the sediment in some mineral components. The commonest cases of selective sorting occur when a mineral has a high specific gravity, such as magnetite, but also occurs for minerals of restricted size range or similar shape. A familiar example of the later cases are zircon rich mineral suites, which are usually the result of selective sorting which concentrates minerals of small size and high density. To determine the influence of grain size on the composition of heavy minerals of the samples studied, plots are prepared showing mineral percentage versus the median grain diameter of the sample.

Disregarding the tendency of the points to be clustered, which is a function of the number of samples collected in any size range of sediment, the scatter of points on Figs. 13 and 14 show but little influence of grain size on mineral percentage. Mineral percentages in this study are mostly the result of factors other than size sorting, a conclusion which agrees with the results of Hutton (1959) who determined the mineral compositions of different size fractions of some samples from Monterey Bay. A possible variant to this relationship is the case of apatite which may be partially size controlled, but the mineral percentages are too low to be certain. Zircon, a mineral of small crystal size and high density, is commonly enriched by selective sorting through the process of residual concentration, but within the sediments of Monterey Bay there is no indication of this occurring.

Selective sorting by means of grain shape, rather than size or density, is a noticeable factor in the marine sediments. The most obvious example is mica, which has a thin plate-like shape that makes it susceptible to transport with finer grained sediment, and for this reason it is not used in setting up heavy mineral provinces. Apatite appears to be selectively sorted, possibly due to its tabular habit. Hornblende is moderately enriched in a few of the finest grained marine samples (see Fig. 15) and visual examination of mineral grains from these samples shows that small hornblende grains commonly occur in the form of flakes, which are hydraulically lighter than rounded grains. The flaky habit of fine grained hornblende perhaps accounts for its concentration in very high percentages in the nonopaque nonmicaceous portion of the heavy mineral fraction of Monterey Fan deep sea sediments.

In the sediments of Monterey Bay density sorting and size sorting are not significant, but the shape of mineral grains does exert a

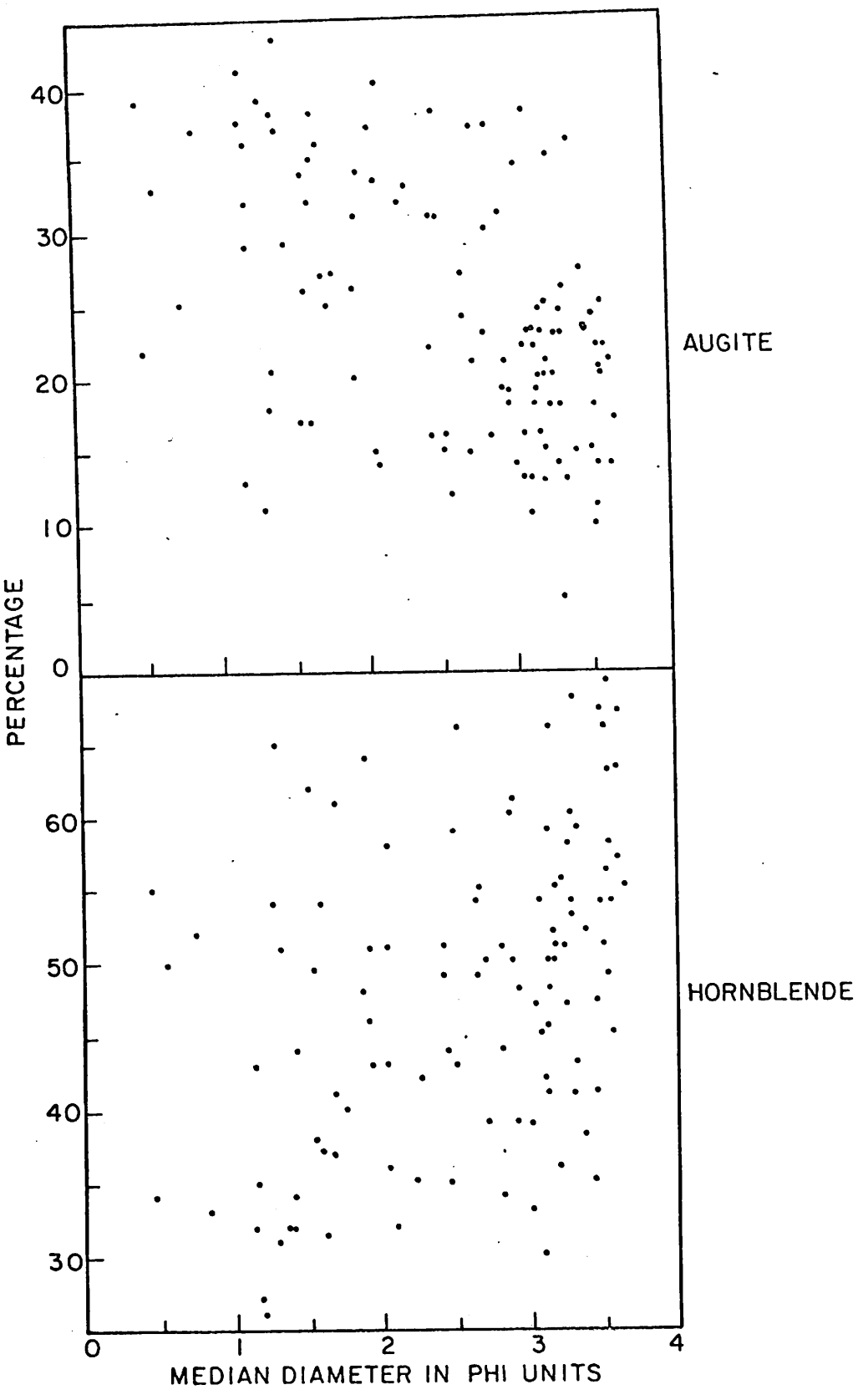

FIG. 13 MINERAL PERCENTAGE vs MEDIAN DIAMETER OF SAMPLE

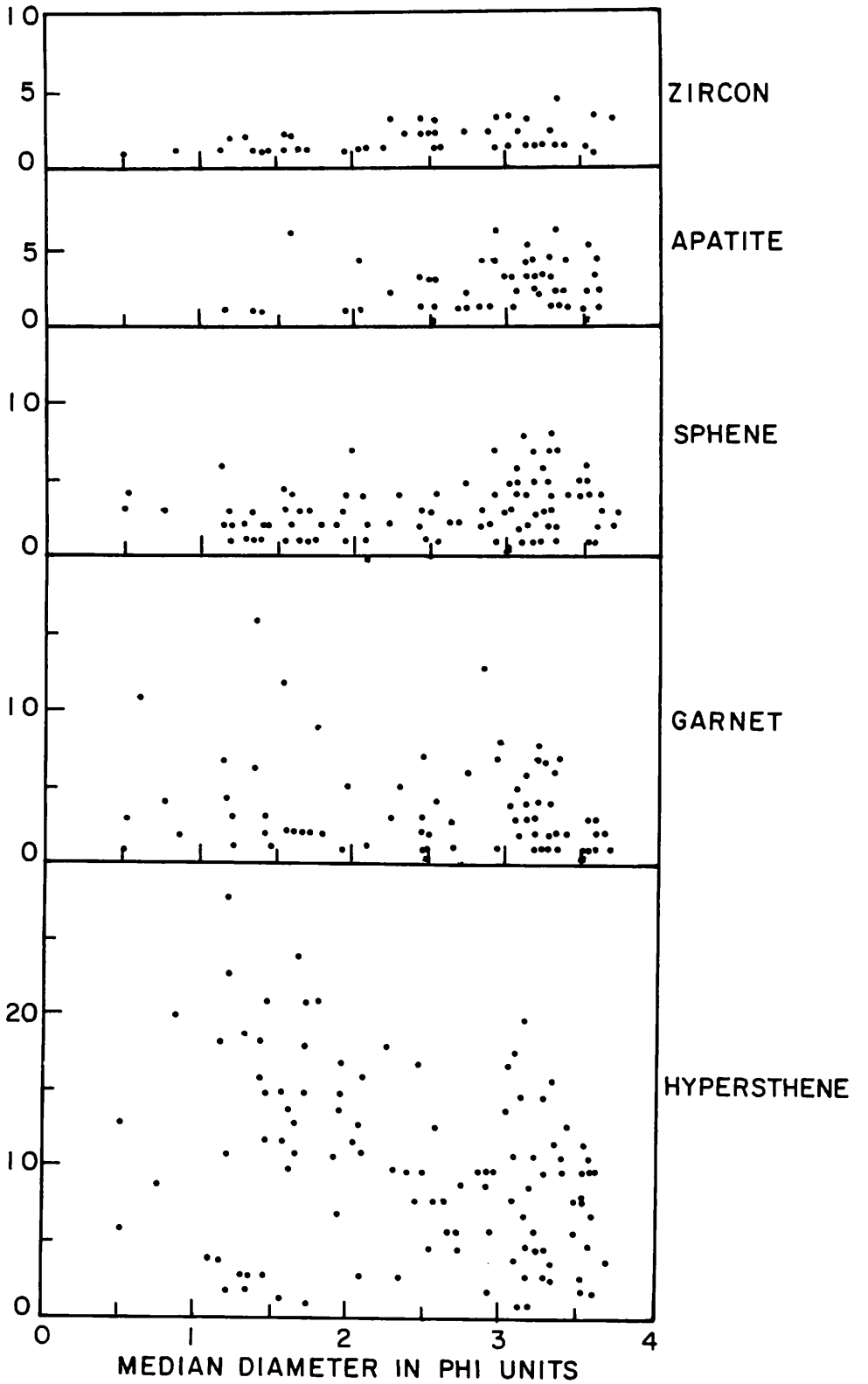

FIG. 14 MINERAL PERCENTAGE vs MEDIAN DIAMETER OF SAMPLE

noticeable effect on mineral concentrations in the fine grained muds. Selective sorting is usually concentrated in coarse grained sediments which are associated with strong wave or current agitation (for examples see Sayles, 1965; Galehouse, 1967). The probability of encountering selective sorting by grain shape has been overlooked because few heavy mineral studies have been made on fine grained sediments. When comparing heavy mineral suites from fine grained and coarse grained sediments for provenance, the hydraulic effects of grain shape must be considered.

MINERAL PROVINCES

To determine the mineral provinces in Monterey Bay mineral percentages for each mineral in the heavy mineral fraction are plotted on a map of the bay, and the ratios of hornblende/augite and augite/hypersthene are similarly treated. Areas of similar values are outlined on the resulting charts. Boundary lines on the separate charts are combined to produce the outlines of the several heavy mineral provinces distinguished. Contouring the charts was attempted, but the mineral percentages vary a great deal from sample to sample and the results of contouring were uninstructive. In an attempt to smooth out sample to sample variation the percentage value from each sample was averaged with the two closest (geographic) samples, but the averaging procedure obscured sharp mineral breaks and overemphasized the importance of samples with highly variant composition, and the technique was used in only a few cases. The charts of the mineral percentage values used in distinguishing the mineral provinces are shown in Figs. 15-27, and the resultant chart of the heavy mineral provinces is shown in Fig. 28.

Figs. 19, 22, and 23 show a distinctive nearshore suite, Province 1, on the beaches and in the nearshore off the mouth of the Salinas River,

and in the bedload of the Salinas River, having a relatively high garnet and brown hornblende content and a low hypersthene content. Province 1 extends offshore to about 100 foot water depth and extends from the head of Monterey Canyon to the town of Monterey. On the west, Province 1 intergrades into an offshore suite through a zone about two miles wide.

Province 3 (Fig. 24 and 25) is a glaucophane rich province in the northeastern part of the bay, extending from the shore to the edge of the continental shelf in the region off the mouth of the Pajaro River. The southern boundary of the province lies entirely along the rim of Monterey Canyon, while the north boundary is gradational, and extends northeastward from the head of Soquel Canyon to the shore. Values of several minerals show a slight change across this north boundary, but the position of the boundary varies for different minerals and includes a mixing zone 2-3 miles wide. Mineralogically Province 3 is defined by the presence of minerals characteristic of the Franciscan Formation, and the minerals lawsonite and jadeite are restricted to it.

Along the north margin of the bay is a high augite, low hornblende suite, shown in Figs. 15 and 17, forming Province 5. This suite is confined to beach samples and was not detected in the marine samples which were taken at depths of 50 feet or greater. On the east it grades into beach samples of the adjoining province.

Separating these three provinces are two areas without distinctive minerals in the heavy mineral suite, which form Provinces 2 and 4. Province 2 lies west of Province 1 in the south part of Monterey Bay, and is bordered on the west and north by Monterey Canyon. Province 4 lies between Provinces 3 and 5 in the northern half of Monterey Bay. It includes all the submarine samples west of Province 3, extending completely

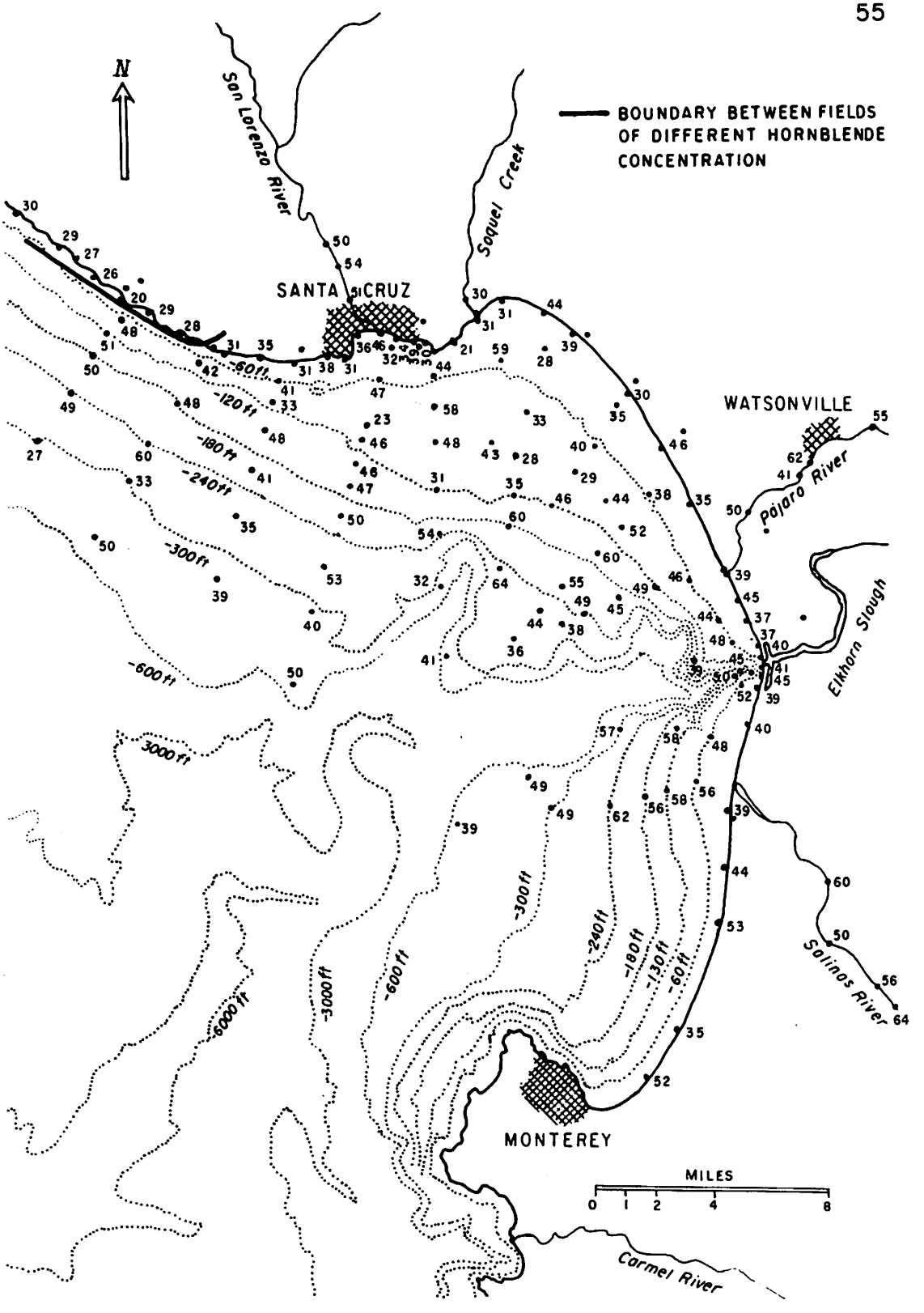

FIG. 15 CHART OF GREEN HORNBLENDE PERCENTAGES

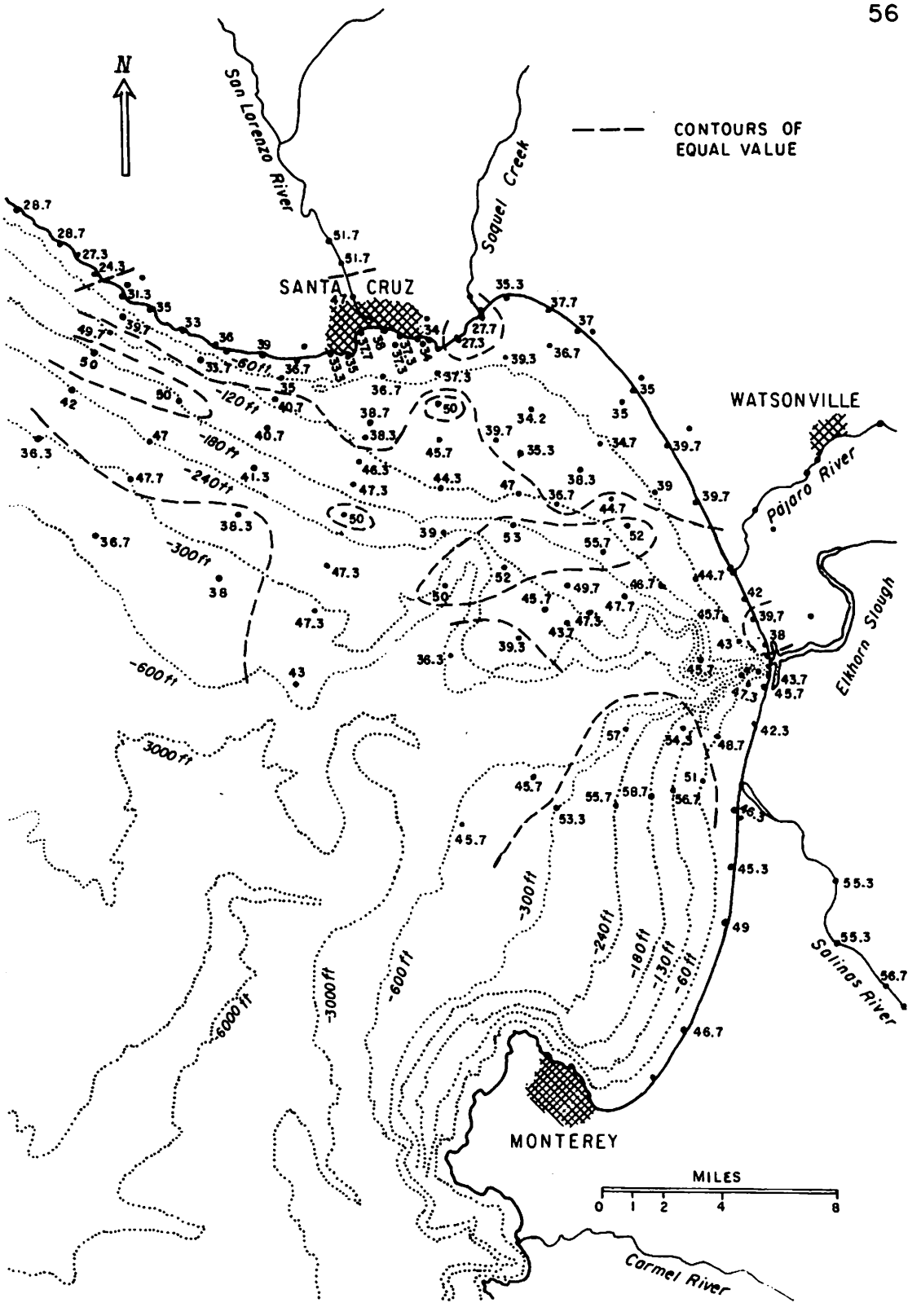

FIG. 16 CHART OF AVERAGED VALUES OF GREEN HORNBLENDE

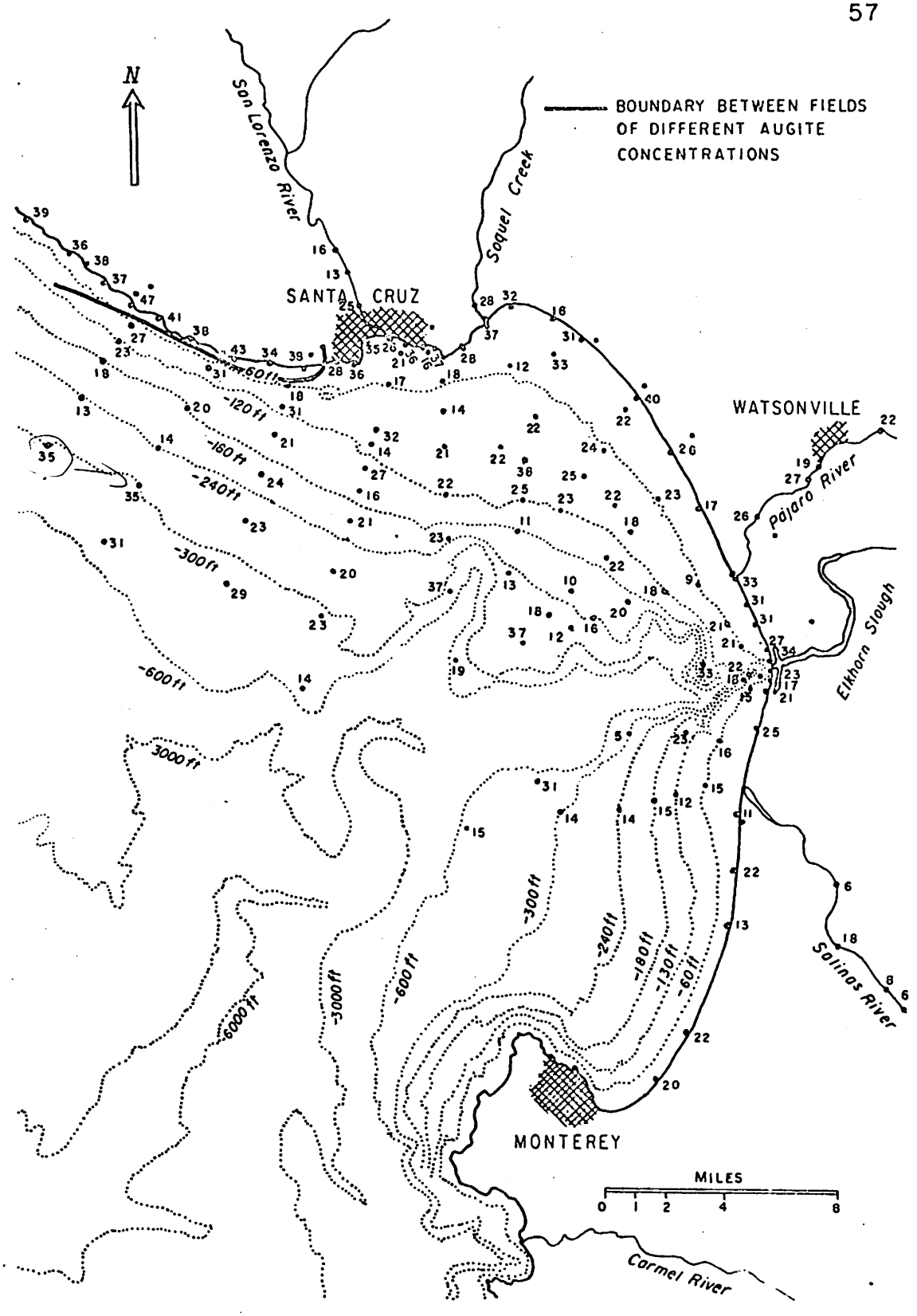

FIG. 17 CHART OF AUGITE PERCENTAGES

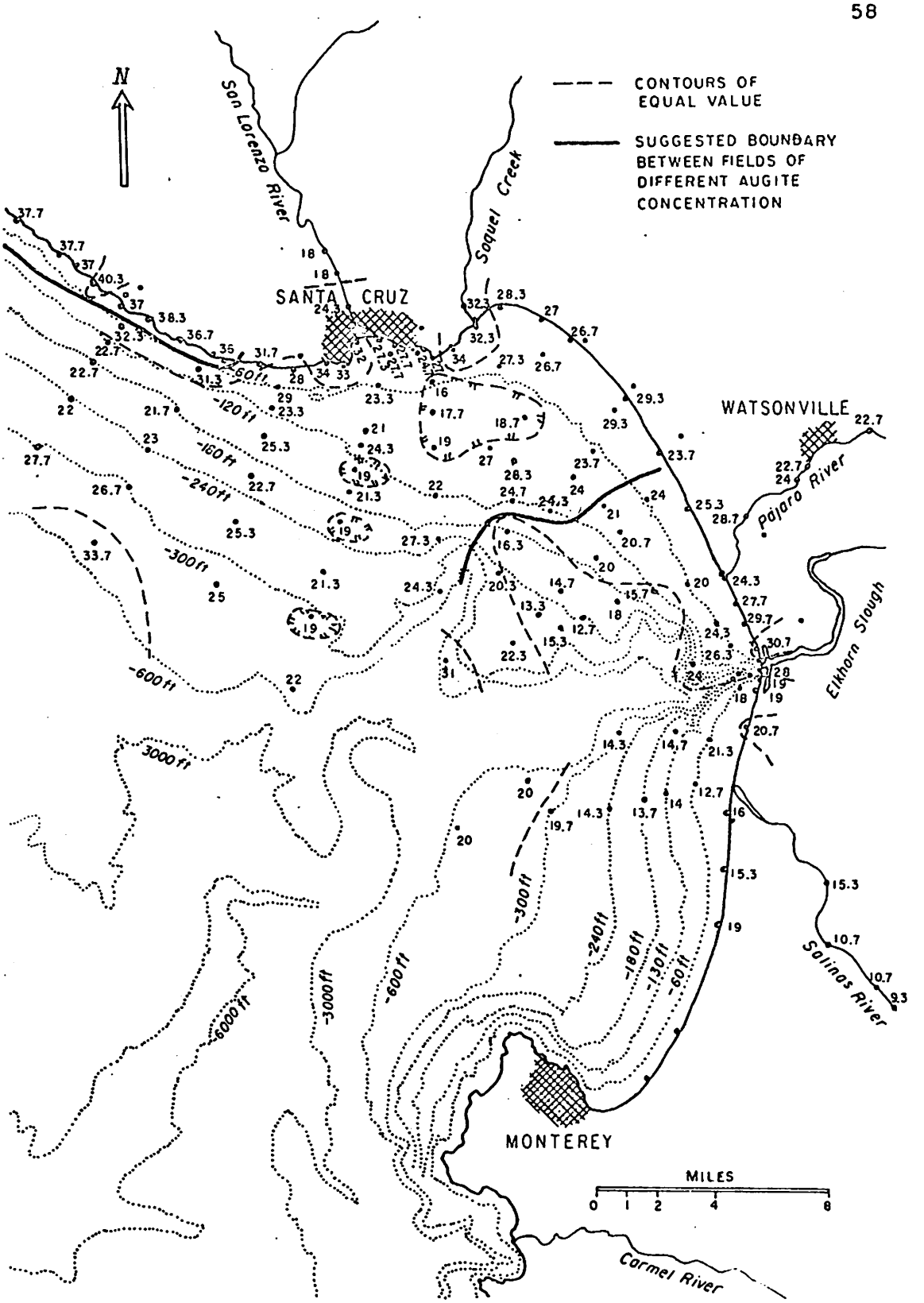

FIG. 18 CHART OF AVERAGED VALUES OF AUGITE

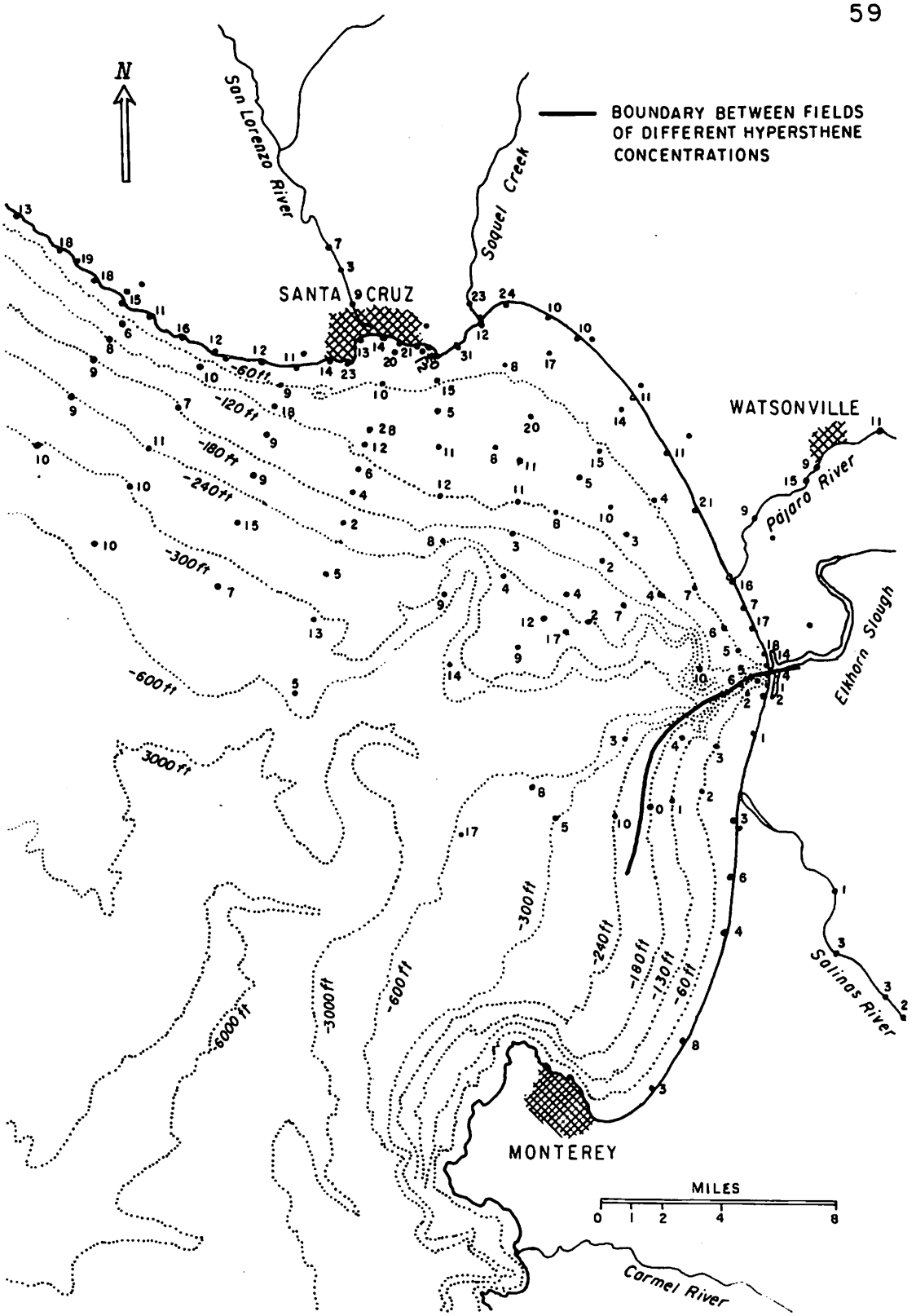

FIG. 19 CHART OF HYPERSTHENE PERCENTAGE VALUES

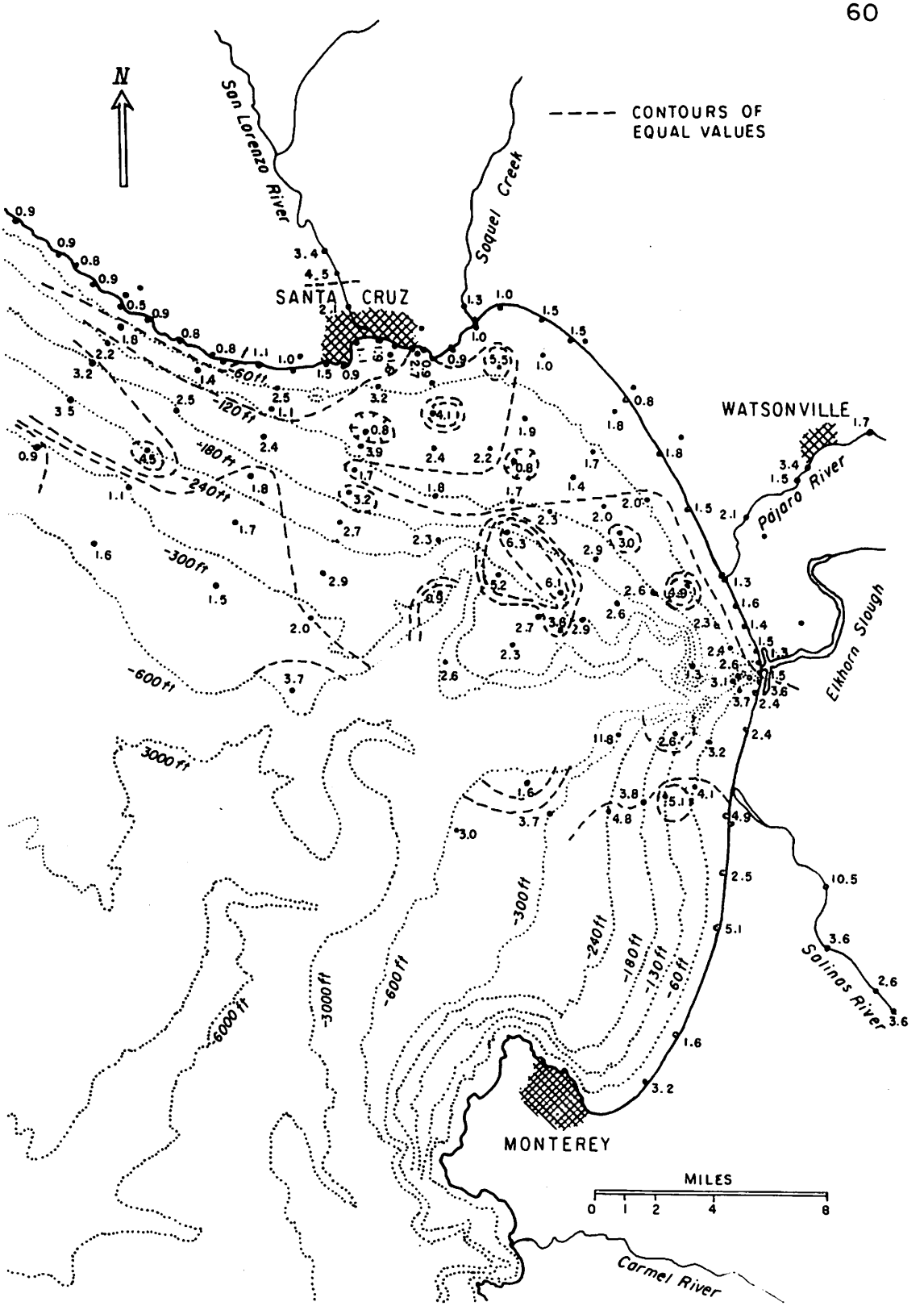

FIG. 20 CHART OF THE HORNBLENDE/AUGITE RATIO VALUES

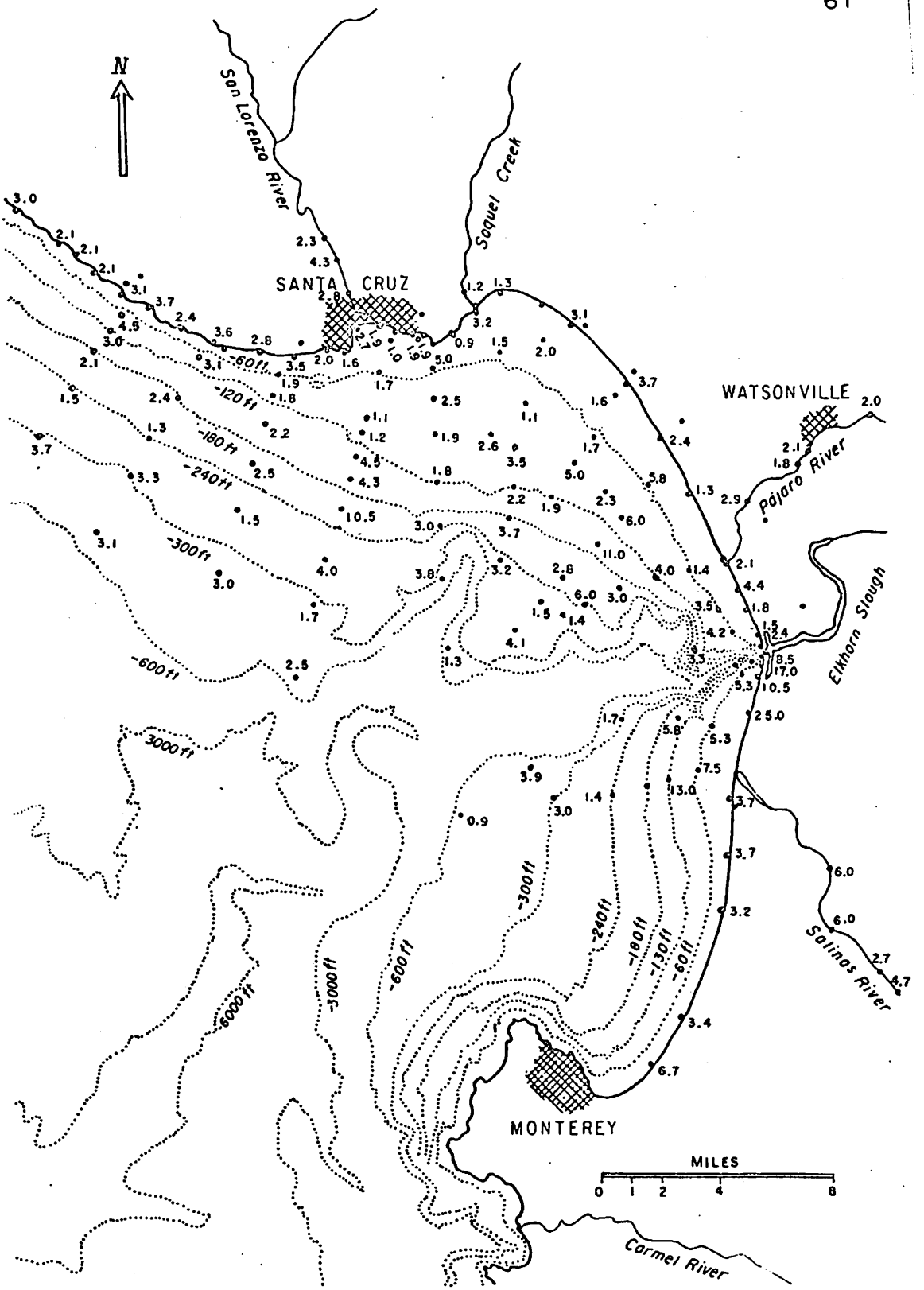

FIG. 21 CHART OF THE AUGITE/HYPERSTHENE RATIO VALUES

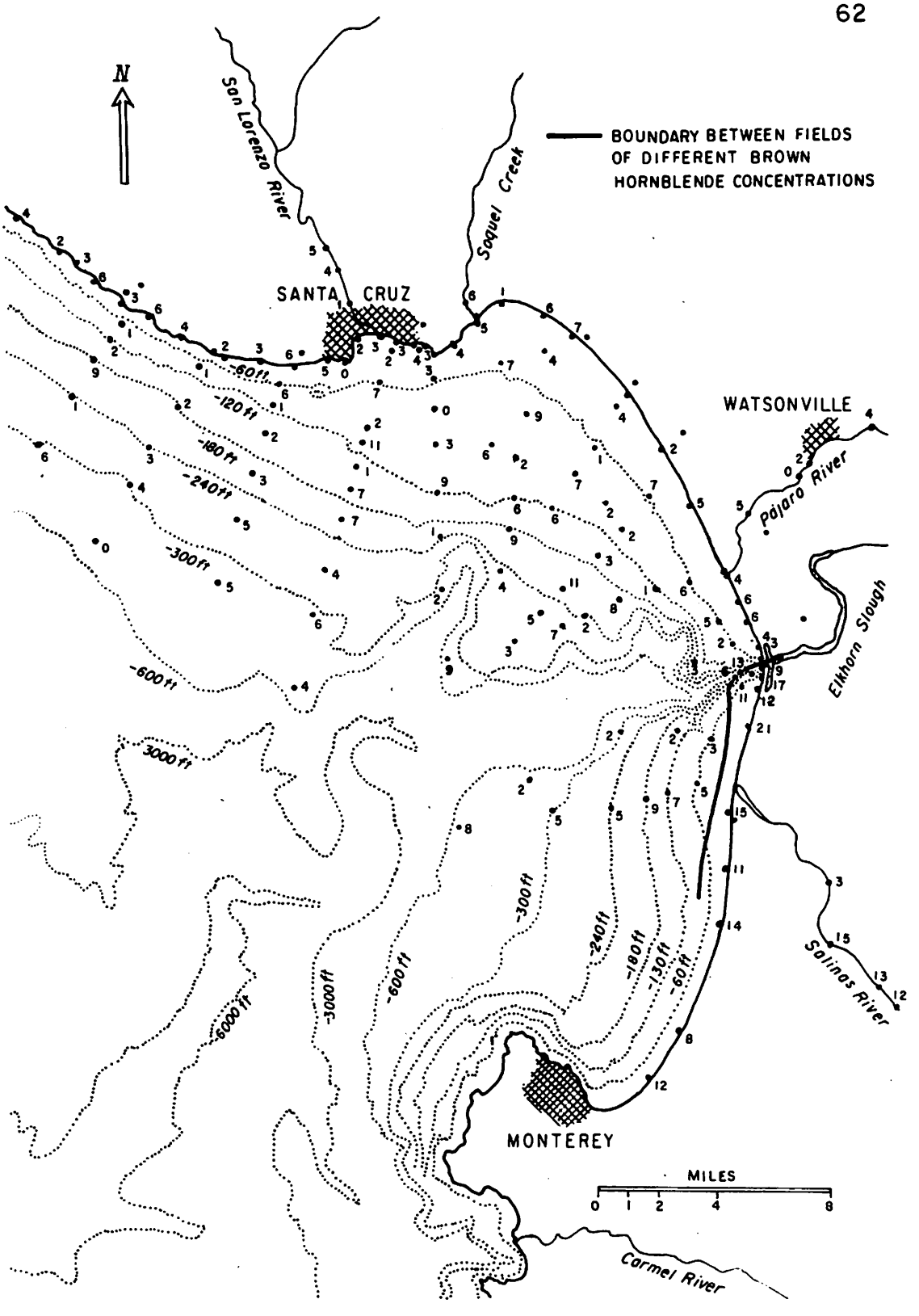

FIG. 22 CHART OF BROWN HORNBLENDE PERCENTAGES

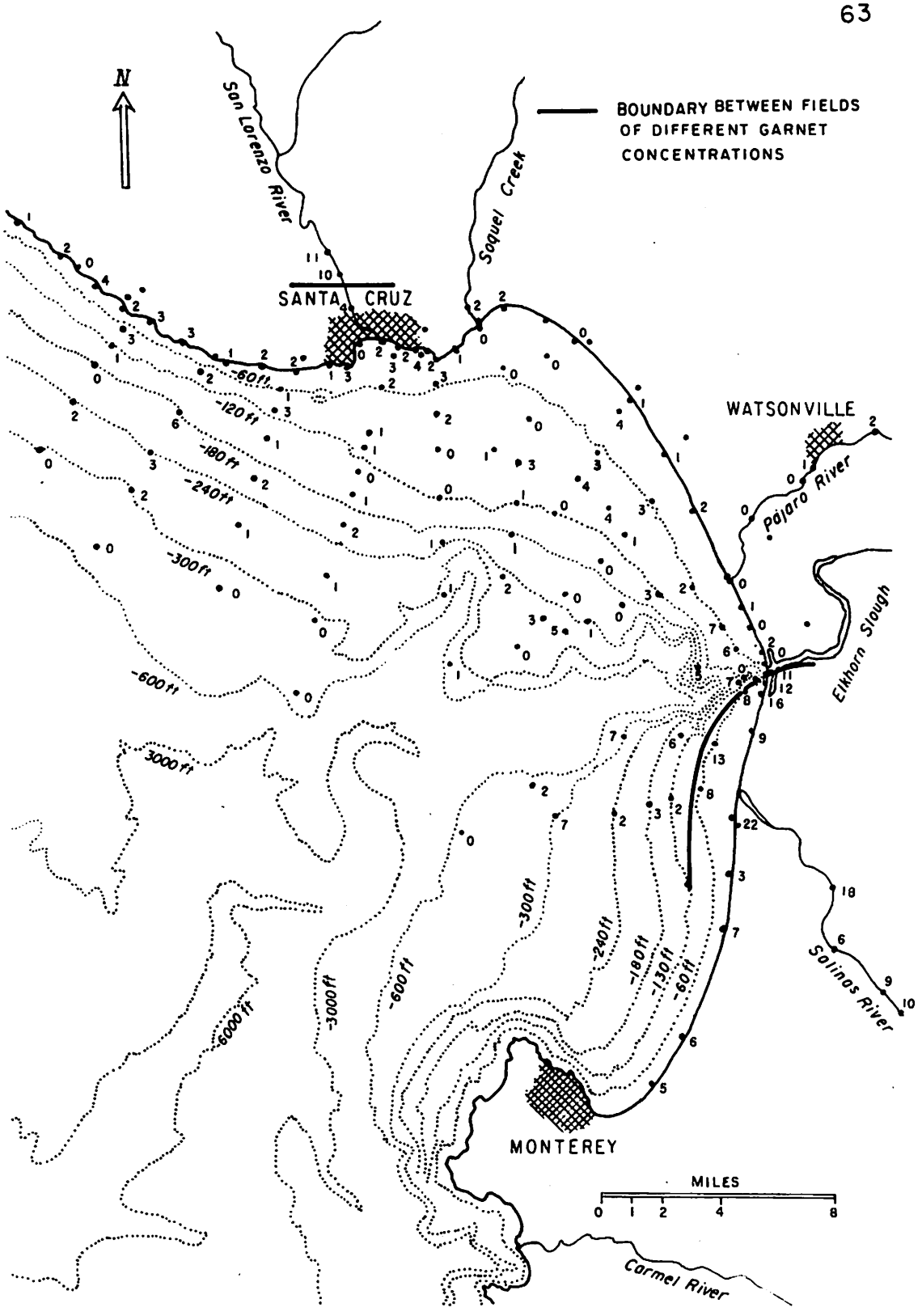

FIG. 23 CHART OF GARNET PERCENTAGES

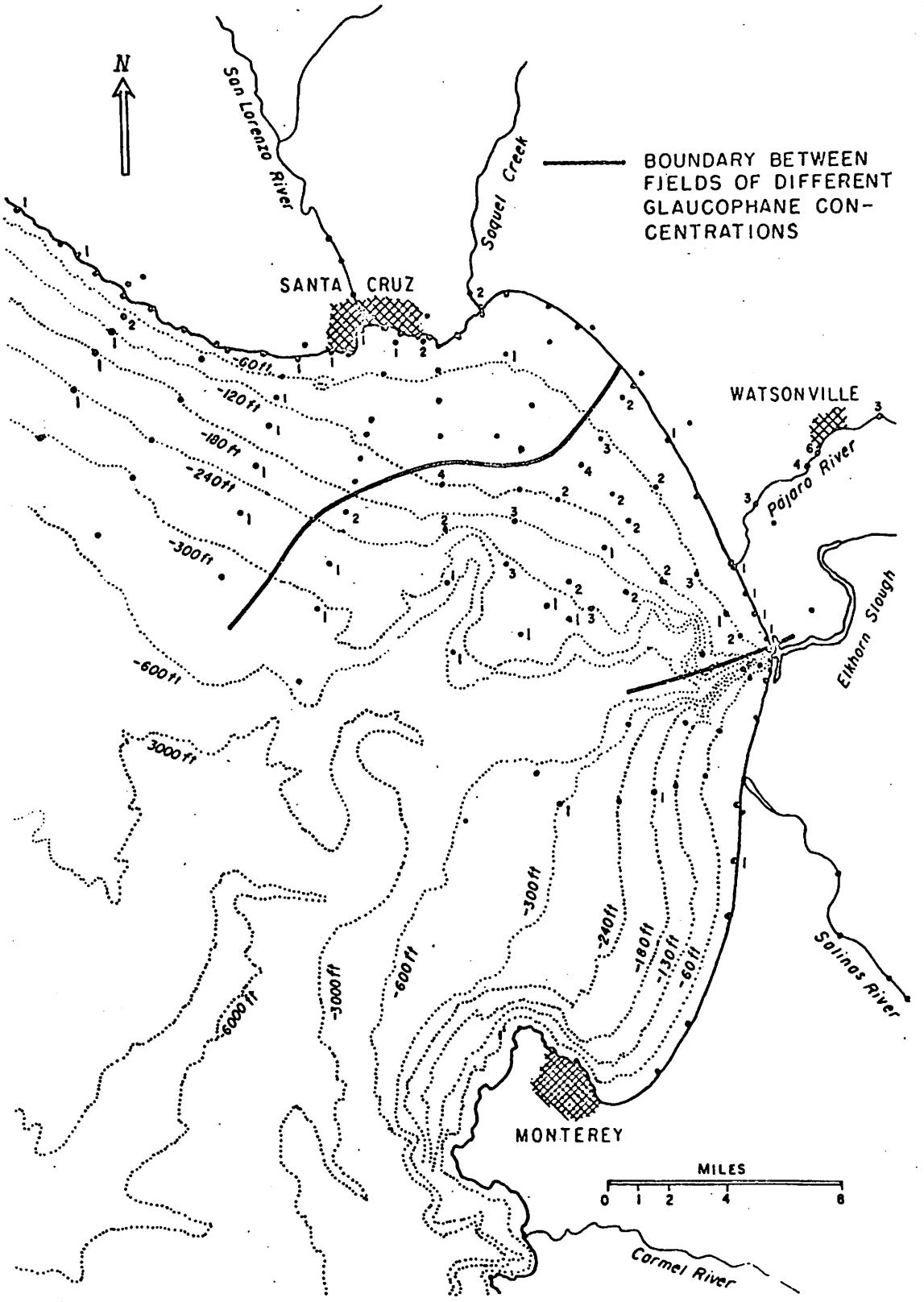

FIG. 24 CHART OF GLAUCOPHANE PERCENTAGES

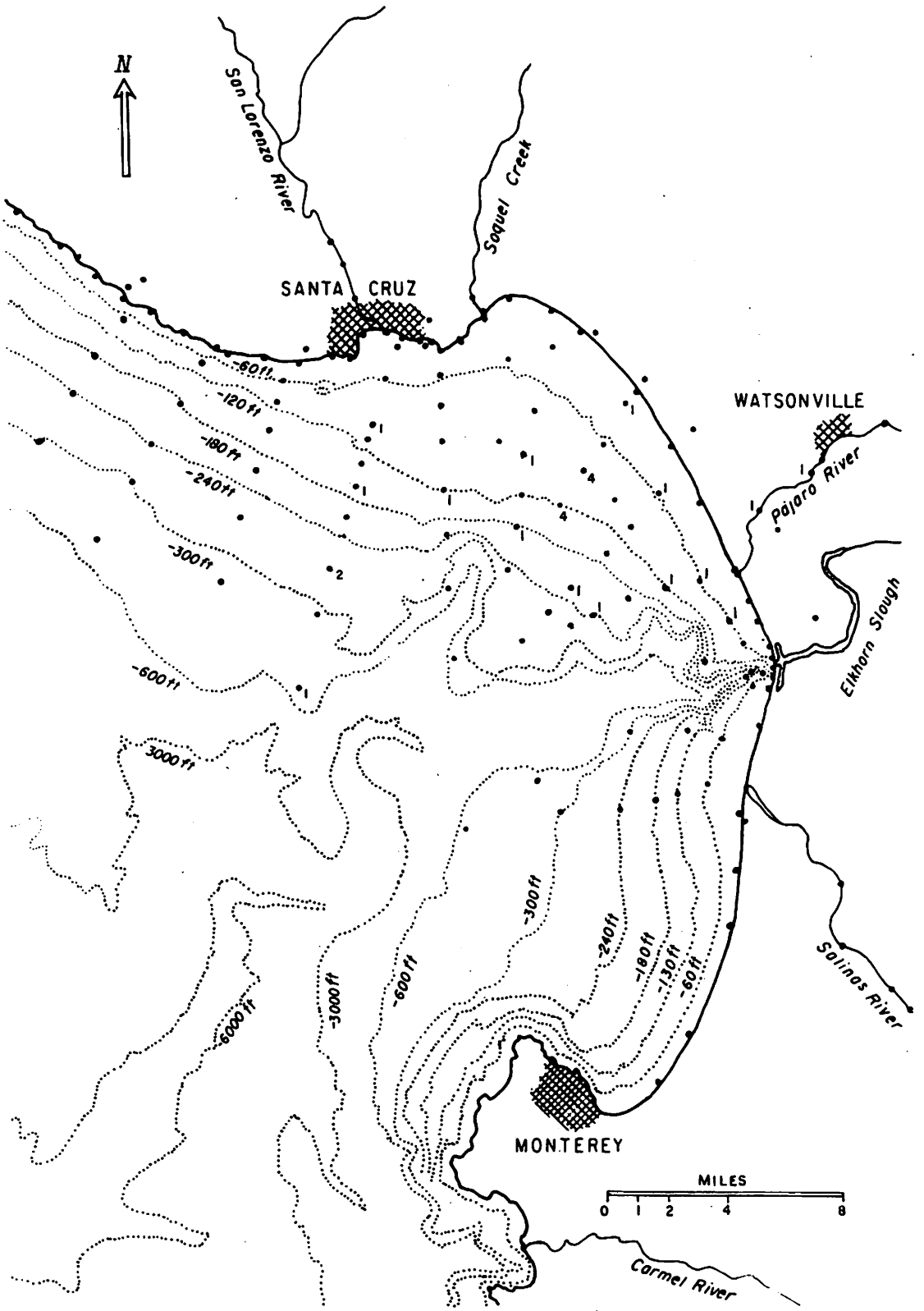

FIG. 25 CHART OF LAWSONITE AND JADEITE PERCENTAGES

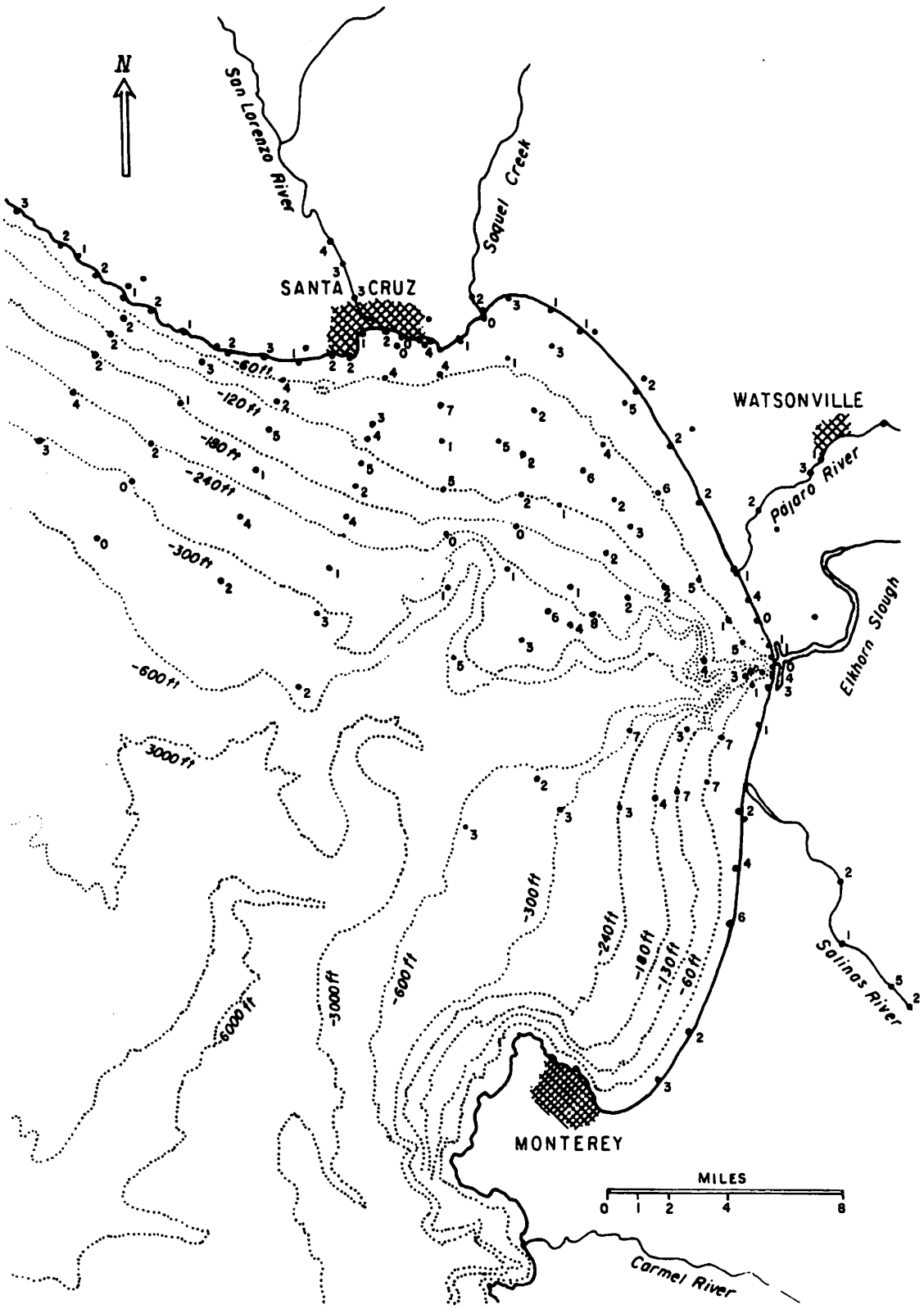

FIG. 26 CHART OF SPHENE PERCENTAGES

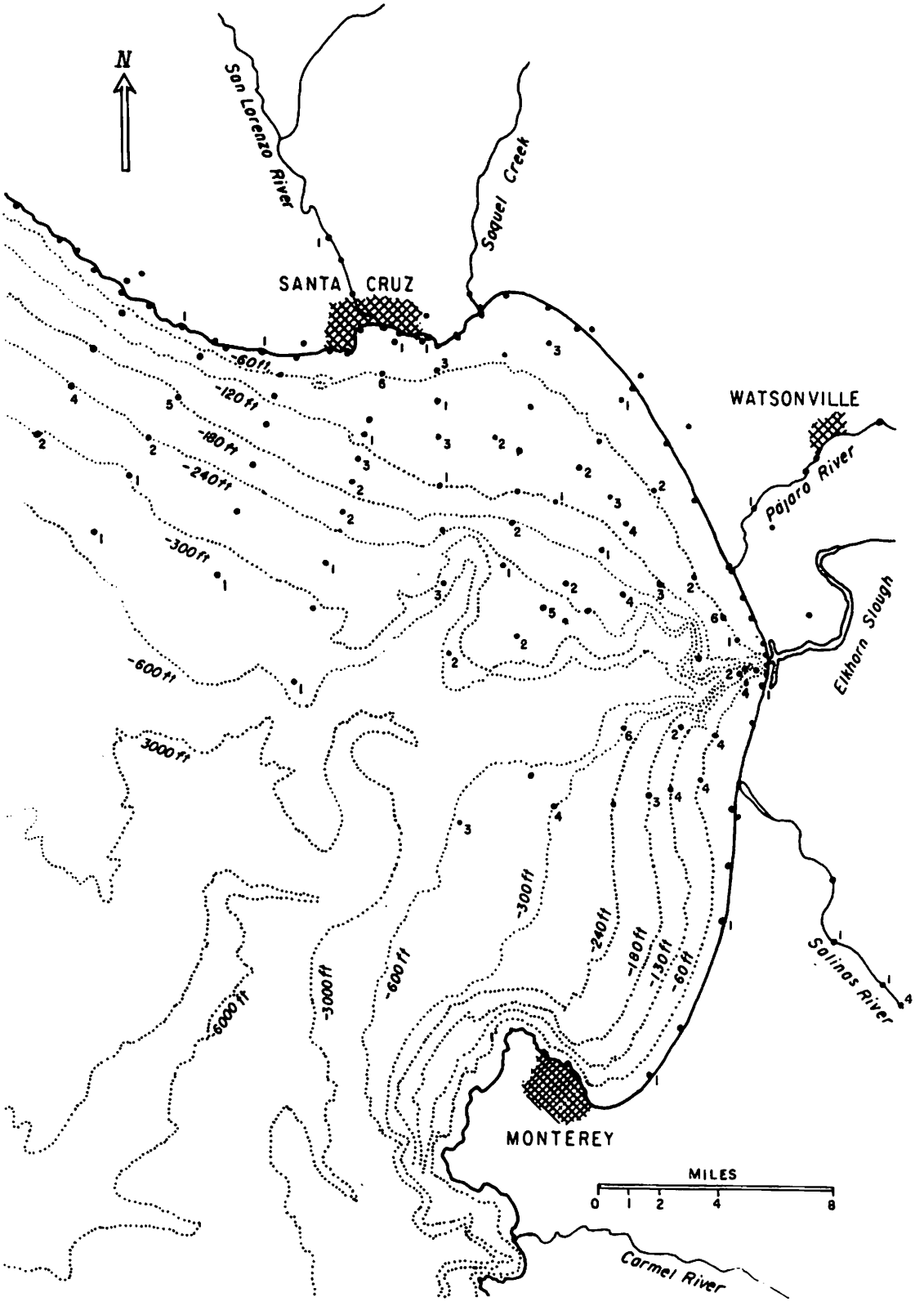

FIG. 27 CHART OF APATITE PERCENTAGES

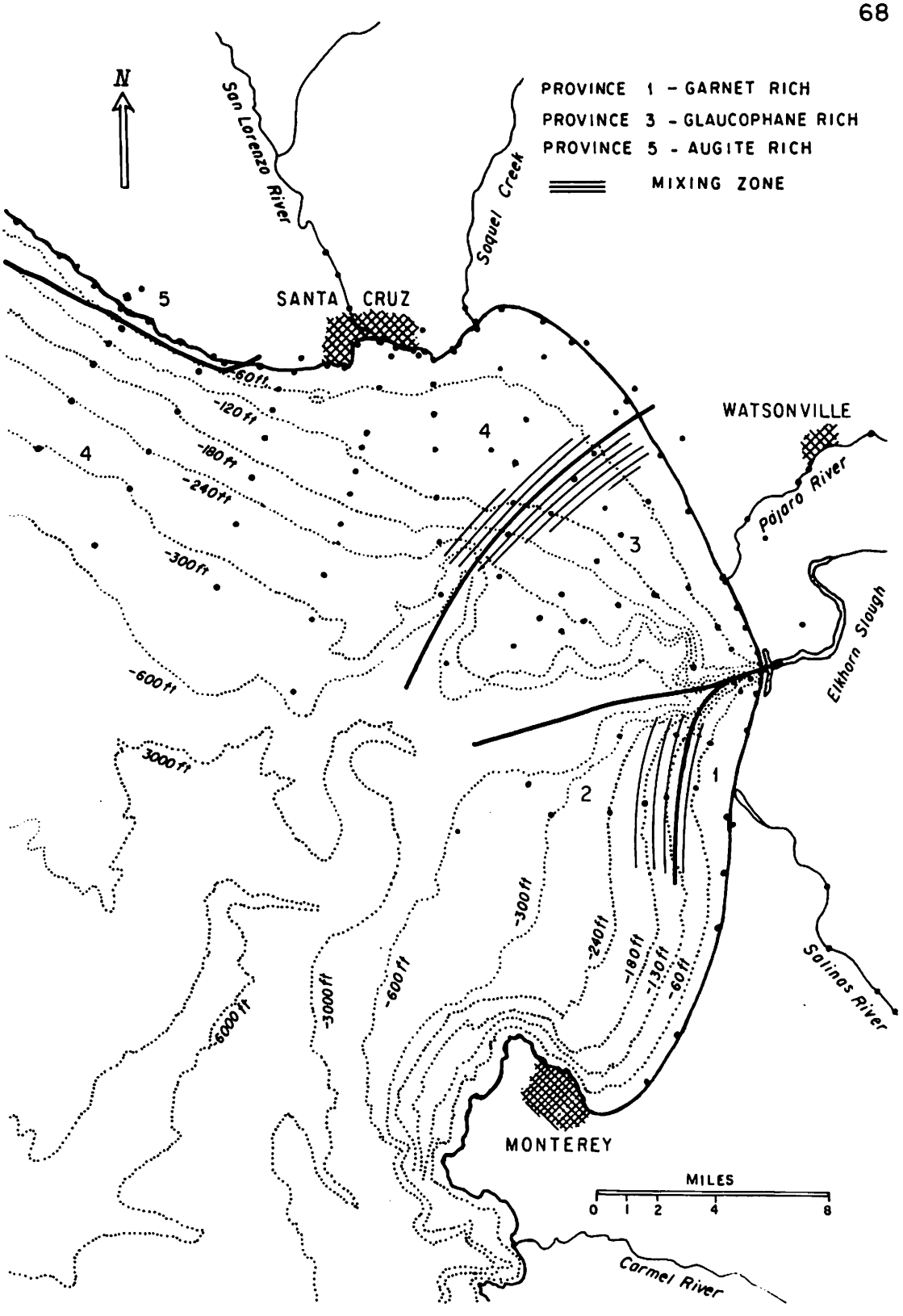

FIG. 28 HEAVY MINERAL PROVINCES

across the continental shelf, and contains considerable heterogeneity in composition.

The heavy mineral provinces are distinguished by the following characters. Province 1 is defined as a garnet rich province, and averages about 10 percent garnet in composition. Province 3 is a glaucophane rich province with an average of 2 percent glaucophane, and has the minerals lawsonite and jadeite restricted to it. Province 5 is an augite rich province with 40 percent augite, twice the augite content of other provinces. Provinces 2 and 4 have no distinguishing minerals and are geographically defined, separating provinces with distinct mineral components, but can be mineralogically distinguished by their lack of the index materials present in the other three provinces.

For comparisons of mineral provinces, the average or mean composition of the province is the best descriptive guide, because it shows all the components in numerical form. The average compositions of the mineral provinces in Monterey Bay are given in Fig. 29, and were calculated by averaging all the marine and beach samples within the province. For Province 1 the river samples were also included because they form an important part of the province. The bulk heavy mineral compositions of the provinces are rather similar, except for Province 5, and the ratios of the three dominant minerals in Provinces 1 - 4 roughly fit the ratio of 4:2:1 for hornblende, augite and hypersthene respectively. In Province 5 augite is the dominant mineral, and the order of mineral abundance is augite, hornblende and hypersthene. The average heavy mineral compositions vary surprisingly little despite the origins of the sediments in greatly different geological terrains, and it is by the minor constituents that they are distinguished. This shows how easily a distinctive suite can lose its identity by either selective sorting or by mixing with other sediment.

	Province 1 - Garnet Rich	Province 2	Province 3 - Glaucophane Rich	Province 4	Province 5 - Augite Rich
Hornblende - Green	48.6	54.0	45.1	40.7	28.0
Hornblende - Brown	10.7	5.0	4.7	4.0	3.7
Oxyhornblende	1.7	1.9	3.6	4.4	2.0
Augite	16.7	16.6	22.5	26.1	40.1
Hypersthene	2.9	6.0	9.0	12.5	15.2
Epidote	2.2	4.6	5.5	4.9	5.7
Garnet	10.9	3.6	2.0	1.4	2.0
Sphene	3.3	4.0	2.9	2.4	1.7
Zircon	1.3	1.0	0.5	0.9	0.4
Apatite	1.2	3.1	1.5	1.0	0.1
Clinozoisite	0.1	0.3	0.4	0.5	0.4
Detrital Carbonate	0.2		0.1	0.4	0.1
Glaucophane		0.3	1.6	0.6	0.2
Lawsonite			0.5	0.1	
Tourmaline			0.1		0.1
Staurolite		0.1			

FIG. 29 AVERAGE COMPOSITIONS OF THE HEAVY MINERAL PROVINCES

PROVENANCE

The heavy mineral provinces can readily be associated with source areas in some cases, having distinctive mineral components, or lying adjacent to known sources of sediment. Province 1 is derived from the Salinas River because (1) the mineral suite present in the river is identical with the mineral suite of the submarine samples, (2) the province is located adjacent to the mouth of the river, and (3) high percentages of garnet are common to both the river and the province. The province represents the spread of sediment outward from the river mouth, but the linear extent of the province along the beaches shows that most sediment dispersal occurs by longshore drift, both north and south, with lesser quantities spreading seaward off the beaches. The spread of Salinas River sediment is cut off on the north by the head of Monterey Canyon which acts as a sediment trap. The effectiveness of this barrier to sediment movement can be seen in the distribution of garnet and glaucophane on opposite sides of Monterey Canyon. These mineral change in abundance abruptly at the canyon head, glaucophane being nearly restricted to the north side, and abundant garnet being restricted to south of the canyon.

Province 1 is similar or equivalent to the hornblende-garnet suite outlined by Galehouse (1967) in the Pliocene deposits of the upper Salinas River Valley. These two suites are both garnet rich and are derived from the same source areas. Drainage patterns in the Salinas Valley have changed since the Pliocene (Baldwin, 1963), but the work of Galehouse shows that the source areas have been in existence since then, and undoubtedly the composition of the mineral provinces has remained constant.

The continental shelf in southern Monterey Bay is an isolated platform, cut off on the north and south, and has no source of sediment other

than the Salinas Valley and Monterey Peninsula. Monterey Canyon blocks sediment transport from the north and the precipitous sea floor south of the Monterey Peninsula blocks sediment transport from the south, therefore the restricted occurrence of the garnet rich suite off the mouth of the Salinas River is hard to explain. The existence of Province 2, which has a mineral composition that is dissimilar to any of the sources that could have supplied sediment to the area, is equally hard to explain. The difference in composition between Province 2 and sediments of the Salinas River is fairly large, and the difference in composition between Province 2 and the heavy mineral suites of the quartz diorites and related rocks of the Monterey Peninsula is even greater. Spotts (1962) determined that quartz diorites and related rocks of the Coast Ranges have heavy mineral suites characteristically containing sphene, zircon and apatite. There are several small drainage basins near the town of Monterey that drain exposures of Miocene sedimentary rock, but these are entirely inadequate in size to produce a mineral suite as widespread as in Province 2.

When all the possible sources are examined for the continental shelf south of Monterey Canyon, none alone could have been the source of Province 2. Therefore, it must be created by mixing of sediment derived from the Monterey Peninsula and the Salinas River. The Salinas River probably supplied most of the sediment to the suite of Province 2, but its influence appears to be masked by additions from other sources. It is possible that the suite was produced during a lower stand of sea level and is a relict suite that is being covered by modern drainage from the Salinas River, but this possibility is rejected because the mineral suite is found in sediment that is completely of modern origin (fine grained muds of the middle continental shelf) and in sediments that are mostly of relict origin

(coarse grained sediments of the outer edge of the continental shelf). The modern sediments off the mouth of the Salinas River are derived for the most part from the Salinas River, yet they do not carry the same mineral suite as the Salinas River and it appears that the effects of selective sorting and mixing with small amounts of relict sediment has had a cumulative effect in establishing a new mineral suite identity.

Province 3 is the province of sediment derived from the Pajaro River. The province is defined on the minerals glaucophane and lawsonite, minerals restricted to the Franciscan Formation. Franciscan Formation terrain is nearly restricted to the Pajaro River drainage basin, so the Pajaro River is clearly the origin of Province 3. Pajaro River sediments extend across eight miles of continental shelf from the shoreline, whereas the Salinas River sediments extend only out to shallow water depths, and the San Lorenzo River sediments cannot be traced beyond its mouth. The sediment carrying capacity of the Pajaro River is not greater than the Salinas River or the San Lorenzo River, and the reason for the wide recognition of Pajaro River sediments is due to the presence of distinct minerals in the suite which can be recognized even after mixing with sediments from other sources.

Province 4 covers a large portion of the north part of Monterey Bay, and is similar in origin to Province 2, being a composite of sediment from many sources where individual contributions cannot be traced because they lack distinctive mineral components. Several sources of sediment border the province on the northeast shore of the bay but none provides distinct sediment that maintains a mineralogic identity once the sediment reaches the marine environment. For example, the San Lorenzo River has a mineral composition that is high in garnet and low in augite,

but sediment of this composition does not extend beyond the mouth of the river. The San Lorenzo River is capable of moving large volumes of sediment into the ocean, as seen by its large size, its steep gradient, and its large volume of water flow, and the river maintains an open channel into the ocean. The inability to detect this contribution in the marine environment is caused either by the actual sediment load being much less than predicted, or by the dynamics of ocean waves and currents being strong enough to obliterate the identity of the sediment by mixing and distributing it widely over the ocean floor. It is not clear which is the cause, but the San Lorenzo sediments do not contain any distinctive minerals that could be recognized in mixtures and apparently the San Lorenzo sediments are underrepresented in the bay in the same manner as the Salinas River sediments. The heavy mineral composition of Province 4 agrees closely with an averaged heavy mineral composition from streams and bedrock around the northeast corner of the bay, and the nearshore portions of the province are certainly derived from local sources.

Much of the sediment of known Pleistocene age lies in Province 4 and it might be assumed that this province is predominantly relict Pleistocene deposits which were transported into the bay by longshore drift during lower sea level. This possibility is rejected because 1) the boundary between Provinces 3 and 4 is nearly perpendicular to the shoreline, not parallel to it, as would be the case if longshore drift were responsible for any part of Province 4, 2). This sediment lacks a high augite content to be expected if it is derived from the northwest, as is Province 5, 3) the nearshore portion of Province 4 could be derived from local sources, and 4) the deeper water sediments contain sediments of Holocene age which are accumulating under modern conditions. While

the sediment in Province 4 is not traceable to any definite source area, it is predominantly of local origin.

Province 5 provides evidence that large amounts of sediment are being transported into the northern part of Monterey Bay by longshore drift. The province has a composition that is dissimilar to Province 4, the offshore suite adjoining it, and also dissimilar to the average composition of the bedrock in the seacliffs and of the several streams draining the adjacent highlands. Sediments derived from Ben Lomond Mountain are often rich in garnet, as seen in sample 1899 and the samples from the San Lorenzo River, but Province 5 shows no garnet enrichment. Also, many of the bedrock samples show a much higher hornblende content than Province 5, eliminating the possibility that the beach sands are of local origin. A source area for the augite rich sands cannot be found within the area studied. The longshore drift for this portion of the coastline is strong and is directed to the southeast. This has transported a new mineral suite into the area from the northwest.

The discrepancy between extent of Salinas River and Pajaro River sediments in Monterey Bay and the respective drainage capacities of these rivers illustrates the difficulties in comparing mineral provinces with source areas. The Pajaro River drainage area is the only source of glaucophane, lawsonite and jadeite, so even where the Pajaro River sediment is mixed with sediment brought in by beach erosion, longshore drift or other sources, the sediment can be identified as being from the Pajaro River. Sediment derived from the Salinas River on the other hand contains minerals common to all provinces, and mixing with sediment of another source would very easily reduce the amounts of garnet and brown hornblende below the level needed to distinguish it, so sediments of Salinas River origin

would be recognized only when completely unmixed. This relationship must be kept in mind; trace minerals of restricted origin will overemphasize the influence of a source, while mineral provinces based on minerals in common with adjacent mineral provinces will tend to underemphasize the influence of its source.

In this study the mineral provinces show no correspondence to the age of the sediments. Pleistocene and Holocene sediments are distinguishable in Monterey Bay on the basis of grain size data, and the boundaries between sediment covers of different age are totally independent of the boundaries between mineral provinces. The boundary of mineral provinces 1 and 2 paralells a boundary between sediment of different age but the two boundaries are separated by a great distance and cannot be associated with each other.

Sayles (1965), Moore (1965), and Cherry (1966) in investigations to the north in the San Francisco region note the existence of an offshore mineral province of similar composition that usually is picked up in depths below 100 feet and is mainly associated with fine grained sediments -- characters that apply to Province 2 and 4 in Monterey Bay. Moore (1965) and Sayles (1965) associate the offshore province they found with a Franciscan Formation source that was spread by longshore drift and by sand dunes during lower sea level stand. Such an explanation of origin has been discounted for Provinces 2 and 4 in Monterey Bay and the origin of this ubiquitous suite in Monterey Bay appears to be entirely through mixing of sediment from many local sources. Without the presence of distinctive minerals in a mineral suite, such as glaucophane for Province 3, it would be very difficult to associate a mineral suite with a specific source area unless it is geographically adjacent to it. Along the central California coast a mixing and averaging of the sediments from the

Franciscan Formation, granitic and Central Valley terrains would produce a mineral suite very close to that found in the "Franciscan" province of Moore (1965) and Sayles (1965) and the "inactive zone" of Cherry (1966), and in Provinces 2 and 4 in Monterey Bay. Distinguishing provenance in this mineralogically similar group of sediments will depend on more detailed mineral identification and investigations of mineral province and provenance problems associated with fine grained sediments.

COMPARISON WITH SEDIMENTS OF MONTEREY CANYON AND MONEREY DEEP-SEA FAN

The continental shelf is not the final resting place for sediment entering Monterey Bay, as it can either be carried out onto the continental shelf and over the edge or it can be transported by longshore drift along the beaches to the head of Monterey Canyon and channeled down the canyon and out of the bay. Sediment that does move out of the bay in either manner moves down the canyon or one of its tributaries and emerges onto the Monterey Deep-Sea Fan. The existence of this process of transportation can be definitely predicted from the topography, morphology and placement of all the main features - shorelines, bay, canyon and fan - but the confirmation that large amounts of sediment are really moving down the canyon has not been made.

To help resolve this problem several samples of surface sediment from the walls and axis of the Monterey Canyon, collected by University of Southern California, and obtained through the courtesy of Dr. Bruce Marten, were examined and the heavy minerals were separated and identified. Of these samples I-7477 is probably the only one that was taken from the exact axis of the canyon and consists of very clean sand with abundant large flakes of mica. The others consist of fine sandy mud and represent quiet water deposition of sediments draping the banks and walls of

the canyon. Mineralogically these sediments are nearly indistinguishable from the sediments covering the continental shelf, having the same minerals in about the same proportions. Sample I-7477, along with samples 1863, 1865 and 1866, were taken in the very head of Monterey Canyon but are not identical with either Province 1 or Province 3 which border the rim of the canyon head, and their composition must be explained by assuming a mixing of sediment from the two provinces. Sample CM-8137, a fine grained sediment from deeper water, has a high garnet content and probably represents sediment derived from Province 1 but the lone occurrence of this distinctive sample does not enable any conclusions to be made about the importance of individual sediment sources. In conclusion the surface sediments from the upper part of Monterey Canyon are very similar to the surface sediments of the continental shelf and were undoubtedly derived from them but the contributions of individual sources has not been traceable within this series of samples. It appears that sediment moving down the canyon assumes a composition that is an average of that found in the various parts of the bay.

Below the canyon lies Monterey Fan which covers at least 20,000 square miles and has its apex at the mouth of the canyon. Dill and others (1954) show that the surface of this fan is channeled and possesses levees in a manner similar to subaerial streams, morphological features that suggest that large volumes of sediment have moved down the canyon and spread out onto the fan. In addition, many people have claimed that the terminous of drainage from the Central Valley of California, during an undetermined period of the late Tertiary, was situated at Monterey Bay (Baldwin, 1963; Martin & Emery, 1967; etc.). Wilde's (1965) study on the Monterey Fan is one of the very few reports that have investigated the mineralogy of deep sea sediments along the northern California coast, and is the only

source of data available for a comparison of the nearshore sediments of Monterey Bay with the sediments of the fan.

Wilde's (1965) identified the heavy minerals of 37 samples from many cores scattered over the fan, taking his samples from sand lenses occurring down to 232 cm. depth in the cores. Reexamining his data from sand lenses down to 100 cm. depth, it is clear that the mineralogy within any single core is nearly uniform from top to bottom so it is safe to compare mineralogies of the various cores despite the small variations of stratigraphic depths of the sand lenses in the cores. Where adequate numbers of nonopaque nonmicaceous grains were available for determination the heavy mineral content is seen to be similar to the average heavy mineralogy of the continental shelf, and taking into account the different identification techniques of different workers, there are no sediment suites or samples dissimilar to sediment assemblages currently found on the adjacent continental shelf.

Upon examining the garnet and glaucophane contents (minerals extremely easy to identify, thereby eliminating personal bias) it is noticeable that the heavy mineral assemblages of about half of the cores can be divided into two groups based on the presence of these minerals, in the same way that Province 1 and 3 are distinguished in Monterey Bay. Cores with high glaucophane content are HMS-10 & 11, and LFGS-68 & 70. Cores with high garnet content are HMS-6, Mare-6 and BP-10; BP-10 also containing a moderately high content of glaucophane. Garnet rich samples are present over the southern half of the area sampled, and glaucophane rich samples are present over the northern half. The sampling area includes the whole of the Monterey Fan and the southern edge of the Delgada Fan. The garnet rich samples are from the Monterey Fan, near the Monterey channels,

while the glaucophane rich samples occur on the northern edge of Monterey Fan and the southern edge of Delgada Fan, associated with the Farallon and Pioneer Canyon-channel system.

Wilde (1964) reported mineralogic differences between sands of the Monterey Fan and Delgada Fan in which Delgada Fan sands had lower amounts of amphibole and higher amounts of clinozoisite-epidote than Monterey Fan sends. A similar mineralogic difference based on the minerals glaucophane and garnet exists between the two fans, although the boundary between the glaucophane and garnet suites is south of the actual transition between Monterey and Delgada fans, and lies upon the north part of Monterey Fan. This mineralogic boundary appears to mark the boundary between sediments transported down the Monterey Canyon to the south, and sediments transported down Pioneer Canyon (and Farallon Canyon) to the north. Although Pioneer Canyon is a minor canyon in size, it has provided a distinctive mineral suite to the sediments of Monterey Fan.

DISTRIBUTION AND THICKNESS OF HOLOCENE SEDIMENTS

The floor of Monterey Bay is covered with bands of sediment of different age and thickness that generally parallel the depth contours. The outermost band on the continental shelf, and the deepest one, contains coarse sediments that are not presently being accumulated, and are of Pleistocene age. Sample 1871, from this band of coarse sediment contains both deep water and shallow water faunal elements. The shallow water faunal elements are dead shells of the gastropod Olivella biplicata, a species that does not live in water depths as deep as that presently covering the locality (Smith & Gordon, 1948). The sample also contains a dead shell of Astarte compacta, a cold water bivalve that has not been reported in Monterey Bay. This species may be represented by Pleistocene shells that lived in

Monterey Bay during a glacial period when marine temperatures were lower along the California coast (Valentine, 1961). These two species of mollusks represent conditions of depth and temperature that are no longer present at the sample location, and are of Pleistocene age.

Sediment shoreward of the outer band of coarse sediment is finer grained and better sorted and is in adjustment with modern conditions of wave agitation. The very fine grained sediment of the middle continental shelf is of Holocene age because it could have accumulated only under modern conditions of wave agitation. From cores taken in this band a minimum depth of the modern sediment cover can be obtained. Mare 2, taken at 210 feet depth on the flat between Soquel and Monterey canyons, penetrated 87 cm. of sediments very similar to the top layer of sediment (Wilde, 1965) indicating the deposition of at least one meter of sediment under uniform conditions associated with present sea level. Mare 3, taken in 300 feet of water off Davenport, penetrated 20 cm. of green muds, of which the deepest contained about 30 percent sand fraction. 20 cm. is a good estimate of the amount of modern sediment deposited in this area, a region receiving little sediment from the adjacent land. Box core MTC-19, from 335 feet depth off the mouth of the Salinas River, contains fine sediment overlying a coarse gravel layer, with fine sediment about 20 cm. in thickness. The Holocene sediment cover is certainly thickest in moderate depths, about 200 feet, and pinches out toward the edge of the continental shelf. It probably also thins toward the shoreline because at 100 feet depth a pre-modern shoreline feature is still noticeable in the surface sediments along the north shore of the bay. In shallower depths than 100 feet no evidence is available on thickness or age of the sediment cover.

The known Holocene sediments of the bay are fine grained sediments. The clay fraction of these sediments is derived from the Salinas and

Pajaro rivers, the mineralogy of the clays in the bay and in the rivers being identical. The origin of the sand fraction is more complex and appears to represent a greater variety of sources, and the details of this has been fully discussed in previous sections. The distribution of clays and sands do not agree in detail, and workers in other areas have noted similar differences (for example, van Andel & Postma, 1954). The distribution of the clays and fine sediment can be explained in terms of the water current pattern in Monterey Bay. The major flow of water off the central California coast is to the south, but during the winter months, when the greater part of the sediment reaches the ocean, a countercurrent forms in Monterey Bay which flows north along the nearshore portions of the bay (Skogsberg & Phelps, 1946). Fine grained sediment reaching the ocean during the existence of this current will be carried to the north and distributed perhaps as far as Ano Nuevo Point. More cores are needed in the northwest part of the bay to see if the Holocene sediment cover thins in a northwest direction, away from the river mouths.

CONCLUSIONS

1. Sediment types within Monterey Bay occur in three widespread bands that are aligned subparallel to the submarine contours. The outermost band lies on the outer edge of the continental shelf and varies from one to three miles in width. It is predominantly of coarse grained sediment, including some cobbles, and is a relict deposit of Pleistocene age. The age of the sediment is determined from a Pleistocene fauna found at locality 1871, and by the fact that sediment as coarse as this is not being accumulated under modern conditions. The middle band is three to four miles wide on the middle continental shelf and grades abruptly into the outer band. It is a band of very fine grained muds and occurs in water depths between

150 and 300 feet. Its age is determined as Holocene because its grain size varies in close relation to modern conditions of wave agitation and depth, and because sediment as fine grained as this is could not have survived disruption during rising sea level at the end of the Wisconsin glaciation at the end of the Pleistocene. The inner band is a few miles wide along the shorelines and it grades completely into the middle band. The inner band is of coarse and medium grained sediments that are being worked by waves close to the shore. It may be of mixed age, because along the north side of the bay a premodern shoreline feature is noticeable in depths of 100 feet, while in areas off the mouths of the Salinas and Pajaro rivers, it is suggestive that this band is of modern origin.

2. The thickness of the Holocene cover is not uniform over the entire bay. The thickest accumulations occur on the middle of the continental shelf at about 200 feet depth and thin in a shoreward and seaward direction. The cover pinches out in a seaward direction against Pleistocene coarser sediments. Shoreward it probably thinks, because Pleistocene features are noticeable in depths of about 100 feet. There is no evidence of the age of the sediment in the nearshore portions of the bay. In the east part of the bay a core in a water depth of 200 feet revealed the Holocene sediment cover to be at least one meter in thickness.

3. The grain size of the sediment cover, out to depths of 300 feet, is in close adjustment to modern conditions of wave agitation. Grain size modes from samples between depths of 50 to 300 feet steadily shift into the finer size ranges with increasing water depth. Between the depths of 100 to 300 feet this is a linear relation with mode values increasing one phi unit for each 75 foot depth increase (see Fig. 11). The unimodal nature of the samples (except for the 100 foot trend in the northeast

corner of the bay) shows that the sediment is not simply being reworked in place, but that it is being transported and deposited under conditions determined by wave agitation. This is excellent evidence that sediment is being moved into deeper water from the shoreline, and being sorted by size before it is deposited, with the finest fraction moving farthest from the shoreline.

4. Five heavy mineral provinces are distinguished in the sediment cover of Monterey Bay. Two of them are identified to source areas; Province 1 is from the Salinas River and Province 3 is from the Pajaro River. Province 5 is restricted to beach sediments along the northern border of the bay, and is transported onto the bay by longshore drift from an unknown source. Two provinces, Province 2 and Province 4, are not associated with definite source areas, but are believed to be derived from local sources. The heavy mineral provinces do not coincide with the age differences of the sediment cover.

5. Heavy mineral provinces 2 and 4 have a similar mode of occurrence, but probably not the same source areas, as a very widespread heavy mineral province in the San Francisco region to the north. The characteristics of this heavy mineral assemblage are a fairly uniform mineralogy, usual association with fine grained sediments in deeper water, and no obvious local source for it. In the San Francisco region this has been called a relict Pleistocene assemblage of Franciscan Formation origin, but in Monterey Bay where this assemblage occurs in two provinces, the grain size data and the aerial distribution of the provinces do not support this interpretation. In the Monterey Bay region this assemblage appears to be a composite one derived from many sources, and the same may be true in the San Francisco region.

6. The Salinas River and the Pajaro River each produce a distinctive mineral suite. These two rivers provide 80 percent of the drainage, and probably deliver a similar proportion of the sediment, reaching Monterey Bay. The rivers drain different geological terrains, and the Pajaro River contains a mineral suite with the characteristic Franciscan Formation minerals glaucophane and lawsonite, while the Salinas River has a mineral suite high in garnet and is associated with metamorphic and granitic bedrock. Sediment from these rivers is traceable over wide areas in Monterey Bay, covering most of the eastern half of the bay. Within the bay the mineral suite from the Pajaro River is more widespread than the mineral suite from the Salinas River, although the Salinas River provides three times as much water drainage as the Pajaro River. The Salinas and Pajaro rivers empty into the bay on opposite sides of Monterey Canyon, and their mineral provinces are restricted to opposite sides of Monterey Canyon. No mixing of sediment from these two provinces occurs except for sediment moved down Monterey Canyon and out of the bay.

7. Longshore drift is strong and present on all of the shorelines of the bay. It is strongest along the north shore of the bay and along the Monterey Peninsula, and is directed eastward. The east shore of the bay is in close adjustment with average wave conditions, so longshore drift forces are weaker, but the beaches contain large amounts of sand and greater volumes of sand are probably moved along the east shore than the north or south shores. The only area of the shore in exact adjustment with the waves is the portion of the shoreline between Marina and Monterey. Along the north shore of the bay eastward directed longshore drift has moved enough sand along the beaches from the northwest to establish a new mineral province in the bay - Province 5.

8. The clay mineralogy of the submarine samples is uniform over the entire bay. Montmorillonite is the dominant mineral, with lesser amounts of kaolinite and small amounts of mica. Chlorite was not detected. The clay mineralogy of the submarine samples is identical to the clay mineralogy of sediments from the Salinas and Pajaro rivers. These rivers provide nearly all of the clay sediment supplied to the bay.

9. Sediment sources for Monterey Bay are known from three areas. The two largest sources are the Salinas and Pajaro rivers, and the other is the movement of beach sand into the north bay by longshore drift. The San Lorenzo River does not provide large amounts of sediment to the bay, providing less sediment than expected from considerations of hydrologic data and basin morphology. Soquel Creek is a striking example of how streams and rivers with bars and lagoons at their mouths can deliver large amounts of sediment to the ocean. An unmeasurable amount of sediment is entering the ocean from the seacliffs along the northeast corner of the bay. The movement of sediment upon entering the ocean is complex, but mineral provinces show that most sediment remains in local areas. Longshore drift distributes the coarser sediment, and the effects of longshore drift are most noticeable in areas where the shoreline is most open to waves. The grain size data of the sediments shows that large amounts of sediment is moving directly offshore from the beaches, with the finer grain sizes moving into deeper water than the coarser sizes and are deposited in close harmony with conditions of wave agitation. Clays may be transported differently than sands, being distributed by water currents within the bay. Sediment is transported out of the bay by movement down Monterey Canyon, where it is channeled onto the deep sea Monterey Fan.

10. Heavy mineral provinces similar to those in Monterey Bay exist on the surface of the deep sea Monterey Fan. From preliminary studies,

two provinces can be distinguished, a glaucophane rich province and a garnet rich province. The glaucophane province lies on the northern part of the fan and the garnet province lies on the central and southern part of the fan. This mineralogic boundary appears to mark a boundary on the fan between sediment derived from the Monterey Canyon system and the Pioneer Canyon system. Glaucophane rich samples are associated with parts of the Monterey Fan close to the Pioneer Canyon and Channel, and garnet rich samples are associated with parts of Monterey Fan close to Monterey Canyon and Channel.

11. Submarine physiography suggests that during the Pleistocene and Holocene the size and position of the head of Monterey Canyon, and the mouth of the Salinas River, have remained the same. Pleistocene entrenchment of the Salinas and Pajaro rivers carved channels that join the upper portion of Monterey Canyon about three miles from the present shoreline. The mouth of the Salinas River has been located in its present position from at least the late Pleistocene, and has deposited a sediment wedge around the present mouth and has cut a channel that extends in a straight line off the present mouth. Monterey Canyon narrows markedly upchannel from its junction with the submerged Pleistocene channels of the Salinas and Pajaro rivers. This does not provide supporting evidence for the theory that the valley containing Elkhorn Slough was the site of outflow for drainage from the Central Valley of California in the late Tertiary or early Quaternary. The valley containing Elkhorn Slough is oversized only to the extent that it appears to be in adjustment with conditions during lower stand of sea level.

REFERENCES

Allen, J. E., 1945, Geology of the San Juan Bautista quadrangle, California: California Div. Mines Bull. 133, p. 75.

Baldwin, T. A., 1963, Land forms of the Salinas Valley, California, in Guidebook to the Salinas Valley and the San Andreas Fault, Pacific Section of the Am. Assoc. Petroleum Geologists and Soc. Econ. Paleontologists and Mineralogists, Annual spring field trip, May 1963, pp. 11-13.

Beveridge, A. J., 1960, Heavy minerals in lower Tertiary formations in the Santa Cruz mountains, California: Jour. Sed. Petrology, v. 30, no. 4, pp. 513-537.

Bowen, O. E., and Gray, C. H., Jr., 1959, Geology and economic possibilities of the limestone and dolomite deposits of the northern Gabilan Range, California: California Div. Mines Spec. Rept. 56, p. 40.

Brindley, G. W., 1951, X-ray identification and crystal structures of clay minerals: London, The Mineralogical Society, p. 345.

Cherry, J. A., 1966, Sand movement along equilibrium beaches north of San Francisco: Jour. Sed. Petrology, v. 36, no. 2, pp. 341-357.

Compton, R. R., 1966, Granitic and metamorphic rocks of the Salinian Block, California Coast Ranges, in Bailey, E. H., ed., Geology of Northern California, California Div. Mines Bull. 190, pp. 277-287.

Curry, J. R., 1960, Sediments and history of Holocene transgression, continental shelf, northwest Gulf of Mexico, in Shepard and others, eds., Recent sediments, northwest Gulf of Mexico: Am. Assoc. Petroleum Geologists, pp. 221-260.

Dill, R. F., Dietz, R. S., and Stewart, H. B., 1954, Deep-sea channels and delta of the Monterey submarine canyon: Geol. Soc. America Bull., v. 65, pp. 191-194.

Folk, R. L., 1966, A review of grain size parameters: Sedimentology, v. 6, no. 2, pp. 73-93.

Friedman, G. M., 1962, On sorting, sorting coefficients and the lognormality of the grain-size distribution of sandstones: Jour. Geology, v. 70, no. 6, pp. 737-753.

Galehouse, J. S., 1967, Provenance and paleocurrents of the Paso Robles Formation, California: Geol. Soc. America Bull., v. 78, no. 8, pp. 951-978.

Galliher, E. W., 1932, Sediments of Monterey Bay, California: State of California, Report XXVIII of the State Mineralogist, v. 28, no. 1, p. 42-79.

_____ 1935, Glauconite genesis: Geol. Soc. America Bull., v. 46, pp. 1351-1366.

Grim, R. E., 1953, Clay mineralogy: New York, McGraw-Hill, p. 384.

Hendricks, E. L., ed., Compilation of records of surface waters of the United States, October 1950 to September 1960, part 11, Pacific slope basins in California: U. S. Geol. Survey Water-Supply Paper 1735, p. 715.

Hutton, C. O., 1959, Mineralogy of beach sands, between Halfmoon and Monterey Bays, California: California Div. Mines Spec. Rept. 59, p. 32.

Ingle, J. C., Jr., 1966, The movement of beach sand: Developments in Sedimentology, v. 5, p. 221.

Johnson, J. W., 1953, Engineering aspects of diffraction and refraction: Am. Soc. Civil Engineers Trans., v. 118, paper 2556, pp. 617-648.

_____ 1956, Dynamics of nearshore sediment movement: Am. Assoc. Petroleum Geologists Bull., v. 40, no. 9, pp. 2211-2232.

Johnson, J. W., O'Brien, M. P., and Isaacs, J. D., 1948, Graphical construction of wave refraction diagrams: U. S. Navy Hydrographic Office Pub. no. 605, p. 75.

Keller, W. D., 1957, The principles of chemical weathering, revised edition: Columbia, Missouri, Lucas Bros., p. 111.

Krumbein, W. C., and Pettijohn, F. J., 1938, Manual of sedimentary petrography: New York, Appleton-Century-Crofts, p. 549.

Leo, G. W., 1961, The plutonic and metamorphic rocks of Ben Lomond Mountain, Santa Cruz County, California: Stanford Univ., Stanford, Calif., Ph.D. thesis, p. 169.

Manning, J. C., 1963, Resume of ground water hydrology in Salinas Valley, California, in Guidebook to the Salinas Valley and the San Andreas Fault, Pacific Section of the Am. Assoc. Petroleum Geologists and Soc. Econ. Paleontologists and Mineralogists, Annual spring field trip, May 1963, pp. 106-109.

Martin, B. D., and Emery, K. O., 1967, Geology of Monterey Canyon, California: Am. Assoc. Petroleum Geologists Bull., v. 51, no. 11, pp. 2281-2304.

Minard, C. R., Jr., 1964, The erosional and depositional history of the coast of northern California: University of California Hydraulic Engineering Laboratory, Tech. Rept. HEL-2-10, p. 63.

Monteath, G. M., Jr., 1965, Environmental analysis of the sediments of southern Monterey Bay, California: U.S. Naval Postgraduate School, Monterey, California, Masters thesis, p. 87.

Moore, D. B., 1965, Recent coastal sediments, Double Point to Point San Pedro, California: University of California Hydraulic Engineering Laboratory, Tech. Rept. HEL-2-14, p. 86.

National Marine Consultants, 1960, Wave statistics for seven deep water stations along the California coast: prepared for U. S. Army Engineer Districts, Los Angeles and San Francisco.

Pettijohn, F. J., 1949, Sedimentary rocks: New York, Harper & Bros., p. 718.

Sayles, F. L., 1965, Coastal sedimentation: Point San Pedro to Miramontes Point, California: University of California Hydraulic Engineering Laboratory, Tech. Rept. HEL-2-15, p. 105.

_____ 1966, A reconnaissance heavy mineral study of Monterey Bay beach sediments: University of California Hydraulic Engineering Laboratory, Tech. Rept. HEL-2-16, p. 20.

Shepard, F. P., and Emery, K. O., 1941, Submarine topography off the California coast: canyons and tectonic interpretation: Geol. Soc. America Spec. Paper 31, p. 171.

Skogsberg, T., and Phelps, A., 1946, Hydrography of Monterey Bay, California and thermal conditions, Part II (1934-1937): Am. Philos. Soc. Proc., 90:5, p. 350-386.

Smith, A. G., and Gordon, M., Jr., 1948, The marine mollusks and brachiopods of Monterey Bay, California, and vicinity: Calif. Acad. Sci. Proc., fourth series, v. XXVI, no. 8, pp. 147-245.

Spotts, J. H., 1962, Zircon and other accessory minerals, Coast Range Batholith, California: Geol. Soc. America Bull., v. 73, no. 10, pp. 1221-1240.

Starke, G. W., and Howard, A. D., 1968, Polygenetic origin of Monterey Submarine Canyon: Geol. Soc. America Bull., v. 79, no. 7, pp. 813-826.

Valentine, J. W., 1961, Paleoecologic molluscan geography of the Californian Pleistocene: University of California Pubs. Geol. Sci., v. 34, no. 7, pp. 309-442.

Van Andel, T. H., 1959, Reflections on the interpretation of heavy mineral analyses: Jour. Sed. Petrology, v. 29, no. 2, pp. 153-163.

_____ 1964, Recent marine sediments of the Gulf of California, in van Andel, T. H., and Shor, G. G., eds., Marine Geology of the Gulf of California, A Symposium: Am. Assoc. Petroleum Geologists Memoir 3, pp. 216-310.

Van Andel, T. H., and Poole, D. M., 1960, Sources of recent sediments in the northern Gulf of Mexico: Jour. Sed. Petrology, v. 30, no. 1, pp. 91-122

Van Andel, T. H., and Postma, H., 1954, Recent sediments of the Gulf of Paria: Koninklijke Acad. Wetenschappen, Verhand, v. 20, 5, p. 245.

Vernon, J. W., 1966, Shelf sediment transport system: Univ. of Southern California, Los Angeles, Calif., Ph.D. thesis, p. 135.

Warshaw, C. M., and Roy, R., 1961, Classification and a scheme for the identification of layer silicates: Geol. Soc. America Bull., v. 72, no. 10, pp. 1455-1492.

Wiegel, R. L., 1964, Oceanographical Engineering: Englewood Cliffs, New Jersey, Prentice-Hall, p. 532.

Wilde, P., 1964, Sand-sized sediment from the Delgada and Monterey Deep-Sea Fans, in Abstracts for 1964: Geol. Soc. America Spec. Paper 82, pp. 224-225.

_____ 1965, Recent sediments of the Monterey Deep-Sea Fan: University of California Hydraulics Laboratory, Tech. Rept. HEL-2-13, p. 153.

Wilson, B. W., Hendrickson, J. A., and Kilmer, R. E., 1965, Feasibility study for a surge-action model of Monterey Harbor, California: U. S. Army Corps of Engineers, Army Engineer Waterways Experiment Station, Contract Report No. 2-136, p. 166.

Sept 1966 ~ 218

APPENDIX A

Location and Description of Samples

Sample Number	Location	Depth	Description
1800	36° 58.2' N. 122° 09.5' W.	75 feet	Marine sediment. Fine sand, containing larger clasts of very fine grained bedrock.
1801	36° 57.8' N. 122° 09.8' W.	120 feet	Marine sediment. Very fine sand.
1802	36° 57.2' N. 122° 10.3' W.	180 feet	Marine sediment. Sandy silt.
1803	36° 56.3' N. 122° 11.2' W.	240 feet	Marine sediment. Green mud.
1804	36° 54.9' N. 122° 12.4' W.	300 feet	Marine sediment. Pebbly sandy silt, very rich in glauconite. Many live brachiopods recovered attached to pebbles, and to each other.
1805	36° 57.0' N. 122° 06.6' W.	85 feet	Marine sediment. Fine sand, containing larger clasts of very fine grained bedrock.
1806	36° 55.8' N. 122° 07.3' W.	180 feet	Marine sediment. Silty sand.
1807	36° 54.7' N. 122° 08.2' W.	240 feet	Marine sediment. Silty green mud.
1808	36° 53.6' N. 122° 09.0' W.	300 feet	Marine sediment. Green mud, contains much glauconite and partially glauconitized clay aggregates.
1809	36° 52.2' N. 122° 10.0' W.	360 feet	Marine sediment. Silty sand, very rich in glauconite and glauconitized clay aggregates.
1810	36° 56.5' N. 122° 03.9' W.	60 feet	Marine sediment. Sand, with very abundant shell fragments. Some small pebbles in the sample.
1811	36° 55.8' N. 122° 04.2' W.	110 feet	Marine sediment. Sand of fine to medium grain size, with abundant coarse shell fragments.

Sample Number	Location	Depth	Description
1812	36° 55.0' N. 122° 04.5' W.	150 feet	Marine sediment. Sandy silt.
1813	36° 53.9' N. 122° 04.9' W.	205 feet	Marine sediment. Green mud.
1814	36° 52.5' N. 122° 05.4' W.	270 feet	Marine sediment. Green mud.
1815	36° 50.5' N. 122° 06.2' W.	330 feet	Marine sediment. Fine sand, with abundant clay aggregates and glauconite.
1816	36° 57.2' N. 122° 00.1' W.	35 feet	Marine sediment. Fine sand, containing larger clasts of very fine grained bedrock.
1817	36° 56.4' N. 122° 00.5' W.	60 feet	Marine sediment. Sandy silt. Close to the whistle buoy, off Santa Cruz Harbor.
1818	36° 55.2' N. 122° 00.8' W.	100 feet	Marine sediment. Gravelly sand, very rich in shell debris, and containing some large cobbles.
1819	36° 54.7' N. 122° 01.0' W.	115 feet	Marine sediment. Very poorly sorted sand, with a mode of coarse sand and a mode of fine sand.
1820	36° 54.1' N. 122° 01.3' W.	130 feet	Marine sediment. Sandy silt.
1821	36° 53.3' N. 122° 01.6' W.	170 feet	Marine sediment. Green silty mud.
1822	36° 52.6' N. 122° 01.9' W.	210 feet	Marine sediment. Green silty mud.
1823	36° 51.3' N. 122° 02.4' W.	270 feet	Marine sediment. Green mud.
1824	36° 49.8' N. 122° 03.0' W.	305 feet	Marine sediment. Sandy mud; a coarser grained sediment but without glauconite.
1825	36° 48.1' N. 122° 03.4' W.	330 feet	Marine sediment. Poorly sorted sand, very rich in glauconite and partially glauconitized clay aggregates.

Sample Number	Location	Depth	Description
1826	Number not used		
1827	36° 57.3' N. 121° 59.1' W.	30 feet	Marine sediment. Fine sand.
1828	36° 56.5' N. 121° 58.6' W.	55 feet	Marine sediment. Very fine sand, with abundant shell fragments.
1829	36° 55.6' N. 121° 58.7' W.	80 feet	Marine sediment. Very fine sand.
1830	36° 54.8' N. 121° 58.6' W.	100 feet	Marine sediment. Very fine sand.
1831	36° 53.3' N. 121° 58.6' W.	120 feet	Marine sediment. Silty sand.
1832	36° 52.1' N. 121° 58.6' W.	230 feet	Marine sediment. Green mud.
1833	36° 50.5' N. 121° 58.6' W.	305 feet	Marine sediment. Pebbly sand.
1834	36° 48.5' N. 121° 58.4' W.	335 feet	Marine sediment. Green mud, very high in clay content.
1835	36° 56.8' N. 121° 56.2' W.	60 feet	Marine sediment. Very fine sand, shell rich.
1836	36° 54.7' N. 121° 57.0' W.	90 feet	Marine sediment. Silty sand.
1837	36° 57.3' N. 121° 54.8' W.	40 feet	Marine sediment. Very fine sand, with extremely abundant juveniles of the clam Tivela stultorum.
1838	36° 55.8' N. 121° 55.4' W.	65 feet	Marine sediment. Very fine sand.
1839	36° 54.3' N. 121° 55.8' W.	85 feet	Marine sediment. Very fine sand.
1840	36° 53.1' N. 121° 56.1' W.	120 feet	Marine sediment. Silty sand.
1841	36° 52.2' N. 121° 56.2' W.	180 feet	Marine sediment. Green mud, slightly sandy.

Sample Number	Location	Depth	Description
1842	36° 51.0' N. 121° 56.4' W.	240 feet	Marine sediment. Green mud, extremely fine grained, nearly 100% silt and clay.
1843	36° 55.3' N. 121° 52.2' W.	35 feet	Marine sediment. Very fine sand.
1844	36° 54.4' N. 121° 53.1' W.	65 feet	Marine sediment. Very fine sand.
1845	36° 53.7' N. 121° 53.7' W.	85 feet	Marine sediment. Very fine sand.
1846	36° 52.8' N. 121° 54.7' W.	120 feet	Marine sediment. Silty sand.
1847	36° 52.8' N. 121° 54.6' W.	120 feet	Marine sediment. Sandy silt.
1848	36° 52.9' N. 121° 52.9' W.	90 feet	Marine sediment. Very fine sand.
1849	36° 53.0' N. 121° 51.4' W.	60 feet	Marine sediment. Very fine sand.
1850	36° 52.2' N. 121° 52.4' W.	100 feet	Marine sediment. Silty sand.
1851	36° 51.5' N. 121° 53.2' W.	160 feet	Marine sediment. Silty mud.
1852	36° 50.6' N. 121° 54.3' W.	220 feet	Marine sediment. Green mud, with sand size fraction composed predominantly of mica flakes.
1853	36° 49.8' N. 121° 55.3' W.	265 feet	Marine sediment. Green mud, with sand size fraction composed predominantly of mica flakes.
1854	36° 49.0' N. 121° 56.2' W.	290 feet	Marine sediment. Sandy silt, with a secondary mode of coarse to medium sized sand grains. Some glauconite present.
1855	36° 50.6' N. 121° 49.8' W.	60 feet	Marine sediment. Fine sand.
1856	36° 50.5' N. 121° 50.9' W.	120 feet	Marine sediment. Very fine sand.

Sample Number	Location	Depth	Description
1857	36° 50.1' N. 121° 52.2' W.	200 feet	Marine sediment. Sandy silt.
1858	36° 49.7' N. 121° 53.5' W.	240 feet	Marine sediment. Green mud.
1859	36° 49.4' N. 121° 54.5' W.	270 feet	Marine sediment. Green mud.
1860	36° 49.5' N. 121° 48.9' W.	65 feet	Marine sediment. Fine sand.
1861	36° 48.8' N. 121° 48.2' W.	65 feet	Marine sediment. Fine sand - with a large amount of hydraulically light materials, wood, non-calcareous organic matter, mica, etc. Near the north buoy at Moss Landing.
1862	36° 48.5' N. 121° 49.7' W.	150 feet	Marine sediment. Fine to medium size sand.
1863	36° 48.2' N. 121° 47.7' W.	185 feet	Marine sediment. Very fine sand, with abundant mica and noncalcareous organic matter. From the head of Monterey Seacanyon.
1864	Number not used.		
1865	36° 48.2' N. 121° 48.1' W.	390 feet	Marine sediment. Fine to medium size sand, with occasional pebble clasts, and large amounts of hydraulically light materials, mica, woody material, etc. The sediment contains extremely little silt or clay fraction, and contrasts markedly with other sediment samples of this depth, resembling much more a shallow near shore sediment. From axis of Monterey Seacanyon.
1866	36° 48.1' N. 121° 48.4' W.	450 feet	Marine sediment. Green mud. From the axis of Monterey Seacanyon.
1867	36° 48.0' N. 121° 48.2' W.	85 feet	Marine sediment. Silty sand, with large amounts of mica. Near the south buoy at Moss Landing.
1868	36° 46.3' N. 121° 49.1' W.	55 feet	Marine sediment. Fine sand.

Sample Number	Location	Depth	Description
1869	36° 46.6' N. 121° 50.3' W.	150 feet	Marine sediment. Silty sand, with large amounts of mica.
1870	36° 46.6' N. 121° 52.2' W.	330 feet	Marine sediment. Green mud.
1871	36° 45.3' N. 121° 55.4' W.	370 feet	Marine sediment. Pebbly sand, small amounts of glauconite present.
1872	36° 45.2' N. 121° 49.5' W.	60 feet	Marine sediment. Fine sand
1873	36° 45.0' N. 121° 50.6' W.	120 feet	Marine sediment. Very fine sand.
1874	36° 44.9' N. 121° 51.3' W.	180 feet	Marine sediment. Sandy silt.
1875	36° 44.7' N. 121° 52.5' W.	240 feet	Marine sediment. Green mud.
1876	36° 44.5' N. 121° 54.6' W.	300 feet	Marine sediment. Green mud, extremely fine grained, nearly 100% silt and clay.
1877	36° 44.2' N. 121° 58.1' W.	400 feet	Marine sediment. Sandy silt, poorly sorted, with abundant glauconite.
1878-1891	Numbers not used.		
1892	UTM grid, zone 10 569,820 m. E. 4097,660 m. N.		Beach sand.
1893	UTM zone 10 571,780 m. E. 4096,030 m. N.		Beach sand. Town of Davenport, at mouth of San Vicente Creek.
1894	UTM zone 10 572,900 m. E. 4095,070 m. N.		Beach sand. At mouth of Liddell Creek.
1895	UTM zone 10 573,920 m. E. 4094,210 m. N.		Beach sand.
1896	Number not used.		

Sample Number	Location	Depth	Description
1897	UTM zone 10 575,180 m. E. 4093,130 m. N.		Beach sand. At mouth of Logan Creek.
1898	UTM zone 10 575,230 m. E. 4093,540 m. N.		Pleistocene terrace deposit. Cobbly black dirt, overlying 4-5' of granite wash on granitic bedrock.
1899	UTM zone 10 575,600 m. E. 4093,590 m. N.		Stream sediment sample, from the very bouldery channel of Laguna Creek.
1900	UTM zone 10 576,490 m. E. 4092,400 m. N.		Beach sand. At the mouth of Majors Creek.
1901	UTM zone 10 576,520 m. E. 4092,400 m. N.		Fine grained mudstone bedrock of Miocene age.
1902	UTM zone 10 578,230 m. E. 4091,250 m. N.		Beach sand. At mouth of Baldwin Creek.
1903	UTM zone 10 579,740 m. E. 4090,210 m. N.		Semi-consolidated sandstone from Pleistocene terrace deposits.
1904	UTM zone 10 579,740 m. E. 4090,210 m. N.		Siliceous mudstone of Miocene age.
1905	UTM zone 10 580,030 m. E. 4090,210 m. N.		Beach sand.
1906	UTM zone 10 582,230 m. E. 4089,890 m. N.		Beach sand. At mouth of Wilder Creek.
1907	UTM zone 10 582,340 m. E. 4089,980 m. N.		Siliceous mudstone bedrock of Miocene age.
1908	UTM zone 10 583,930 m. E. 4089,530 m. N.		Beach sand. Natural Bridges State Park.
1909	UTM zone 10 584,060 m. E. 4089,440 m. N.		Pleistocene terrace deposits, of pebbly black dirt.

Sample Number	Location	Depth	Description
1910	UTM zone 10 583,740 m. E. 4090,680 m. N.		Fine grained mudstone bedrock of Miocene age.
1911	UTM zone 10 585,500 m. E. 4089,830 m. N.		Beach sand.
1912	UTM zone 10 586,730 m. E. 4089,770 m. N.		Beach sand. Pt. Santa Cruz.
1913	UTM zone 10 586,730 m. E. 4089,770 m. N.		Fine grained sandstone bedrock of Pliocene age.
1914	UTM zone 10 587,070 m. E. 4090,900 m. N.		Beach sand. At Municipal Pier, Santa Cruz.
1915	UTM zone 10 586,980 m. E. 4092,520 m. N.		River sediment sample from the San Lorenzo River.
1916	UTM zone 10 585,510 m. E. 4095,530 m. N.		River sediment sample from the San Lorenzo River.
1917	UTM zone 10 588,720 m. E. 4091,110 m. N.		Fine grained sandstone bedrock of Pliocene age.
1918	UTM zone 10 588,570 m. E. 4091,110 m. N.		Beach sand.
1919	UTM zone 10 589,330 m. E. 4090,890 m. N.		Beach sand. At the mouth of Schwans Lagoon.
1920	UTM zone 10 590,020 m. E. 4090,750 m. N.		Siliceous mudstone bedrock of Pliocene age, at Black Pt.
1921	UTM zone 10 590,420 m. E. 4091,710 m. N.		Pleistocene terrace deposits of semi-consolidated sandstone.
1922	UTM zone 10 590,660 m. E. 4090,480 m. N.		Beach sand.

Sample Number	Location	Depth	Description
1923	UTM zone 10 591,330 m. E. 4090,100 m. N.		Pleistocene terrace deposits of unconsolidated gravelly sand, at Soquel Point.
1924	UTM zone 10 591,330 m. E. 4090,100 m. N.		Fine grained silty sandstones of Pliocene age, at Soquel Point.
1925	UTM zone 10 592,120 m. E. 4090,600 m. N.		Beach sand.
1926	UTM zone 10 592,120 m. E. 4090,600 m. N.		Fine grained mudstone bedrock of Pliocene age.
1927	UTM zone 10 593,320 m. E. 4092,050 m. N.		Beach sand. At mouth of Soquel Creek, in Capitola.
1928	UTM zone 10 593,380 m. E. 4092,120 m. N.		Poorly consolidated sandstone bedrock of Pliocene age.
1929	UTM zone 10 592,910 m. E. 4093,000 m. N.		Stream sediment sample in Soquel Creek, from just above the head of the lagoon formed at the mouth of the stream.
1930	UTM zone 10 594,560 m. E. 4092,730 m. N.		Beach sand.
1931	UTM zone 10 596,900 m. E. 4092,110 m. N.		Pleistocene terrace deposit of gravelly sand.
1932	UTM zone 10 596,900 m. E. 4092,110 m. N.		Unconsolidated sands and gravels of Pliocene age.
1933	UTM zone 10 598,600 m. E. 4091,030 m. N.		Unconsolidated sands of Plio-Pleistocene age.
1934	UTM zone 10 598,600 m. E. 4091,030 m. N.		Unconsolidated sands of Plio-Pleistocene age.
1935	UTM zone 10 598,630 m. E. 4091,870 m. N.		Beach sand.

Sample Number	Location	Depth	Description
1936	UTM zone 10 599,140 m. E. 4090,810 m. N.		Poorly consolidated sandstone of Plio-Pleistocene age.
1937	UTM zone 10 601,440 m. E. 4087,670 m. N.		Beach sand.
1938	UTM zone 10 601,440 m. E. 4087,670 m. N.		Unconsolidated sands of Plio-Pleistocene age.
1939	UTM zone 10 601,560 m. E. 4089,120 m. N.		Unconsolidated sands of Plio-Pleistocene age.
1940	UTM zone 10 602,670 m. E. 4085,310 m. N.		Beach sand.
1941	UTM zone 10 602,720 m. E. 4085,210 m. N.		Unconsolidated sands of Plio-Pleistocene age.
1942	UTM zone 10 603,840 m. E. 4086,480 m. N.		Poorly consolidated sandstone of Plio-Pleistocene age.
1943	UTM zone 10 603,610 m. E. 4083,600 m. N.		Beach sand.
1944	UTM zone 10 603,610 m. E. 4083,600 m. N.		Unconsolidated sands of Plio-Pleistocene age.
1945	UTM zone 10 606,070 m. E. 4079,060 m. N.		Dune sand.
1946	UTM zone 10 606,070 m. E. 4078,840 m. N.		Beach sand. Mouth of the Pajaro River.
1947	UTM zone 10 607,170 m. E. 4079,900 m. N.		From depositional terrace of the Salinas and Pajaro Rivers; ferruginously coated sands from the upper part of the terrace. Exposed in a quarry along the Pajaro River.

Sample Number	Location	Depth	Description
1948	UTM zone 10 607,170 m. E. 4079,900 m. N.		From a depositional terrace of the Salinas and Pajaro Rivers; gray sands from the lower part of the terrace, at modern river level. Exposed in a quarry along the Pajaro River.
1949	UTM zone 10 610,330 m. E. 4083,470 m. N.		River sediment sample of the Pajaro River. From the freeway crossing of the river just west of Watsonville.
1950	UTM zone 10 606,720 m. E. 4077,320 m. N.		Beach sand.
1951	UTM zone 10 606,110 m. E. 4076,260 m. N.		Beach sand.
1952	UTM zone 10 606,180 m. E. 4076,260 m. N.		Dune sand.
1953	UTM zone 10 609,780 m. E. 4077,000 m. N.		From a depositional terrace of the Salinas River, exposed along the north side of Elkhorn Slough.
1954	UTM zone 10 607,840 m. E. 4075,880 m. N.		Beach sand.
1955	UTM zone 10 608,060 m. E. 4074,080 m. N.		Beach sand. At the north jetty of Moss Landing.
1956	UTM zone 10 608,170 m. E. 4073,730 m. N.		Beach sand. At the south jetty of Moss Landing.
1957	UTM zone 10 608,110 m. E. 4073,240 m. N.		Beach sand.
1958	UTM zone 10 607,770 m. E. 4072,260 m. N.		Beach sand.
1959	UTM zone 10 607,160 m. E. 4069,580 m. N.		Beach sand.

Sample Number	Location	Depth	Description
1960	UTM zone 10 607,280 m. E. 4069,580 m. N.		Dune sand.
1961	UTM zone 10 606,620 m. E. 4066,080 m. N.		Beach sand. At mouth of the Salinas River.
1962	UTM zone 10 607,030 m. E. 4065,790 m. N.		Dune sand.
1963	UTM zone 10 611,930 m. E. 4059,580 m. N.		River sediment sample from the Salinas River.
1964	36° 37' 50" N. 121° 40' 45" W.		River sediment sample from the Salinas River.
1965	UTM zone 10 606,620 m. E. 4063,660 m. N.		Beach sand.
1966	UTM zone 10 606,230 m. E. 4061,150 m. N.		Beach sand.
1967	UTM zone 10 603,440 m. E. 4054,180 m. N.		Beach sand.
1968	UTM zone 10 601,540 m. E. 4051,840 m. N.		Beach sand.
1969-1970 - Numbers not used.			
1971	UTM zone 10 611,930 m. E. 4062,720 m. N.		River sediment sample from the Salinas River.
1972	36° 39' 20" N. 121° 42' 50" W.		River sediment sample from the Salinas River.
1973	36° 38' 50" N. 121° 42' 00" W.		River sediment sample from the Salinas River.
1974	36° 37' 20" N. 121° 40' 05" W.		River sediment sample from the Salinas River.

Sample Number	Location	Depth	Description
1975	UTM zone 10 607,620 m. E. 4082,030 m. N.		River sediment sample from the Pajaro River.
1976	UTM zone 10 611,040 m. E. 4084,620 m. N.		River sediment sample from the Pajaro River.
1977	UTM zone 10 615,750 m. E. 4084,230 m. N.		River sediment sample from the Pajaro River.
1978	UTM zone 10 585,800 m. E. 4094,910 m. N.		River sediment sample from the San Lorenzo River.
MTC-19	36° 43.7' N. 121° 56.4' W.	335 feet	Two samples taken from a box core; one at 7.5-12.5 cm. from the top, consisting of a muddy sand, and the other at 27-32 cm. from the top of the core, and consisting of a pebbly sand.
MTC-58	36° 42.6' N. 122° 01.0' W.	4675 feet	A box core 20 cm. long, mostly cobbly sand, with a thin top layer of silty mud. One sample taken 17-18 cm. from the top, of sand and gravel.
Mare. #2	36° 51' N. 121° 55' W.	225 feet	A 60 cm. long core, of all mud. Samples taken at top, middle and bottom of the core.
Mare. #3	36° 55' N. 122° 11' W.	290 feet	A 20 cm. long core, of all mud. Samples taken at top and at 18 cm. from the top.
M-6-8164	Start: 36° 48' 30" N. 121° 53' 00" W. Finish: 36° 48' 28" N. 121° 52' 15" W.	880-300 feet	Dredge sample, of fine mud.
BM-8136	36° 47' 45" N. 121° 52' 00" W.	1150 feet	Grab sample; of fine mud.
CM-8137	36° 46' 45" N. 121° 56' 15" W.	2380 feet	Grab sample; of sandy mud.
BS-8149	36° 48' 28" N. 122° 04' 14" W.	2500 feet	Grab sample; of fine mud.
I-7477	36° 47' 20" N. 121° 49' 00" W.	400 feet	Core; sample taken from the top.

APPENDIX B

Pipette Analysis

Weight of Suspension in Grams

	1818	1820	1821	1822	1823	1824	1826
< 4Φ	.051	.105	.218	.180	.223	.099	.120
< 4¼Φ	.046	.070	.158	.151	.211	.080	.113
< 4½Φ	.040	.049	.098	.108	.190	.074	.103
< 4 3/4Φ	.034	.036	.081	.093	.168	.066	.095
< 5Φ	.030	.029	.061	.072	.145	.060	.084
< 5¼Φ	.025	.024	.048	.060	.127	.055	.079
< 5½Φ	.023	.020	.041	.052	.113	.049	.071
< 5 3/4Φ	.020	.019	.036	.045	.098	.044	.065
< 6Φ	.020	.018	.034	.041	.089	.039	.059
< 6¼Φ	.019	.016	.033	.038	.078	.036	.054
< 6½Φ	.016	.015	.029	.033	.072	.033	.050
< 6 3/4Φ	.016	.014	.028	.031	.065	.030	.045
< 7Φ	.015	.013	.027	.029	.060	.027	.040

Weight of Sediment Within Size Classes in Grams

4Φ-4¼Φ	.005	.035	.060	.029	.012	.014	.007
4¼Φ-4½Φ	.006	.021	.060	.043	.021	.011	.010
4½Φ-4 3/4Φ	.006	.013	.017	.015	.022	.008	.008
4 3/4Φ-5Φ	.004	.007	.020	.021	.023	.006	.011
5Φ-5¼Φ	.005	.005	.013	.012	.018	.005	.005
5¼Φ-5½Φ	.002	.004	.007	.008	.014	.006	.008
5½Φ5 3/4Φ	.003	.001	.005	.007	.015	.005	.006
5 3/4Φ-6Φ	0	.001	.002	.004	.009	.005	.006
6Φ-6¼Φ	.001	.002	.001	.003	.011	.003	.005
6¼Φ-6½Φ	.003	.001	.004	.005	.006	.003	.004
6½Φ-6 3/4Φ	0	.001	.001	.002	.007	.003	.005
6 3/4Φ-7Φ	.001	.001	.001	.002	.005	.003	.005

Principal Mode

-	3 3/4Φ*	4Φ*	4¼Φ	4 3/4Φ

*Determined with aid of sand fraction size analysis

Weight of Suspension in Grams

	1872	1873	1874	1875	1876	1877
< 4Φ	.015	.043	.247	.281	.282	.343
< 4¼Φ	.012	.024	.176	.260	.280	.336
< 4½Φ	.008	.018	.119	.231	.277	.332
< 4 3/4Φ	.008	.015	.089	.199	.270	.331
< 5Φ	.008	.013	.066	.161	.265	.324
< 5¼Φ	.009	.012	.055	.134	.255	.316
< 5½Φ	.007	.011	.049	.116	.245	.308
< 5 3/4Φ	.007	.011	.043	.100	.227	.298
< 6Φ	.006	.010	.040	.090	.215	.290
< 6¼Φ		.011	.039	.082	.198	.279
< 6½Φ		.010	.038	.075	.186	.267
< 6 3/4Φ			.037	.070	.175	.254
< 7Φ			.038	.066	.164	.240

Weight of Sediment Within Size Classes in Grams

4Φ-4¼Φ	.003	.019	.071	.021	.002	.007
4¼Φ-4½Φ	.004	.006	.027	.029	.003	.004
4½Φ-4 3/4Φ	0	.003	.030	.032	.007	.001
4 3/4Φ-5Φ	0	.002	.023	.038	.005	.007
5Φ-5¼Φ		.001	.011	.027	.010	.008
5¼-5½Φ	.001	.001	.006	.018	.010	.008
5½Φ-5 3/4Φ	0	0	.006	.016	.018	.010
5 3/4Φ-6Φ		.001	.003	.010	.012	.008
6Φ-6¼Φ			.001	.008	.013	.011
6¼Φ-6½Φ		.001	.001	.007	.012	.012
6½Φ-6 3/4Φ			.001	.005	.011	.013
6 3/4Φ-7Φ				.004	.011	.014

Principal Mode

3Φ*	3¼Φ*	3 3/4Φ*	4 3/4Φ	5½Φ

*Determined with aid of sand fraction size analysis.

APPENDIX C

Grain Size Analysis Data

	1800	1801	1802	1803	1804	1805	1806	1807
Phi Unit								
-1.0 >1.981mm	0	0	0	0	0	0	0	0
-0.75 } 1.397 >	0	0	0	0	0	0	0	0
-0.50 }	0	0	0	0	0	0	0	0
-0.25 } .991	0	0	0	0	0	0	0	0
0.0 }	0	0	0	0	0	0	0	0
+0.25 } .701	0	0	0	0	0.1	0	0.1	0
+0.50 }	0	0	0	0	0.4	0.2	0.1	0
+0.75 } .495	0	0	0	0	0.7	0.4	0.1	0
+1.0 }	0	0	0	0.1	1.4	1.1	0.1	0
+1.25 } .351	0	0	0.2	0.1	3.1	2.5	0.1	0
+1.50 }	0	0	0.2	0.2	5.8	4.7	0.3	0
+1.75 } .246	0.1	0.3	0.2	0.3	8.8	7.6	0.7	0
+2.0 }	0.3	1.0	0.4	0.4	12.6	14.0	1.1	0
+2.25 } .175	1.7	3.1	0.8	0.8	17.9	26.8	2.0	0
+2.50 }	25.0	24.1	2.5	0.9	24.9	47.0	3.4	0
+2.75 } .124	52.7	52.8	24.0	1.6	33.9	69.9	15.4	0.2
+3.0 }	76.7	75.7	46.7	8.4	45.8	84.3	27.7	2.3
+3.25 } .088	86.1	85.2	61.3	23.0	58.9	89.3	38.3	9.0
+3.50 }	88.8	86.9	69.1	46.8	68.0	91.0	50.1	28.6
+3.75 } .061	89.6	88.9	74.3	66.9	74.0	91.8	62.0	58.2
+4.0 }	89.9	89.1	77.9	78.2	78.2	92.0	71.3	79.2
Quartile Values								
Q_1	2.48	2.48	2.71	3.21	2.31	2.19	2.78	3.40
Q_2	2.67	2.67	2.92	3.42	2.85	2.49	3.17	3.58
Q_3	2.88	2.87	3.18	3.63	3.23	2.74	3.56	3.77
Sorting Coefficient								
So_Φ	0.20	0.195	0.235	0.21	0.46	0.275	0.39	0.185
Skewness								
Sk_Φ	+0.01	+0.005	+0.025	0.00	-0.08	-0.025	0.00	+0.005
Modes								
	2.65	2.65	2.80	2.95	1.55	2.55	2.80	3.65
				3.45	3.05		3.50	

	1808	1809	1810	1811	1812	1813	1814
Phi Unit							
-1.0	0	0	0	0	0	0	0
-.75	0	0	0	0	0	0	0
-.50	0	0	0	0	0	0	0
-.25	0	0	0.2	0	0	0	0
0.0	0	0	0.3	0	0	0	0
+.25	0	0	0.3	0	0	0	0.1
+.50	0	0	0.4	0	0	0	0.1
+.75	0	0.8	0.5	0.3	0	0	0.2
+1.0	0	1.1	0.7	1.7	0.1	0	0.3
+1.25	0	2.3	1.0	5.6	0.1	0	0.4
+1.50	0.1	4.2	1.9	14.7	0.2	0	0.5
+1.75	0.5	5.9	3.3	25.3	0.2	0	0.6
+2.0	1.0	8.0	5.3	33.5	0.3	0	0.6
+2.25	1.4	12.3	8.5	39.9	0.4	0.1	0.7
+2.50	2.2	21.5	14.3	45.2	0.5	0.1	0.9
+2.75	5.6	34.2	21.5	50.9	0.7	0.2	5.9
+3.0	10.7	53.0	32.4	59.3	4.6	0.8	17.6
+3.25	15.4	73.5	43.4	66.5	15.6	8.9	33.6
+3.50	21.7	84.0	51.7	72.2	34.1	27.5	53.6
+3.75	29.5	88.1	57.6	77.0	59.7	57.5	69.8
+4.0	38.0	89.7	61.0	80.0	76.4	79.8	76.7
Quartile Values							
Q_1	2.95	2.51	2.53	1.62	3.32	3.43	3.03
Q_2	3.40	2.91	2.97	2.25	3.54	3.60	3.32
Q_3	3.72	3.16	3.31	3.03	3.73	3.77	3.55
Sorting Coefficient							
So_{Φ}	0.385	0.325	0.39	0.705	0.205	0.17	0.26
Skewness							
Sk_{Φ}	-0.065	+0.075	-0.05	+0.075	-0.015	0.00	-0.03
Modes							
	2.95	1.40	3.15	1.60	3.45	3.65	3.40
		3.05		2.65			

	1815	1816	1817	1818	1819	1820	1821	1822	1823
Phi Unit									
-1.0	0	0.4	0	0	0	0	0	0	0
-.75	0	0.5	0	0	0	0	0	0	0
-.50	0	0.7	0	0	0	0	0	0	0
-.25	0.1	0.9	0.1	0.3	0	0	0.1	0	0
0.0	0.1	1.0	0.5	1.2	0	0.1	0.2	0	0
+.25	0.2	1.1	1.1	5.1	0	0.1	0.2	0	0.1
+.50	0.3	1.3	2.9	12.6	0.4	0.1	0.2	0	0.1
+.75	0.7	1.9	6.7	23.7	2.1	0.1	0.3	0	0.1
+1.0	1.1	2.8	9.7	34.3	9.9	0.2	0.3	0	0.2
+1.25	1.8	4.3	21.4	45.1	24.1	0.3	0.3	0.1	0.4
+1.50	2.6	7.8	38.2	53.6	32.1	0.5	0.3	0.1	0.4
+1.75	3.5	12.1	48.2	60.2	36.6	0.6	0.4	0.1	0.5
+2.0	4.6	25.0	54.0	66.5	41.7	0.8	0.4	0.2	0.6
+2.25	5.9	32.7	58.0	72.9	48.4	1.9	0.7	0.3	0.7
+2.50	19.0	45.7	60.7	77.3	58.8	2.3	0.8	0.6	0.9
+2.75	36.9	52.4	62.7	79.5	69.8	3.8	1.0	0.7	2.2
+3.0	61.1	60.0	65.6	80.3	76.8	12.8	1.4	2.1	5.0
+3.25	78.9	68.1	69.2	81.2	78.6	24.3	4.2	6.7	10.2
+3.50	86.6	77.4	75.0	82.7	82.0	41.2	14.9	19.7	22.7
+3.75	89.3	85.3	81.5	84.7	85.0	64.7	34.0	43.1	41.6
+4.0	90.2	88.3	86.7	86.2	87.3	80.1	58.8	63.7	58.7
Quartile Values									
Q_1	2.54	1.85	1.26	+.72	1.20	3.17	3.51	3.44	3.34
Q_2	2.84	2.46	1.61	1.21	2.07	3.49	3.69	3.64	3.58
Q_3	3.07	3.20	2.95	1.92	2.65	3.69	3.85	3.78	3.78
Sorting Coefficient									
So_Φ	.265	.675	.845	.60	.725	.26	.17	.17	.22
Skewness									
Sk_Φ	-.035	+.065	+.495	+.11	+.145	-.06	-.01	-.03	-.02
Modes									
	2.85	1.90	0.65	0.70	1.15	2.15		3.70	3.70
		2.35	1.35		2.50	3.70			
		3.35	3.60		3.45				

	1824	1825	1827	1828	1829	1830	1831	1832
Phi Unit								
-1.0	0	0	0	0	0	0	0	0
-0.75	0	0	0	0	0	0	0	0
-0.50	0	0	0	0	0	0	0	0
-0.25	0	0	0.1	0	0	0	0	0
0.0	0	0	0.1	0	0	0	0	0
+0.25	0	0.4	0.2	0.1	0	0	0	0
+0.50	0	2.1	0.5	0.1	0	0	0	0
+0.75	0	3.8	1.4	0.1	0	0.1	0	0
+1.0	0	5.7	3.2	0.1	0.1	0.1	0	0
+1.25	0	8.7	6.4	0.3	0.1	0.1	0	0
+1.50	0.1	13.0	11.0	1.1	0.1	0.2	0	0
+1.75	0.2	15.6	16.2	2.2	0.3	0.3	0	0
+2.0	0.3	18.3	25.3	3.8	0.7	0.5	0	0.1
+2.25	0.5	24.5	37.3	7.6	1.4	0.9	0.1	0.2
+2.50	8.0	34.3	48.6	13.3	2.7	1.5	0.1	0.3
+2.75	24.0	47.1	61.3	21.6	6.8	5.7	0.3	1.5
+3.0	48.5	67.4	73.9	34.2	18.9	21.5	2.7	6.2
+3.25	69.4	78.5	84.8	52.3	37.5	44.0	15.4	15.0
+3.50	83.7	83.7	89.9	75.0	64.3	69.0	32.2	29.9
+3.75	94.4	86.6	91.0	85.9	80.9	81.2	52.5	48.7
+4.0	100.0	88.5	91.3	89.0	86.6	85.2	66.3	63.0
Quartile Values								
Q_1	2.76	2.15	1.94	2.63	3.05	3.00	3.26	3.26
Q_2	3.02	2.70	2.53	3.16	3.30	3.23	3.49	3.53
Q_3	3.34	3.00	2.88	3.40	3.51	3.43	3.71	3.72
Sorting Coefficient								
So_Φ	.29	.425	.47	.385	.23	.215	.225	.23
Skewness								
Sk_Φ	+.03	-.125	-.12	-.145	-.02	-.015	-.005	-.04
Modes								
	2.95	1.35	2.20	3.35	3.35	3.30	3.60	3.60
		2.85	2.75					

	1833	1834	1835	1836	1837	1838	1839	1840	1841	1842	1843
-1.0	0	0	0	0	0	0	0	0	0	0.4	0
-0.75	0.1	0	0	0	0	0	0	0	0	0.4	0
-0.50	0.6	0	0	0	0	0	0	0	0	0.4	0
-0.25	1.3	0	0.1	0	0	0.1	0	0	0	0.4	0
0.0	2.4	0.1	0.1	0	0	0.7	0.1	0	0	0.4	0
+0.25	3.2	0.2	0.2	0	0.3	0.9	0.1	0	0	0.6	0.6
+0.50	4.9	0.2	0.6	0	1.0	1.7	0.2	0	0	0.7	0.8
+0.75	7.4	0.3	0.8	0	1.9	2.3	0.3	0	0	0.9	1.0
+1.0	9.5	0.3	1.3	0.2	3.0	3.1	0.4	0	0	0.9	1.5
+1.25	10.8	0.3	2.7	0.7	4.3	4.0	0.7	0	0.1	1.0	2.1
+1.50	12.0	0.4	4.7	1.4	6.0	4.9	1.0	0	0.1	1.2	2.9
+1.75	14.1	0.5	7.3	2.3	7.9	5.9	1.4	0	0.2	1.3	3.6
+2.0	20.1	0.6	13.7	3.2	9.4	6.9	1.8	0	0.3	1.8	4.7
+2.25	29.7	1.4	28.2	4.3	11.3	9.2	2.0	0.1	0.4	2.3	6.0
+2.50	45.9	3.7	39.3	5.5	17.0	13.2	2.7	0.2	0.5	5.4	10.7
+2.75	63.7	12.9	54.8	13.2	27.3	20.4	10.3	0.4	0.7	11.4	21.8
+3.0	79.7	23.3	66.9	25.7	42.6	33.9	30.0	9.4	2.4	19.4	40.4
+3.25	85.8	36.7	76.6	46.7	62.6	54.7	57.6	33.1	11.9	30.2	66.3
+3.50	88.0	52.9	82.3	66.8	79.2	73.9	76.7	63.0	28.0	44.1	79.2
+3.75	89.4	67.1	85.2	77.3	86.5	83.8	84.2	82.5	49.0	61.5	85.6
+4.0	90.3	75.9	86.8	82.1	89.3	87.7	87.0	90.5	62.5	72.7	88.8
Quartile Values											
Q_1	2.09	2.89	2.14	2.89	2.64	2.78	2.91	3.16	3.33	2.96	2.76
Q_2	2.49	3.27	2.57	3.19	3.03	3.14	3.11	3.34	3.54	3.36	3.04
Q_3	2.80	3.56	2.96	3.42	3.30	3.37	3.33	3.54	3.72	3.64	3.26
Sorting Coefficient											
So_Φ	.355	.335	.41	.265	.33	.295	.21	.19	.195	.34	.25
Skewness											
Sk_Φ	-.045	-.045	-.02	-.035	-.06	-.065	+.01	+.01	-.015	-.06	-.03
Modes											
	0.65	3.40	2.15	1.75	1.70	1.25	1.75	3.35	3.60	2.75	1.40
	2.60		2.85	3.20	3.10	3.15	3.10			3.55	3.10

	1844	1845	1846	1847	1848	1849	1850	1851	1852	1853
-1.0	0	0	0	0	0	0	0	0	0	0
-0.75	0	0	0	0	0	0	0	0	0	0
-0.50	0	0	0	0	0	0	0	0	0	0
-0.25	0	0	0	0	0	0	0	0	0	0
0.0	0	0	0	0.1	0	0	0	0	0	0
+0.25	0	0	0	0.1	0	0	0	0	0	0
+0.50	0	0	0	0.1	0	0	0	0.1	0	0.1
+0.75	0.3	0.1	0	0.1	0	0	0	0.1	0	0.1
+1.0	0.9	0.3	0.1	0.1	0	0.1	0	0.1	0	0.2
+1.25	1.4	0.7	0.1	0.3	0	0.1	0	0.1	0	0.3
+1.50	2.0	1.1	0.2	0.3	0.1	0.1	0	0.1	0	0.3
+1.75	2.7	2.0	0.2	0.6	0.1	0.1	0	0.1	0	0.7
+2.0	3.3	3.2	0.4	0.8	0.2	0.1	0	0.2	0.1	0.9
+2.25	4.9	5.7	1.0	1.0	0.3	0.3	0.2	0.4	0.2	1.3
+2.50	6.9	8.0	2.9	1.4	0.7	1.0	0.4	0.9	0.4	2.0
+2.75	14.9	14.1	6.7	2.3	1.3	10.7	1.0	1.3	1.1	3.7
+3.0	29.7	23.5	13.0	4.0	17.0	33.4	15.2	2.1	2.7	7.3
+3.25	51.5	43.9	27.1	16.2	38.9	57.4	36.4	4.8	4.8	13.0
+3.50	72.3	68.0	52.8	37.0	62.7	74.1	60.0	8.8	8.2	23.2
+3.75	83.3	80.5	74.8	62.3	78.0	83.6	77.7	15.6	13.7	33.8
+4.0	87.2	84.0	84.4	76.5	85.6	87.6	87.3	24.0	18.4	54.2
Quartile Values										
Q_1	2.87	2.94	3.15	3.29	3.06	2.88	3.08	3.36	3.22	3.27
Q_2	3.17	3.23	3.40	3.51	3.28	3.10	3.32	3.63	3.54	3.56
Q_3	3.40	3.45	3.60	3.69	3.52	3.35	3.56	3.82	3.76	3.77
Sorting Coefficient										
So_Φ	.265	.255	.225	.20	.23	.235	.24	.23	.27	.25
Skewness										
Sk_Φ	-.035	-.035	-.025	-.02	+.01	+.015	0.00	-.04	-.05	-.04
Modes										
	1.65	2.20		3.55	3.30	3.00	3.30			
	3.20	3.30								

	1854	1855	1856	1857	1858	1859	1860	1861	1862	1863
-1.0	0	0	0	0	0	0	0	0	0	0
-0.75	0	0	0	0	0	0	0	0	0	0
-0.50	0	0	0	0	0	0	0	0	0	0
-0.25	0	0	0	0	0	0.1	0	0	0	0
1.0	0.5	0	0	0	0	0.2	0	0	0	0
+0.25	1.7	0	0	0	0	0.3	0.1	0	0	0
+0.50	3.6	0	0	0	0	0.3	0.1	0	0	0
+0.75	5.4	0	0	0	0	0.3	0.1	0	0	0
+1.0	7.2	0	0	0.1	0	0.6	0.1	0	0	0.1
+1.25	8.3	0	0	0.1	0	0.8	0.1	0	0.1	0.1
+1.50	9.2	0	0	0.2	0	1.6	0.1	0	1.0	0.1
+1.75	10.0	0	0	0.3	0	2.7	0.1	0.1	3.3	0.1
+2.0	10.8	0	0	0.4	0.1	4.4	0.2	0.4	17.5	0.3
+2.25	12.7	0	0.1	0.5	0.2	6.6	0.7	1.6	42.8	0.9
+2.50	24.7	0.2	0.2	0.7	0.5	13.0	3.0	20.8	62.3	2.4
+2.75	42.6	10.0	4.1	0.8	1.1	20.8	22.7	41.9	75.4	12.0
+3.0	63.0	30.3	21.1	1.6	3.8	30.3	51.3	67.2	82.9	28.7
+3.25	71.1	55.2	47.8	8.2	7.7	40.6	74.7	81.2	86.7	51.3
+3.50	76.8	74.7	69.8	21.3	11.3	52.3	85.0	86.7	88.9	68.5
+3.75	81.1	82.9	81.0	39.4	14.9	61.9	88.3	89.7	90.3	78.5
+4.0	83.3	85.2	85.2	54.5	16.7	67.6	89.6	91.4	91.0	83.3
Quartile Values										
Q_1	2.41	2.89	3.00	3.37	3.03	2.61	2.75	2.53	1.93	2.88
Q_2	2.74	3.12	3.20	3.58	3.31	3.08	2.95	2.74	2.28	3.15
Q_3	2.99	3.34	3.41	3.77	3.57	3.46	3.16	3.03	2.59	3.38
Sorting Coefficient										
So_Φ	.29	.225	.205	.20	.27	.425	.205	.25	.33	.25
Skewness										
Sk_Φ	-.04	-.005	+.005	-.01	-.01	-.045	+.005	+.04	-.02	-.02
Modes										
	0.45	3.25	3.15		3.25	3.30	2.90	2.85	2.15	3.15
	2.90									

	1865	1866	1867	1868	1869	1870	1871	1872	1873	1874
-1.0	0	0	0	0	0	0	0	0	0	0
-0.75	0	0	0	0	0	0	0	0.1	0	0
-0.50	0	0	0	0	0	0	0.7	0.1	0	0
-0.25	0.2	0	0	0	0	0	2.1	0.2	0	0
0.0	0.3	0	0	0	0	0	3.9	0.3	0	0
+0.25	0.6	0	0	0	0	0	6.8	0.4	0	0
+0.50	1.0	0	0	0	0	0	8.5	0.4	0	0
+0.75	1.4	0	0	0	0	0	10.0	0.4	0.1	0
+1.0	2.0	0	0	0	0	0	11.4	0.4	0.1	0
+1.25	2.8	0	0	0.2	0	0.1	13.1	0.5	0.1	0
+1.50	4.0	0	0	0.2	0	0.1	15.2	0.7	0.1	0
+1.75	5.4	0.1	0.1	0.3	0	0.2	18.2	0.7	0.1	0
+2.0	7.6	0.8	0.2	0.6	0.1	0.3	23.6	0.8	0.1	0
+2.25	20.3	2.4	0.7	1.3	0.2	0.7	33.3	1.4	0.2	0
+2.50	41.4	4.2	1.6	10.2	0.7	1.4	44.5	4.6	1.0	0.2
+2.75	62.1	12.1	5.8	33.3	3.6	6.1	58.4	24.0	8.5	0.8
+3.0	75.9	20.7	25.6	60.4	17.1	18.4	75.1	48.8	24.7	5.4
+3.25	82.6	29.6	49.0	78.7	34.7	32.8	83.1	73.0	47.1	13.6
+3.50	85.2	41.2	71.4	87.1	60.9	53.7	85.5	85.7	67.5	32.3
+3.75	86.9	52.1	81.9	89.3	79.5	72.9	86.4	89.7	79.5	59.3
+4.0	88.4	58.9	85.2	90.0	86.2	84.5	86.7	90.7	84.3	82.7
Quartile Values										
Q_1	2.27	2.96	2.96	2.63	3.07	3.05	1.93	2.73	2.96	3.35
Q_2	2.53	3.25	3.18	2.85	3.33	3.36	2.47	2.96	3.19	3.57
Q_3	2.80	3.46	3.40	3.07	3.54	3.62	2.84	3.19	3.44	3.77
Sorting Coefficient										
So_Φ	.265	.25	.22	.22	.235	.285	.455	.23	.24	.21
Skewness										
Sk_Φ	+.005	-.04	0.00	0.00	-.025	-.025	-.085	0.00	+.01	-.01
Modes										
	2.50	3.45	3.25	2.80	3.40	3.50	0.10	3.05	3.20	3.45
							2.70			

	1875	1876	1877	1892	1893	1894	1895	1897	1900	1902
-1.0	0	0.1	0	0.8	0	0	0	0	0.3	0
-0.75	0	0.1	0	2.9	0	0	0	0	0.3	0
-0.50	0	0.1	0	6.0	0	0	0	0	0.3	0
-0.25	0	0.1	0	10.4	0	0	0	0	0.4	0
0.0	0	0.2	0	19.7	0.4	0.5	0.6	0	0.8	0
+0.25	0	0.2	0.5	30.6	1.6	1.7	2.9	0	2.7	0.2
+0.50	0	0.2	1.3	47.0	3.3	4.7	10.4	0	9.0	2.7
+0.75	0.2	0.2	2.7	64.0	5.9	10.3	11.9	0.3	21.0	13.8
+1.0	0.3	0.3	4.4	75.4	10.6	20.1	37.1	1.5	32.6	24.3
+1.25	0.4	0.4	6.6	83.6	27.3	38.5	53.1	10.1	47.1	32.6
+1.50	0.7	0.8	9.8	87.2	53.7	62.9	69.6	37.3	64.0	56.7
+1.75	0.8	1.0	15.7	88.0	71.1	75.9	80.0	57.8	75.7	72.6
+2.0	0.9	1.6	23.7	88.1	82.9	83.4	85.8	72.1	82.6	83.8
+2.25	0.9	3.0	32.3	88.3	90.0	88.3	88.5	80.8	84.7	90.4
+2.50	1.1	7.7	40.1	88.4	93.0	90.4	89.7	83.9	85.7	93.1
+2.75	1.7	14.2	50.0	88.4	93.7	91.0	90.0	84.5	85.9	94.0
+3.0	3.3	22.7	61.9	88.4	94.0	91.2	90.1	84.6	85.9	94.1
+3.25	7.9	31.5	69.0	88.5	94.1	91.3	90.2	84.6	85.9	94.2
+3.50	18.1	41.1	72.7	88.5	94.1	91.5	90.2	84.6	85.9	94.7
+3.75	38.9	50.9	74.9	88.5	94.1	91.8	90.2	84.6	85.9	94.8
+4.0	60.2	59.2	76.4	88.5	94.1	92.0	90.2	84.6	85.9	94.8
Quartile Values										
Q_1	3.45	2.78	1.87	-0.2	1.22	1.05	+0.77	1.34	0.76	1.00
Q_2	3.65	3.22	2.45	+0.48	1.42	1.31	1.16	1.54	1.18	1.38
Q_3	3.82	3.59	2.78	+0.8	1.74	1.58	1.48	1.83	1.51	1.73
Sorting Coefficient										
So_Φ	.185	.405	.455	.50	.26	.265	.355	.245	.375	.365
Skewness										
Sk_Φ	+.015	-.035	-.125	-.18	+.06	+.005	-.035	+.045	-.045	-.015
Modes										
		3.55	2.10							
			2.85							

	1905	1906	1908	1911	1912	1914	1915	1917	1918	1919
-1.0	0	0	0	0	0	0	1.1	0	0	1.1
-0.75	0	0	0	0	0	0	2.6	0	0	1.1
-0.50	0	0	0	0	0	0	4.8	0	0	1.1
-0.25	0	0	0	0	0.1	0	9.9	0	0	1.5
0.0	0	0	0	0.1	0.2	0	15.1	0	0	1.8
+0.25	0	0.1	0.4	0.3	1.1	0.3	19.6	0	0.1	2.3
+0.50	0.5	0.6	1.5	2.1	3.2	1.0	27.8	0	0.6	3.3
+0.75	3.8	2.6	3.9	7.7	13.6	4.8	38.4	0	3.2	5.4
+1.0	12.6	7.4	7.2	13.6	28.1	10.6	48.7	0	9.2	10.4
+1.25	27.3	17.2	12.3	28.3	42.4	18.5	58.2	0	18.6	20.6
+1.50	50.6	39.1	28.3	49.5	57.8	32.6	66.3	0.2	36.2	39.1
+1.75	68.6	57.6	46.2	57.9	68.7	51.4	70.7	0.7	54.5	58.7
+2.0	80.4	72.4	60.7	79.4	74.9	70.2	72.9	2.0	68.8	75.3
+2.25	86.4	83.5	72.1	87.2	78.2	85.9	73.8	11.7	78.3	87.8
+2.50	88.2	88.7	77.2	88.7	79.0	93.0	74.5	30.7	82.7	94.2
+2.75	88.7	90.1	78.7	89.7	79.0	94.9	74.9	49.6	84.3	96.4
+3.0	88.7	90.6	78.8	89.9	79.0	95.3	75.2	67.6	84.6	97.4
+3.25	88.7	90.8	79.0	90.0	79.0	95.3	75.5	82.7	84.7	97.8
+3.50	88.7	90.9	79.0	90.2	79.0	95.3	75.9	93.0	84.7	97.9
+3.75	88.7	91.0	79.0	90.5	79.0	95.3	75.9	98.5	84.8	98.0
+4.0	88.7	91.0	79.0	90.7	79.0	95.3	75.9	101.3	84.8	98.0
Quartile Values										
Q_1	1.18	1.32	1.36	1.17	0.83	1.30	0.21	2.42	1.28	1.36
Q_2	1.43	1.57	1.65	1.45	1.19	1.65	0.75	2.76	1.58	1.70
Q_3	1.72	1.92	1.98	1.77	1.52	1.97	1.22	3.13	1.88	2.02
Sorting Coefficient										
So_Φ	.27	.30	.31	.30	.345	.335	.505	.355	.30	.33
Skewness										
Sk_Φ	+.02	+.05	+.02	+.02	-.015	-.015	-.035	+.015	0.00	-.01

	1920	1922	1925	1927	1928	1930	1931	1932	1933	1935
-1.0	0.1	4.5	0	0	0	0	0	1.5	0	0
-0.75	0.1	5.5	0	0	0	0	0	2.0	0	0
-0.50	0.1	7.1	0	0	0	0.3	0	2.3	0	0
-0.25	0.2	10.5	0	0	0	1.0	0	2.9	0	0
0.0	0.2	15.3	0.8	0.3	0	1.6	1.0	3.8	0	0
+0.25	0.2	20.4	2.7	0.4	0.5	2.0	3.5	5.3	0.1	0.5
+0.50	0.2	28.2	6.1	0.7	1.0	3.3	5.9	7.8	0.1	0.8
+0.75	0.2	42.0	17.9	1.4	2.4	6.5	13.1	10.3	0.1	1.3
+1.0	0.3	53.9	33.0	2.5	6.6	13.8	24.9	12.2	0.1	3.0
+1.25	0.3	65.3	48.4	4.6	29.1	26.1	35.9	13.5	0.1	5.9
+1.50	0.4	78.3	63.0	7.2	59.7	40.9	47.4	14.3	0.2	12.4
+1.75	0.4	85.5	74.7	18.8	74.4	57.0	55.7	14.8	0.3	32.2
+2.0	0.7	89.8	82.2	35.4	82.9	72.6	62.1	15.5	0.7	51.2
+2.25	2.1	92.2	86.0	54.3	88.3	87.6	68.0	20.9	2.0	70.7
+2.50	17.8	93.1	87.4	70.0	91.0	95.7	73.5	34.4	24.7	82.7
+2.75	33.8	93.7	88.0	78.0	92.5	98.1	77.9	52.8	54.8	87.5
+3.0	42.7	94.8	88.0	80.5	93.6	98.6	81.7	77.0	79.0	89.3
+3.25	59.5	94.8	88.0	80.9	94.5	98.9	84.3	87.0	87.3	90.0
+3.50	69.1	94.8	88.1	81.0	95.0	98.9	86.6	89.4	89.3	90.2
+3.75	75.4	94.8	88.1	81.1	95.3	98.9	88.3	90.6	90.1	91.3
+4.0	79.2	94.8	88.1	81.1	95.9	98.9	89.8	91.3	90.5	91.3
Quartile Values										
Q_1	2.53	+0.36	+0.83	1.72	1.21	1.23	0.97	2.30	2.48	1.65
Q_2	2.84	+0.85	1.19	2.06	1.37	1.63	1.55	2.67	2.67	1.94
Q_3	3.24	1.33	1.57	2.33	1.68	2.03	2.21	2.90	2.86	2.22
Sorting Coefficient										
So_Φ	.355	.485	.37	.305	.235	.40	.62	.30	.19	.285
Skewness										
Sk_Φ	+.045	-.005	+.01	-.035	+.075	0.00	+.04	-.07	0.00	-.005

	1937	1938	1940	1941	1943	1944	1945	1946	1949	1950
-1.0	0	0.4	0	0	0	0	0	0	0	0
-0.75	0	1.0	0	0	0	0	0	0	0	0
-0.50	0	1.6	0	0	0	0	0	0	0	0
-0.25	0	2.0	0.1	0.2	0	0	0	0	0	0
0.0	0	2.7	0.2	0.8	0	0	0.1	0	0.3	0
+0.25	0	3.7	0.5	1.7	0.2	0	0.1	0	0.7	0
+0.50	0.1	5.1	0.7	2.3	1.2	0.2	0.2	0	1.1	0
+0.75	0.3	8.6	1.1	2.7	4.8	1.6	0.7	0.1	2.3	0.2
+1.0	0.7	14.8	2.4	3.3	10.1	6.4	1.7	0.7	5.0	0.4
+1.25	1.5	25.2	6.0	4.8	18.0	19.6	4.0	2.0	11.9	1.5
+1.50	4.9	42.6	15.8	10.0	29.6	38.8	15.5	7.0	31.3	11.4
+1.75	13.0	55.8	32.2	22.7	43.0	56.3	37.0	19.4	54.3	29.8
+2.0	33.1	67.1	54.4	37.9	56.3	69.8	59.9	39.3	70.9	52.1
+2.25	56.2	77.6	73.5	54.0	69.5	79.9	78.0	60.4	83.5	74.3
+2.50	74.6	84.6	85.9	68.0	81.5	85.8	91.9	78.9	91.2	88.3
+2.75	84.9	88.3	91.0	77.4	87.2	88.7	95.4	89.8	95.1	94.8
+3.0	88.0	89.8	92.3	83.7	88.8	89.9	96.7	93.8	97.3	95.0
+3.25	88.8	90.4	92.6	86.7	89.2	90.4	97.1	94.8	98.4	95.3
+3.50	88.9	90.9	92.7	88.1	89.4	90.9	97.4	95.1	99.3	95.4
+3.75	89.0	91.3	93.2	89.2	89.5	91.0	97.8	95.3	99.9	95.6
+4.0	89.1	91.6	93.7	90.0	89.6	91.4	97.9	95.4	100.2	95.7
Quartile Values										
Q_1	1.87	1.22	1.62	1.75	1.34	1.29	1.60	1.79	1.43	1.67
Q_2	2.12	1.55	1.92	2.10	1.78	1.59	1.87	2.08	1.70	1.97
Q_3	2.37	2.04	2.19	2.49	2.19	1.99	2.18	2.38	2.06	2.22
Sorting Coefficient										
So_Φ	.25	.41	.285	.37	.425	.35	.29	.295	.315	.275
Skewness										
Sk_Φ	0.00	+.08	-.015	+.02	-.015	+.05	+.02	+.005	+.045	-.025

	1951	1952	1954	1955	1956	1957	1958	1959
-1.0	0	0	0	0	1.8	0	0	0
-0.75	0	0	0	0	3.0	0	0	0
-0.50	0	0	0	0	4.8	0	0.1	0
-0.25	0	0	0	0	8.4	0.2	0.7	0
0.0	0	0	0	0	16.3	1.4	3.5	0
+0.25	0	0	0	0.3	26.3	3.4	9.0	0
+0.50	0	0	0	1.0	42.0	7.0	16.8	0.4
+0.75	0	0.2	0.3	2.4	57.2	11.3	24.9	1.0
+1.0	0.2	1.1	1.5	4.5	68.0	17.1	33.4	2.3
+1.25	1.8	5.2	7.9	8.1	78.4	28.4	45.6	4.8
+1.50	10.0	24.6	29.7	15.0	85.1	44.1	60.3	19.0
+1.75	28.7	52.7	49.6	29.8	88.7	61.2	76.7	48.0
+2.0	51.9	75.5	67.1	52.5	90.3	78.3	88.3	73.6
+2.25	74.7	88.8	81.6	76.9	91.3	89.8	96.0	87.3
+2.50	87.8	93.6	89.6	91.8	91.8	94.2	99.3	91.2
+2.75	92.8	94.8	91.6	96.8	92.0	95.3	100.1	92.1
+3.0	94.0	95.1	92.0	97.8	92.2	95.7	100.5	92.3
+3.25	94.3	95.2	92.1	97.9	92.9	95.9	100.7	92.6
+3.50	94.4	95.4	92.2	98.0	93.0	96.0	100.9	92.7
+3.75	94.7	95.4	92.4	98.1	93.3	96.0	101.0	92.9
+4.0	94.9	95.4	92.6	98.2	93.5	96.1	101.0	93.0
Quartile Values								
Q_1	1.69	1.50	1.41	1.68	+.20	+.18	+.79	1.53
Q_2	1.97	1.71	1.72	1.97	+.59	1.55	1.34	1.74
Q_3	2.21	1.97	2.03	2.10	1.06	1.91	1.73	1.96
Sorting Coefficient								
So_Φ	.26	.235	.31	.21	.43	.865	.47	.215
Skewness								
Sk_Φ	-.02	+.025	0.00	-.08	+.04	-.505	-.08	+.005

	1960	1961	1962	1963	1964	1965	1966	1968
-1.0	0	0	0.9	0	0	0	0	0
-0.75	0	0	0.9	0.5	0	0.6	0	0
-0.50	0	0.2	0.9	1.7	0	3.0	0.3	0
-0.25	0	0.6	0.9	2.3	0	8.9	0.8	0
0.0	0.6	2.2	1.5	3.2	0	18.6	1.9	0.1
+0.25	2.5	5.2	3.0	4.8	0	30.0	3.7	0.3
+0.50	7.4	10.2	7.9	7.6	0	38.2	7.2	0.4
+0.75	16.7	16.1	18.2	12.1	0	47.2	17.5	0.9
+1.0	31.5	25.9	34.9	22.1	0.1	54.9	31.2	2.0
+1.25	51.8	43.9	55.1	41.2	0.2	62.7	53.6	4.7
+1.50	66.7	63.0	75.4	62.0	1.1	70.1	73.0	15.9
+1.75	77.8	78.5	86.4	76.7	9.6	73.7	83.1	27.4
+2.0	86.3	83.4	91.3	86.3	37.8	75.3	87.5	32.8
+2.25	91.5	92.8	94.3	91.7	60.0	75.9	89.0	60.0
+2.50	93.7	93.8	95.7	93.8	75.3	76.0	89.4	72.2
+2.75	94.3	94.0	96.0	94.8	84.2	76.0	89.7	77.1
+3.0	94.7	94.1	96.1	95.2	88.7	76.0	89.7	77.7
+3.25	94.9	94.1	96.2	95.7	90.5	76.0	89.8	78.0
+3.50	95.1	94.2	96.2	95.8	91.8	76.0	90.0	78.1
+3.75	95.2	94.3	96.3	96.0	92.9	76.0	90.1	78.1
+4.0	95.4	94.4	96.3	96.1	93.3	76.0	90.2	78.1
Quartile Values								
Q_1	+.89	+.96	+.87	1.04	1.87	-0.01	+.88	1.57
Q_2	1.20	1.30	1.18	1.33	2.07	+0.49	1.17	1.94
Q_3	1.60	1.61	1.46	1.66	2.38	1.07	1.41	2.22
Sorting Coefficient								
So_Φ	.355	.325	.295	.31	.255	.54	.265	.325
Skewness								
Sk_Φ	+.045	-.015	-.015	+.02	+.055	+.05	-.025	-.045

APPENDIX D

Heavy Mineral Composition of Sediment Samples

	1800	1801	1802	1803	1804	1805	1806	1807	1808	1809
Green Hornblende	48	52	51	51	28	43	48	60	34	50
Brown Hornblende	1	2	9	1	6	1	2	3	4	
Oxyhornblende	3	2	3	3	5	3	3	4	3	1
Augite	27	24	19	15	37	31	20	14	36	31
Hypersthene	6	8	9	10	10	10	7	11	11	10
Epidote	4	5	4	7	6	2	5	1	7	5
Garnet	3	1		2		2	6	3	2	
Sphene	2	2	2	4	3	3	1	2		
Zircon	1			1		2			2	
Apatite				4	2		5	2	1	1
Clinozoisite			1	1	2	1	1			2
Detrital Carbonate	3	3	1			2	2			
Glaucophane	2	1	1	1						
Lawsonite										
Jadeite										
Tourmaline										
Andalusite										
Sillimanite										
Staurolite										
Biotite	5		63	13	2		15	17	1	3
Organic Carbonate										
Composites - Opaques	45	67	73	25	56	42	25	48	49	47
Hornblende/ Augite Ratio	1.8	2.2	3.2	3.5	0.9	1.4	2.5	4.5	1.1	1.6
Augite/Hyper-sthene Ratio	4.5	3.0	2.1	1.5	3.7	3.1	2.9	1.3	3.3	3.1

	1810	1811	1812	1813	1814	1815	1816	1817	1818	1819
Green Hornblende	42	34	49	42	36	39	33	47	24	47
Brown Hornblende	6	1	2	3	5	5	2	7	2	11
Oxyhornblende	8	4	4	7	2	1	8	3	4	2
Augite	19	32	22	25	24	30	22	17	32	15
Hypersthene	10	18	10	10	16	10	21	10	28	13
Epidote	7	2	5	5	9	11	6	2	4	5
Garnet	1	3	1	2	1		3	2	1	1
Sphene	4	2	5	1	4	2		4	3	4
Zircon	3	3		3	1		3		1	1
Apatite						1	1	6		1
Clinozoisite				1	1					
Detrital Carbonate								2		
Glaucophane		1	1	1	1		1			
Lawsonite									1	
Jadeite										
Tourmaline			1							
Andalusite										
Sillimanite										
Staurolite						1				
Biotite	6		5	24	12		4	11	5	1
Organic Carbonate										
Composites - Opaques	50	49	17	33	56	39	35	35	24	33
Hornblende/ Augite Ratio	2.5	1.1	2.4	1.8	1.7	1.5	1.6	3.2	0.8	3.9
Augite/Hyper-sthene Ratio	1.9	1.8	2.2	2.5	1.5	3.0	1.0	1.7	1.1	1.2

	1820	1821	1822	1823	1824	1825	1827	1828	1829
Green Hornblende	46	48	50	54	41	51	39	45	58
Brown Hornblende	1	7	7	4	6	4	4	3	
Oxyhornblende	4	6	4	6	3	10	7	2	7
Augite	27	17	21	20	24	15	16	18	14
Hypersthene	6	4	2	5	14	6	13	15	5
Epidote	5	7	4	4	8	8	7	3	2
Garnet		1	2	1			4	3	2
Sphene	5	2	4	1	3	2	4	4	7
Zircon		3		1			2	3	2
Apatite	3	2	2	1		1	1	3	1
Clinozoisite	1	1	1			1	1		2
Detrital Carbonate	2	1	1			1			
Glaucophane			2	1	1		2	1	
Lawsonite		1		2		1			
Jadeite									
Tourmaline									
Andalusite									
Sillimanite									
Staurolite									
Biotite	7	3	15	15		13	1	5	10
Organic Carbonate								1	1
Composites - Opaques	22	46	33		39	73	38	29	36
Hornblende/ Augite Ratio	1.7	3.2	2.7	2.9	2.0	3.7	2.7	2.7	4.1
Augite/Hyper-sthene Ratio	4.5	4.3	10.5	4.0	1.7	2.5	1.9	5.0	2.5

	1830	1831	1832	1833	1834	1835	1836	1837	1838	1839
Green Hornblende	48	32	55	33	42	59	44	29	33	28
Brown Hornblende	3	9	1	2	9	7	6	4	9	2
Oxyhornblende	8	5	4	5	1	7	5	3	8	11
Augite	21	23	24	38	20	12	23	34	22	38
Hypersthene	11	13	8	10	15	8	9	17	20	11
Epidote	3	6	3	5	4	2	3	3	4	2
Garnet			1	1	1		1			3
Sphene	1	5		1	5	1	5	3	2	2
Zircon	1		1			3	1	3	1	2
Apatite	3	1		3	2		2	3		
Clinozoisite	1	1		1			1	1		
Detrital Carbonate			1						1	
Glaucophane		4	2	1	1	1				
Lawsonite										1
Jadeite		1								
Tourmaline										
Andalusite										
Sillimanite										
Staurolite										
Biotite	13	7	32	1	4	4	11	2	6	
Organic Carbonate									1	
Composites - Opaques	38	34	51	80	61	52	20	70	57	31
Hornblende/ Augite Ratio	2.4	1.8	2.3	0.9	2.6	5.5	2.2	1.0	1.9	0.8
Augite/Hyper-sthene Ratio	1.9	1.8	3.0	3.8	1.3	1.5	2.6	2.0	1.1	3.5

	1840	1841	1842	1843	1844	1845	1846	1847	1848	1849
Green Hornblende	37	60	64	35	40	29	46	47	45	38
Brown Hornblende	6	9	4	4	1	7	6	7	2	7
Oxyhornblende	4	6	1	7	3	4	6	3	3	11
Augite	26	11	13	22	24	25	23	15	23	23
Hypersthene	12	3	4	14	15	5	8	8	10	4
Epidote	10	4	4	5	6	7	6	7	6	3
Garnet	1	1	2	4	3	4		1	4	3
Sphene	2		1	5	4	6	1	4	2	6
Zircon			1	1		1	1			
Apatite		2	1	1		2	1	1	3	2
Clinozoisite	1		1			1				
Detrital Carbonate			1		1	1				
Glaucophane		3	3	2	3	4	2	3	2	2
Lawsonite		1				3		4		1
Jadeite						1				
Tourmaline										
Andalusite										
Sillimanite	1									
Staurolite										
Biotite	5	69	503	1	4	2	2	5	2	1
Organic Carbonate		4	20							
Composites - Opaques	36	97	105	103	38	47	42	46	36	60
Hornblende/ Augite Ratio	1.7	6.3	5.2	1.8	1.7	1.4	2.3	3.2	2.0	2.0
Augite/Hyper-sthene Ratio	2.2	3.7	3.2	1.6	1.7	5.0	2.9	1.9	2.3	5.8

	1850	1851	1852	1853	1854	1855	1856	1857	1858	1859
Green Hornblende	52	60	56	44	36	48	51	46	51	40
Brown Hornblende	2	3	11	5	3	6	1	8	2	7
Oxyhornblende	6	5	4	1	2	1	2	3	3	6
Augite	18	22	11	18	37	11	20	21	18	13
Hypersthene	3	2	4	12	9	8	5	7	3	18
Epidote	9	3	5	4	4	9	9	6	10	6
Garnet	1			3		2	3		1	5
Sphene	3	2	1	6	3	5	2	2	8	4
Zircon					2	2	1			
Apatite	4	1	2	5	2	2	3	4		
Clinozoisite		1	1		1	1		1		
Detrital Carbonate										
Glaucophane	2	1	2	1	1	3	2	2	3	1
Lawsonite			1			1	1		1	
Jadeite										
Tourmaline				1						
Andalusite										
Sillimanite			2			1				
Staurolite										
Biotite	3	17	21	3	2		1	5	2	1
Organic Carbonate			1					1		
Composites - Opaques	52	61	43	41	67	70	71	37	40	64
Hornblende/ Augite Ratio	3.0	2.9	6.1	2.7	2.3	4.9	2.6	2.6	2.9	3.6
Augite Hypersthene Ratio	6.0	11.0	2.8	1.5	4.1	1.4	4.0	3.0	6.0	1.4

	1860	1861	1862	1863	1865	1866	1867	1868	1869
Green Hornblende	44	48	39	45	46	50	53	48	58
Brown Hornblende	5	2	3	11	13	6	6	3	2
Oxyhornblende	4	3	1	2	3	4	1		
Augite	21	21	33	19	23	18	16	16	23
Hypersthene	6	5	10	1	5	6	3	3	4
Epidote	3	4	5	3	4	3	6	3	2
Garnet	7	6	5	4		7	8	13	6
Sphene	1	5	4	8	1	3	1	7	3
Zircon	1	2		3	1	1		2	
Apatite	6	1		4	3	2	4	4	2
Clinozoisite		1			1			1	
Detrital Carbonate							2		
Glaucophane	1	2							
Lawsonite	1								
Jadeite									
Tourmaline									
Andalusite									
Sillimanite									
Staurolite									
Biotite	8	11		3	17	13	5	1	18
Organic Carbonate									
Composites - Opaques	42	49	59	42	62	40	52	19	42
Hornblende/ Augite Ratio	2.3	2.4	1.3	2.9	2.6	3.1	3.7	3.2	2.6
Augite/Hyper-sthene Ratio	3.5	4.2	3.3	19.0	4.6	3.0	5.3	5.3	5.8

	1870	1871	1872	1873	1874	1875	1876	1877
Green Hornblende	57	49	56	59	57	62	50	40
Brown Hornblende	2	2	5	7	9	5	5	8
Oxyhornblende	4	5	2		1	1	1	3
Augite	5	31	15	13	16	14	15	16
Hypersthene	3	8	2	1		10	5	17
Epidote	5	1	1	6	4	3	9	7
Garnet	7	2	8	2	3	2	7	
Sphene	7	2	7	7	4	3	3	3
Zircon	4			1				2
Apatite	6		4	4	3		4	3
Clinozoisite					2			
Detrital Carbonate								
Glaucophane					1		1	
Lawsonite								
Jadeite								
Tourmaline								
Andalusite								
Sillimanite								
Staurolite								1
Biotite	20	3	2	12	17	101	39	10
Organic Carbonate	1					2		
Composites - Opaques	54	42	23	35	25	31	68	42
Hornblende/ Augite Ratio	11.8	1.6	4.1	5.1	3.8	4.8	3.7	3.0
Augite/Hyper-sthene Ratio	1.7	3.9	7.5	13.0		1.4	3.0	0.9

	1892	1893	1894	1895	1897	1898	1899
Green Hornblende	30	30	28	26	21	50	22
Brown Hornblende	4	2	3	6	3	2	1
Oxyhornblende	4	2	1	2	2	2	
Augite	39	37	39	37	47	17	22
Hypersthene	13	18	19	18	15	4	
Epidote	4	7	8	4	5	6	1
Garnet	1	2		4	2	4	47
Sphene	3	2	1	2	1	12	2
Zircon					1	2	5
Apatite						1	
Clinozoisite				1	2		
Detrital Carbonate	1						
Glaucophane	1		1				
Lawsonite							
Jadeite							
Tourmaline					1		
Andalusite							
Sillimanite							
Staurolite							
Biotite	3	2				9	8
Organic Carbonate	2						
Composites - Opaques	83	54	56	52	46	87	67
Hornblende/ Augite Ratio	0.9	0.9	0.8	0.9	0.5	3.1	1.0
Augite/Hypersthene Ratio	3.0	2.1	2.1	2.1	3.1	4.3	

	1900	1901	1902	1903	1904	1905	1906	1907	1908	1909
Green Hornblende	29	25	28	64	30	32	35	25	31	65
Brown Hornblende	6	1	4	3	2	2	3		6	
Oxyhornblende	2		2	1	1	1	3		3	4
Augite	41	33	38	13	15	43	34	31	38	19
Hypersthene	11	16	16	11	9	12	12	3	11	1
Epidote	6	5	6	3	2	6	4	1	6	3
Garnet	3	6	3	1	14	1	2	31	2	4
Sphene	2	1	1	1	2	2	3	1	1	3
Zircon		4	1	2	15	1	2	7		
Apatite		8	1	1	8		1	1		
Clinozoisite					2		1		1	1
Detrital Carbonate										
Glaucophane									1	
Lawsonite										
Jadeite										
Tourmaline		1								
Andalusite										
Sillimanite										
Staurolite										
Biotite		5		1	14				3	
Organic Carbonate	1									
Composites - Opaques	64	64	53	90	116	42	38	104	54	41
Hornblende/ Augite Ratio	0.9	0.8	0.8	5.1	2.1	0.8	1.1	0.8	1.0	3.4
Augite/Hyper-sthene Ratio	3.7	2.1	2.4	1.2	1.7	3.6	2.8	1.0	3.5	19.0

	1910	1911	1912	1913	1914	1915	1916	1917	1918	1919
Green Hornblende	5	39	31	47	36	51	50	38	46	34
Brown Hornblende	1	5		12	2	1	5	2	3	3
Oxyhornblende	1		2	16	6	5	1	2	2	3
Augite	16	29	36	16	35	25	16	26	26	36
Hypersthene	5	15	23	1	13	9	7	27	14	21
Epidote	1	7	3	1	6	2	1	5	5	1
Garnet	13	1	3			4	11		2	2
Sphene	48	2	2	2	1	3	4		2	
Zircon	9						4			
Apatite				2						
Clinozoisite		1					1			
Detrital Carbonate										
Glaucophane	1	1		2	1					
Lawsonite				1						
Jadeite										
Tourmaline										
Andalusite										
Sillimanite										
Staurolite										
Biotite	27			2	1	4	14	1	1	
Organic Carbonate							1			
Composites - Opaques	113	32	59	23	46	99	67	22	57	55
Hornblende/ Augite Ratio	0.4	1.5	0.9	3.7	1.1	2.1	3.4	1.5	1.9	1.0
Augite/Hyper-sthene Ratio	3.2	2.0	1.6	16.0	2.7	2.8	2.3	1.0	1.9	1.7

	1920	1921	1922	1923	1924	1925	1926	1927	1928	1929
Green Hornblende	34	79	30	21	49	22	37	31	26	30
Brown Hornblende	5	5	3	7	3	5	2	5	4	6
Oxyhornblende	7	4	5	15	10	2	15	10	4	7
Augite	26	3	37	25	22	29	34	37	30	28
Hypersthene	26	1	20	26	8	31	8	12	34	23
Epidote	1	3	1	4	2	7	1	4	2	
Garnet	1	1	2			1				2
Sphene					1	1	1			2
Zircon		1	1	1		2				
Apatite					4		1	1		
Clinozoisite				1						
Detrital Carbonate										
Glaucophane		2	1		1		1			2
Lawsonite		1								
Jadeite										
Tourmaline										
Andalusite										
Sillimanite										
Staurolite										
Biotite	4		1	1		4		1		2
Organic Carbonate										
Composites - Opaques	48	88	80	103	50	50	31	32	43	101
Hornblende/ Augite Ratio	1.5	28.0	0.9	1.1	2.4	0.9	1.1	1.0	1.0	1.3
Augite/Hyper-sthene Ratio	1.0	3.0	1.9	1.0	2.8	0.9	4.3	3.2	0.9	1.2

	1930	1931	1932	1933	1934	1935	1936	1937	1938	1939
Green Hornblende	31	44	44	51	46	39	66	30	40	68
Brown Hornblende	1	6	4	4	2	7	3	2	8	3
Oxyhornblende	1	19	4	7	8	5	10	7	5	8
Augite	32	16	30	26	31	31	11	40	28	13
Hypersthene	24	10	8	2	5	10	1	11	6	2
Epidote	5	1	5	3	2	6	1	5	3	1
Garnet	2			2	1		1	1	3	1
Sphene	3	1		3	1	1	3	2	3	
Zircon	1	3		1			3		4	2
Apatite										
Clinozoisite			1	1	2	1		1		1
Detrital Carbonate										
Glaucophane			2		2		1			1
Lawsonite			2					1		
Jadeite										
Tourmaline										
Andalusite										
Sillimanite										
Staurolite										
Biotite		4	1	2	4	1				
Organic Carbonate										
Composites - Opaques	53	113	50	92	93	59	84	52	189	75
Hornblende/ Augite Ratio	1.0	3.1	1.6	2.1	1.5	1.5	6.3	0.8	1.7	5.5
Augite/Hypersthene Ratio	1.3	1.6	3.8	13.0	6.2	3.1	11.0	3.7	4.7	6.5

	1940	1941	1942	1943	1944	1945	1946	1947	1948	1949
Green Hornblende	46	40	59	35	41	31	39	54	65	41
Brown Hornblende	2	2	8	5	1	2	4		1	
Oxyhornblende	5	4	3	5		7	2	9	5	4
Augite	26	36	21	27	36	32	33	16	15	27
Hypersthene	11	8	5	21	13	20	16	12	2	15
Epidote	5	5	3	3	3	3	3		4	4
Garnet	1	1		2	1			3	1	
Sphene	2	2		2	5	2	1	1	2	3
Zircon			1			2		1	1	
Apatite		2								
Clinozoisite	1						1		2	1
Detrital Carbonate										
Glaucophane	1					1	1	2	1	4
Lawsonite								2	1	1
Jadeite										
Tourmaline										
Andalusite										
Sillimanite										
Staurolite										
Biotite	1	2	1		1		4	2		
Organic Carbonate							2			
Composites - Opaques	68	52	43	73	44	83	46	141	76	38
Hornblende/ Augite Ratio	1.8	1.2	3.2	1.5	1.2	1.0	1.3	3.4	4.4	1.5
Augite/Hyper-sthene Ratio	2.4	4.5	4.2	1.3	2.8	1.6	2.1	1.3	7.5	1.8

	1950	1951	1952	1953	1954	1955	1956	1957	1958	1959
Green Hornblende	45	37	26	37	37	40	41	45	39	40
Brown Hornblende	6	6	4	3	4	3	9	17	12	21
Oxyhornblende	1	6	2	1	4	1	1	1	2	
Augite	31	31	33	38	27	34	33	17	21	25
Hypersthene	7	17	24	3	18	14	4	1	2	1
Epidote	3	2	4	6	5	4	1		2	3
Garnet	1		1	4	2		11	12	16	9
Sphene	4		3	4	1	1		4	3	1
Zircon			1	1	1	1		2	1	
Apatite						1			1	
Clinozoisite				3		1				
Detrital Carbonate	1							1	1	
Glaucophane	1	1	1		1					
Lawsonite										
Jadeite										
Tourmaline			1							
Andalusite										
Sillimanite										
Staurolite										
Biotite			1			1	3	1	3	
Organic Carbonate	1									
Composites - Opaques	62	56	93	78	90	48	67	45	36	34
Hornblende/ Augite Ratio	1.6	1.4	0.9	1.1	1.5	1.3	1.5	3.6	2.4	2.4
Augite/Hyper-sthene Ratio	4.4	1.8	1.4	12.7	1.5	2.4	8.3	17.0	10.5	25.0

	1960	1961	1962	1963	1964	1965	1966	1967	1968
Green Hornblende	44	39	33	50	37	44	53	35	52
Brown Hornblende	14	15	10	15	14	11	14	8	12
Oxyhornblende	1	3	2	3		3		5	2
Augite	17	11	20	18	14	22	13	27	20
Hypersthene	2	3	2	3	3	6	4	8	3
Epidote	1	3		3		4	1	7	2
Garnet	16	22	30	6	20	3	7	6	5
Sphene	2	2	1	1	7	4	6	2	3
Zircon	1	2	2		1	1	1	2	
Apatite	2			1	4		1		1
Clinozoisite						1			
Detrital Carbonate									
Glaucophane						1			
Lawsonite									
Jadeite									
Tourmaline									
Andalusite									
Sillimanite									
Staurolite									
Biotite	1	1		6	3		3	3	1
Organic Carbonate									
Composites - Opaques	41	52	76	57	46	55	61	44	52
Hornblende/ Augite Ratio	3.4	4.9	2.1	3.6	3.6	2.5	5.1	1.6	3.2
Augite/Hyper-sthene Ratio	8.5	3.7	10.0	6.0	4.7	3.7	3.2	3.4	6.7

	1971	1972	1973	1974	1975	1976	1977	1978
Green Hornblende	60	56	64	62	50	62	55	54
Brown Hornblende	3	13	12	3	5	2	4	4
Oxyhornblende	3	1	2	2			2	1
Augite	6	8	6	13	26	19	22	13
Hypersthene	1	3	2	1	9	9	11	3
Epidote	1	1	1		1		1	1
Garnet	18	9	10	14		1	2	10
Sphene	2	5	2	3	2	1		3
Zircon	6	3	1	1	1			10
Apatite		1		1	1			1
Clinozoisite					1			
Detrital Carbonate								
Glaucophane					3	6	3	
Lawsonite								
Jadeite					1			
Tourmaline								
Andalusite								
Sillimanite								
Staurolite								
Biotite	6	1	7	23	4	3	4	17
Organic Carbonate								
Composites - Opaques	38	35	66	65	97	120	22	56
Hornblende/ Augite Ratio	10.5	8.6	12.7	5.0	2.1	3.4	2.7	4.5
Augite/Hyper-sthene Ratio	6.0	2.7	3.0	13.0	2.9	2.1	2.0	4.3

	MTC-19 7-12 cm.	MTC-19 27-32 cm.	MTC-58	Mare 3 0 cm.	Mare 3 18 cm.
Green Hornblende	34	38	57	47	43
Brown Hornblende	1	4	2	4	2
Oxyhornblende	7	3	3	1	1
Augite	39	23	23	24	31
Hypersthene	5	10	8	12	13
Epidote	5	6		1	6
Garnet	4	3	3	3	
Sphene	4	5	4	3	
Zircon	1	2		1	3
Apatite		4		2	1
Clinozoisite		2		1	
Detrital Carbonate					
Glaucophane				1	
Lawsonite					
Jadeite					
Tourmaline					
Andalusite					
Sillimanite					
Staurolite					
Biotite	1	1	17	1	
Organic Carbonate					
Composites - Opaques	62	44	49	74	76
Hornblende/ Augite Ratio	0.9	1.8	2.6	2.1	1.5
Augite/Hyper-sthene Ratio	7.8	2.3	2.9	2.0	2.4

	I-7477	BM-8136	CM-8137	BS-8149	M-6-8164
Green Hornblende	68	60	50	52	42
Brown Hornblende	6	6	5	5	6
Oxyhornblende	3	3	3	3	4
Augite	12	13	19	27	24
Hypersthene	2	5	3	4	13
Epidote	1				
Garnet	4	2	11	2	2
Sphene	2	3	1	1	3
Zircon		4	6	3	3
Apatite	2	2	2	2	2
Clinozoisite					
Detrital Carbonate					
Glaucophane		1		1	1
Lawsonite					
Jadeite					
Tourmaline		1			
Andalusite					
Sillimanite					
Staurolite					
Biotite	95	24	9	34	2
Organic Carbonate					
Composites - Opaques	60	44	62	77	86
Hornblende/ Augite Ratio	6.2	5.1	2.9	2.1	2.0
Augite/Hyper-sthene Ratio	6.0	2.6	6.3	6.8	1.8

APPENDIX E

Faunal Survey

This survey is a listing of species of animals with calcareous skeletons obtained during the marine sampling program. Many identifications were made through the courtesy of Allyn G. Smith of the California Academy of Sciences, and the author is greatly indebted to Allyn G. Smith and Leo Hertlein, both of the California Academy of Sciences, for help in many other identifications. Further information on the assemblages and distributions of marine mollusks and brachiopods is available in The Marine Mollusks and Brachiopods of Monterey Bay, California, and Vicinity, Smith and Gordon, (1948). For localities, see Fig. 1 and Appendix A.

1800

Scaphopods: Cadulus fusiformis Pilsbry & Sharp

1802

Scaphopods: Cadulus fusiformis Pilsbry & Sharp
Bivalves: Macoma yoldiformis Carpenter

1804

Brachiopods: Laqueus californianus (Koch)
Gastropods: Crepipatella lingulata (Gould)
Bivalves: Cyclopecten (Delectopecten) vancouverensis (Whiteaves)
Nemocardium centifilosum (Carpenter)

1805

Gastropods: Crepidula adunca Sowerby
Scaphopods: Cadulus fusiformis Pilsbry & Sharp
Bivalves: Nuculana penderi (Dall & Bartsch)
Glans carpenteri Lamy

1806

Bivalves: Macoma yoldiformis Carpenter

1809

Brachiopods: Laqueus californianus (Koch)
Gastropods: Polinices draconis (Dall)
Bivalves: Acila castrensis (Hinds)
Cardita (Cyclocardia) ventricosa subsp. montereyensis Smith & Gordon
Nemocardium centifilosum (Carpenter)
Amygdalum pallidula (Dall)

1810

Corals:	Paracyathus stearnsii Verrill
Brachiopods:	Terebratalia transversa subsp. caurina (Gould)
	Terebratulina unguicula (Carpenter)
Gastropods:	Scissilabra dalli Bartsch
	Diodora aspersa (Eschscholtz)
	Crepipatella lingulata (Gould)
	Ocenebra interfossa subsp. clathrata (Dall)
	Nassarius cooperi (Forbes)
	Mitrella tuberosa (Carpenter)
	Bittium sp.
	Balcis berryi (Bartsch)
	Turbonilla (Strioturbonilla) torquata Gould
Scaphopods:	Dentalium berryi Smith & Gordon
Bivalves:	Nuculana penderi (Dall & Bartsch)
	Pecten (Chlamys) hericeus Gould
	Glans carpenteri Lamy
	Protothaca staminea (Conrad)
	Tivela stultorum (Mawe)
	Macoma sp.
	Botula californiensis (Philippi)
	Sphenia pholadidea Dall

1811

Corals:	Paracyathus stearnsii Verrill
Brachiopods:	Terebratalia transversa subsp. caurina (Gould)
	Terebratulina unguicula (Carpenter)
Bivalves:	Nuculana penderi (Dall & Bartsch)
	Pecten (Chlamys) hericeus Gould

1812

Gastropods:	Nassarius perpinguis (Hinds)

1816

Brachiopods:	Laqueus californianus (Koch)
Gastropods:	Calliostoma canaliculatum (Martyn)
	Nassarius mendicus (Gould)
	Olivella biplicata (Sowerby)
Bivalves:	Cryptomya californica (Conrad)

1818

Corals:	Paracyathus stearnsii Verrill
Brachiopods:	Terebratalia transversa subsp. caurina (Gould)
	Terebratulina unguicula (Carpenter)
Gastropods:	Calliostoma gloriosum Dall ?
	Homalopoma carpenteri (Pilsbry)
	Homalopoma paucicostatum (Dall)
	Nassarius mendicus (Gould)
	Nassarius mendicus (Gould) forma cooperi (Forbes)
	Ocenebra cf. O. interfossa subsp. clathrata (Dall)
	Halistylus pupoides (Carpenter)
	Kurtzia gordoni Bartsch
	Acteocina exima (Baird)

	Scaphopods:	Dentalium neohexagonum Sharp & Pilsbry
	Bivalves:	Nuculana penderi (Dall & Bartsch)
		Pecten (Chlamys) hericeus Gould ?
		Pseudochama granti Strong
		Glans carpenteri Lamy
		Pitar newcombianus (Gabb)
		Tivela stultorum (Mawe)
		Mactra sp.
1819		
	Scaphopods:	Dentalium semipolitum Broderip & Sowerby
1820		
	Scaphopods:	Cadulus fusiformis Pilsbry & Sharp
	Bivalves:	Nuculana taphria (Dall)
1822		
	Scaphopods:	Cadulus fusiformis Pilsbry & Sharp
1825		
	Corals:	Caryophyllia alaskensis Vaughan
	Gastropods:	Ocenebra interfossa subsp. clathrata (Dall)
		Nassarius insculptus (Carpenter)
		Amphissa versicolor Dall
		Amphissa versicolor subsp. incisa Dall
		Mitrella gouldii (Carpenter)
		Polinices sp.
		Admete sp.
	Bivalves:	Pseudochama granti Strong
		Tellina carpenteri Dall
1827		
	Gastropods:	Olivella biplicata (Sowerby)
1828		
	Gastropods:	Nassarius cf. N. mendicus (Gould)
		Nassarius perpinguis (Hinds)
		Olivella biplicata (Sowerby)
	Bivalves:	Nuculana taphria (Dall)
		Protothaca staminea (Conrad)
		Clinocardium nuttallii (Conrad)
1831		
	Gastropods:	Mitrella gouldii (Carpenter)
1833		
	Gastropods:	Amphissa cf. A. versicolor subsp. incisa Dall
		Turritella cooperi Carpenter
		Cyclichna attonsa (Carpenter)
1835		
	Gastropods:	Nassarius mendicus (Gould)
	Scaphopods:	Cadulus fusiformis Pilsbry & Sharp

1866

Scaphopods: Dentalium rectius Carpenter

1869

Gastropods: Mitrella gouldii (Carpenter)
Scaphopods: Cadulus fusiformis Pilsbry & Sharp

1870

Bivalves: Acila castrensis (Hinds)

1871

Bivalves: Pecten (Chlamys) cf. P. (C.) hindsii Carpenter
Cardita (Cyclocardia) ventricosa subsp. montereyensis Smith & Gordon
Psephidia ovalis Dall ?

1874

Scaphopods: Cadulus fusiformis Pilsbry & Sharp

1875

Bivalves: Pandora filosa (Carpenter)
Cardita (Cyclocardia) ventricosa subsp. montereyensis Smith & Gordon

1876

Gastropods: Mitrella gouldii (Carpenter)
Bivalves: Cardita (Cyclocardia) ventricosa subsp. montereyensis Smith & Gordon

1877

Bivalves: Nemocardium centifilosum (Carpenter)
Cardita (Cyclocardia) ventricosa subsp. montereyensis Smith & Gordon
Amygdalum pallidula (Dall)